Preparation of Functional PolyHIPE polymers for Agro-process and Bio-process applications

Thesis submitted to Newcastle University for the Degree of Doctor of Philosophy in Chemical Engineering

Deepashree Thumbarathy

School of Chemical Engineering and Advanced Materials

Newcastle University, United Kingdom

December 2017

Abstract

Porous polymers containing specific functional groups are attracting scientific interest due to their diverse applications. Polymerized high internal phase emulsions, or polyHIPEs are porous polymers which can be moulded into beads, membranes, films or monoliths. The characteristics of polyHIPEs are their low density, internal pore architecture and interconnectivity along with their high porosity which make them extensively applicable in separation processes, medicine and tissue engineering, agriculture and catalyst supports. However, the major drawback in exploiting the full potential of these polymers is that most of the techniques carried out for functionalization concentrate on their external surfaces. This thesis describes the development of functionalized polyHIPEs as catalyst supports and agricultural soil additive.

Firstly, this work highlights the preparation, sulphonation and characterization of polyHIPE polymers. Sulphonation via microwave irradiation enhances the polyHIPE morphology whilst increasing the specific surface area. PolyHIPEs produced with low surface area (ca. 9 m^2/g) were successfully enhanced to 110 m^2/g without compromising their mechanical stability. Subsequently, these sulphonated polyHIPEs exhibited hydrophilic behaviour capable of absorbing up to 1700 times their own weight of water. These polyHIPEs also demonstrated good ion exchange capacity of 3.4 meq/g. They were further tested for catalytic biofilm growth with *Shewanella Oneidensis MR-1* and the hierarchical structure of the pores and interconnects facilitated the transport into the material. These sulphonated polyHIPEs with high ion exchange capacity, hydrophilicity and thermal stability suggest potential application as a catalyst support. In addition, surface area with good bio-compatibility also suggests agricultural application.

Secondly, to further increase the specific surface area hypercrosslinked polyHIPEs were synthesized and functionalized. PolyHIPEs were prepared using a novel approach of depositing the metal catalyst at the synthesis stage. The incorporation of the catalyst precursor before polymerization into a monolithic

support was demonstrated for the first time. This method enables homogenous distribution of the catalyst throughout the open cellular structure imparting catalytic functionalization. We showed catalyst size can be controlled and BET surface area up to 911 m^2/g can be achieved by varying the homogenization time. These catalytic hypercrosslinked polymers with accessible porosity and transport pores can remove diffusional barriers for the reactants and products. However, addition of porogens and hypercrosslinking reduces the mechanical and thermal properties of the polyHIPEs. Hypercrosslinked sulphonated polyHIPEs were more robust than those prepared with porogens.

Finally, the sulphonated polyHIPEs were investigated for their water absorption capacity in sandy loam and clay loam soils. Addition of small quantities of these polyHIPEs improved the hydrological properties in both the soils. Incorporation of 1% of SPHPA10 polyHIPEs had significant effect on soil water retention characteristics in sandy loam soils, resulting in 3 fold increase in moisture content at field capacity as compared to the control. The most intensive impact in readily available water capacity (RAWC) was seen in 0.5% polyHIPE treatment in both sandy loam and clay loam soils which showed increased retention capacity of 68.9% and 52.8% respectively. The experiments suggest that application of lower levels of SPHPA10 polyHIPEs (0.25-0.5%) may be recommended in both type of soils.

Declaration

This thesis is submitted in fulfilment of the requirements for the degree of Doctor of Philosophy at Newcastle University. I hereby declare that the work described in this thesis is solely my own work except where acknowledged in the text. This work has not been submitted for any other degree or qualification and it was carried out entirely by myself under the supervision of Prof. S. J. Bull and Dr. E. Stockdale in Newcastle University during the period from January 2013 to June 2016.

Acknowledgement

I would like to express my sincere appreciation to my supervisor Prof. Steve Bull for his supervision, guidance and the freedom in my scientific research. His encouragement, feedback and patience helped me immensely throughout my study. I am also thankful to Prof. Galip Akay for giving me the opportunity to start this work.

I would also like to express my gratitude to Dr. Elizabeth Stockdale for her supervision, guidance and advice on the soil works carried out at the School of Agriculture, Food and Rural Development, Newcastle University.

I would like to thank a number of technical staff at the Chemical Engineering department (CEAM), Rob Dixon, Paul Sterling and Simon Daley for their continuous support. Special thanks to all the technical staff at Advance chemical and material Analysis (ACMA), Medical School, School of Agriculture, Food and Rural Development and Analytical Service Unit at the School of Chemistry for their assistance and help in analyses of my samples. I am grateful to all my colleagues and friends at CEAM for making my PhD journey enjoyable in and out of working premises. Sincere thanks to Justine for all the timely reminders.

Last but not least, I would like to extend my deepest gratitude to my family for their immense love, endless prayers and encouragement. The support from my mum and dad has been my biggest motivation. A special thought goes to my brother and sister for their never-ending love and understanding. To my beloved husband, Sudhir and wonderful daughter Annanya, thank you very much for your love, patience and undivided support which kept me going throughout the years especially during the most difficult times.

Conference and Publications

G. Akay, P.P Greco, H. Hasan and D. Thumbarathy, ***Preparation of Catalytic Hypercrosslinked PolyHIPE Polymers***, European Polymer Congress – Pisa (Italy), epf2013.

Thumbarathy D and Bull SJ, **Preparation and Functionalization of Monolith high surface area polyHIPEs polymers,** *ECCE10+ECAB3+EPIC5, Sept27th-Oct 1st2015- Nice, France.* Conference presentation.

Table of Contents

List of Figures

List of Tables

List of Abbreviations

API	agro process intensification
ATRP	Atom-Transfer Radical-Polymerization
AWC	Available Water Capacity
BET	Brunauer-Emmett-Teller
CB	Chlorobenzene
CEB	2-Chloroethylbenzene
CEC	Cation Exchange Capacity
CL	Clay Loam soil
DCE	1, 2- Dichloroethane
DVB	Divinylbenzene
FC	Field Capacity
FTIR	Fourier Transform Infrared
GMA	Glycidyl methacrylate
HEMA	2-Hydroxyethyl Methacrylate
HIPE	High internal phase emulsion
HLB	Hydrophile- Lipophile Balance
HX	Hypercrosslinked
IEC	Ion Exchange Capacity
IUPAC	International Union of Pure and Applied Chemistry
MOF	Metal Organic Frameworks
o/w	Oil-in-Water emulsion
o/w/o	Oil in water in oil emulsion
PolyHIPE	Polymerized High Internal Phase Emulsion
PHP	polyHIPE polymer
PMMA	poly methyl-methacrylate
PI	Process intensification
PGA	polyglutaraldehyde
PWP	Permanent Wilting Point
RAFT	Reversible Addition-Fragmentation chain Transfer
RAWC	Readily Available Water Capacity
SEM	Scanning Electron Microscopy
SL	Sandy Loam soil

Span 80	Sorbitan monooleate
SP	Saturation Percentage
STY	Styrene
STY-DVB	Styrene- Divinylbenzene
TAWC	Total Available Water Capacity
TGA	Thermogravimetric Analysis
TEM	Transmission Electron Microscopy
UV	Ultraviolet light
VBC	Vinylbenzyl Chloride
w/o	Water-in-Oil emulsion
w/o/w	Water in oil in water emulsion

Chapter 1 Introduction

1.1 Introduction

In recent years, microporous materials with large specific surface areas have generated a great deal of interest in research and development. Microporous material allows diffusion and can facilitate bulk transport through large micro- interconnects (Akay, 2004). Moreover, porous polymers have sufficient conformational and rotational flexibility which enables them to maximize intermolecular and intramolecular forces affecting the intrinsic properties of the polymers (McKeown and Budd, 2011).

PolyHIPEs represent cellular micro porous materials which are prepared via high internal phase emulsion (HIPE). PolyHIPEs are characterized with highly controllable physical and chemical properties and their name was coined at the Unilever Research Laboratories, Port Sunlight UK (Barby and Haq, 1985). Design, synthesis and development of polyHIPEs reveal their functional characteristics related to their internal pore architecture, low density, interconnectivity and chemical/biochemical functionality of the walls, making them a micro-structured material for a wide range of applications. These novel micro porous polymers are used either as monolithic micro-reactors for chemical or bio-chemical conversions, or absorbents/membranes or indeed as combination of these basic modes of operation. Hence applications of polyHIPE in analytical science (Marques and Fernandes, 2011), bio-process intensification (Akay *et al.*, 2005a; Akay *et al.*, 2005b), functional porous materials (Kimmins and Cameron, 2011), catalyst supports (Pulko *et al.*, 2010; Kimmins *et al.*, 2014) and medicine and tissue engineering (Akay *et al.*, 2004; Bokhari *et al.*, 2005) have been demonstrated.

In agriculture, polyHIPE functions as a soil additive which remains in the soil as bio-microreactor and associates with plant roots (Burke *et al.*, 2010). This novel method termed as Agro Process Intensification (A-PI) lead to biomass and crop yield enhancement thus enhancing productivity (Akay and Fleming, 2012). Bio process intensification based on the ‘confinement phenomenon’ in which the

micro-organism behavior is dependent on the pore size and biochemical nature of the confinement environment may also be developed as a part of the agro process intensification (Akay and Burke, 2012). The polyHIPEs in a form of micro-bioreactors are utilized as soil additives acting as synthetic rhizosphere for bacterial support with no barrier due to its interconnecting porous structure. Thus this porous and hydrophilic structure facilitates the water, nutrients and bacterial interaction to the roots of the plant. This microporous polymer creates a suitable environment for the biocatalysts and microorganisms which can enhance selectivity, thus resulting in phenomenon based intensification (Akay *et al.*, 2005b). In addition to this attribute, ion-exchange capacity is also an essential functionality of polyHIPEs in agriculture (Akay and Burke, 2010; Burke *et al.*, 2010; Akay and Burke, 2012) and separation process (Akay and Vickers, 2010; Marques and Fernandes, 2011; Akay, 2012; Akay *et al.*, 2012). Ion-exchange media consists of a three dimensional network of hydrocarbon chains containing cationic or anionic groups. Anionic functional groups such as sulphate, sulfonate, phosphate and carboxylate are present on cation exchange matrices and on the other hand anion exchange matrices usually contain the cationic tertiary and quaternary ammonium groups $-NH_3^+$ or $-N^+(CH_3)_3$. Ion-exchange materials are generally water insoluble, but can swell to a limited degree (Helfferich, 1962). These materials contain acidic or basic functional groups and are essentially cross-linked polyelectrolytes. The efficacy of polyHIPE based ion-exchangers mainly depends on the degree of cross-linking and accessibility of the ion-exchange sites which accelerates the exchange kinetics (Wakeman *et al.*, 1998; Akay *et al.*, 2004; Akay *et al.*, 2005b; Akay, 2006; Akay *et al.*, 2010). The size of the ions being exchanged along with high surface area of polyHIPE with small diffusion length may also influence the kinetics of ion exchange.

One of the methods used for developing high surface area in porous polymers is hypercrosslinking. Hypercrosslinked material contains very fine pores. The hypercrosslinking reaction involves swelling the polymer in a good solvent such as dichloroethane (DCE) which causes the space formation between the monomers. It is followed by crosslinking the polymer using the Friedel-Crafts reaction, which results in connection of the neighbouring polymer chains. The swollen or the expanded state of the polymer is retained on

hypercrosslinking even after removal of the solvent thus enhancing its surface area and increasing its free volume (Veverka and Jerabek, 1999). Thus, hypercrosslinking procedure along with Friedel-Crafts chemistry creates a micro porous structure within the polymer network. The resultant polyHIPE exhibits an enhanced surface area interconnected porous structure. Jerabek *et al.* (2008) reported introduction of porogenic solvents into the continuous phase during the preparation of polyHIPEs can yield material with surface area up to 720 m^2/g. Ahn *et al.* (2006) investigated the synthesis parameters such as vinylbenzene chloride monomer concentration, catalyst and solvent choice on the pore properties of the resulting polymeric network. Hypercrosslinking reaction with $FeCl_3$ showed extensive microporosity within only 15 minutes of initiating the cross linking reaction yielding a surface area of approximately 1200 m^2/g which enhanced steadily in 18 hours to approximately 2000 m^2/g. These hypercrosslinked polymers with high microporosity have potential application in gas adsorption and separation processes. Similarly, the interconnected open pore structure of polyHIPE allow dynamic exchange of ions and can play a major role in supply of nutrient ions essential for plant growth. Thus polyHIPEs can be a meaningful tool for controlling the ion exchange kinetics resulting in a variety of applications in the agriculture and environmental fields.

Surprisingly, very little has been published about the water uptake capacity and its effect in different types of soil for hydrophilic polyHIPEs. Soil particles are classified into three major groups; sand, silt and clay. Sandy soils may exhibit limited productivity due to their low water holding capacity and excessive percolation losses. Sand particles are large and allow good aeration. On the other hand, clay particles are very small in size and hence clay soils may store a large amount of water, but the small pores make it difficult for the roots to extract the required water for the plant growth. Silt particles are medium sized and have properties in between sand and clay particles (Weil, 2016). Weil (2016) states that loamy soil is beneficial for plant growth because it has sand, silt and clay particles in relatively equal amounts which aids water retention and aeration within the soil. Loamy soils helps in retaining the nutrients well, also allowing excess of water to drain. Thus two different types of soil, sandy loam and clay

loam considered in this study will help in understanding the water uptake and movement in these soils with the addition of sulphonated polyHIPEs.

With regular irrigation and rainfall water is retained in the soils, however under semiarid conditions with annual rainfall between 250 -500 mm may cause dry regions within the soils, whereas arid conditions (less than 250 mm of annual rainfall) will require frequent irrigation (Troeh, 1993). Burke *et al.* (2010) have claimed that sulphonated hydrophilic polymers exhibited water absorption capacities of 10 fold and 18 fold with pore sizes of 20 and 150 µm respectively. Soil mixed with these polymer particles was subjected to different watering schedule for the plant growth to reflect semiarid and arid conditions. These polymers also showed increase in dry biomass yield of rye grass by about 30, 140 and 300% respectively (with increasing water stress) in normal, semiarid and arid conditions. Similarly Akay and Fleming (2012), demonstrated increase in dry grass shoot by about 145% after 12 weeks of growth with the addition of sulphonated polyHIPEs as soil additives. However, both the studies did not highlight the type of soils used which may affect the water movement and its uptake with the addition of the polymers. Similarly the effect of pore sizes and water retained within the soils has not been accounted in these studies.

1.2 Motivation of study

Several studies have investigated hydrophilic polymers as soil additives, however the relation between the polymer morphologies and its water uptake in soils remains largely unexplored. Furthermore, the influence of the polymer morphology and pore sizes for biofilm formation which affects the soil microbial community, is still unknown. In addition, the development of tailored intensified bioreactors by the incorporation of catalyst has not been widely explored. Bioreactors can stimulate the soil microorganism growth which play a fundamental part in breaking down the organic material in soils and converting them into nutrients essential for the plants, thus impacting the physical, chemical and bio-chemical properties of soil (Weil, 2016). Hierarchically porous polymer with highly interconnected structure and enhanced surface area can be efficiently used as a catalyst support, provided the structure is robust with accessible pores.

Aiming to develop a better understanding of how to prepare, tailor and functionalize hydrophilic polyHIPEs, the first part of the thesis deals with preparation and sulphonation of polyHIPEs. The effect of sulphonation and enhancement of the specific surface area were investigated. It has previously not been investigated whether sulphonated polyHIPE provides a good substrate for the growth of the micro-organism. Furthermore, it still remains a challenge to fabricate micro porous material with controlled morphology and interconnected pore structure facilitating the transport of microorganism from one region of the polymer to another. In agriculture, it is essential to transport water and nutrients throughout the soil as the roots can uptake the water and nutrients to maintain conditions beneficial for plant growth. The proof of concept in this study, will help to clarify the impact of functionalization and tailored morphology on water uptake and ion exchange capacity and biofilm growth on these polyHIPEs. Previous studies have shown that polymeric catalyst supports requires large specific surface area and good thermal stability (Sulman *et al.*, 2011; Sulman *et al.*, 2012). Therefore, the second part of the thesis highlights the relationship between the synthesis conditions and catalyst distribution in the resultant polyHIPE. Surface area enhancement via the hypercrosslinking method is also investigated.

Finally, to provide a better fundamental understanding between the water uptake in different types of soils which effects the plant growth and biomass yield, sulphonated polyHIPEs were investigated for water retention capacity in sandy loam and clay loam soils. Sandy loam soils can easily drain water and exhibit poor water holding capacity due to the high percentage of sand particles in the soil, whereas clay loam soil have good water retaining capacity, but the water may be trapped in smaller pores making it difficult for the plant to use. Data obtained from both the sandy and clay loam soils will be analysed with a one-way analysis of variance (ANOVA) to examine how the addition of sulphonated polyHIPEs aid in moisture retention to improve the hydrological properties of the soil.

1.3 Aims and Objectives

There were two primary aims for this thesis. The first aim was to prepare and functionalize sulphonated polyHIPE materials to be used as soil additives. The

second aim was to enhance the surface area through hypercrosslinking and addition of porogens whilst investigating catalytic functionalisation.

These aims were achieved by the following specific objectives:

1) PolyHIPEs with controlled morphology of pores and interconnects were produced.
2) These materials were then functionalized via microwave irradiation and then characterized for their ion exchange capacity, hydrophilicity and bio-compatibility
3) By addition of porogens and using hypercrosslinking technique, influence on the pore size and interconnects and overall morphology of the polyHIPEs was investigated along with catalyst distribution.
4) Investigating the morphology of sulphonated polyHIPEs and test it in sandy loam and clay loam soils for water absorption capacity.

1.4 Scope and Organization of Thesis

After a brief introduction and motivation for the study, the remainder of this thesis is organized in seven chapters.

- **Chapter 2** covers the theoretical background for the study, starting with literature review on emulsions, high internal phase emulsions (HIPEs) and polyHIPEs. It also details comprehensive review on polymers in agriculture.
- **Chapter 3** details all the materials, experimental procedures and characterization techniques carried out throughout the study.
- **Chapter 4** presents the experimental outputs generated from preparation and sulphonation of polyHIPE materials. Characteristics features like the pores and the interconnected network of the polyHIPE along with its physical and chemical properties are discussed. The last section of this chapter briefly discusses the catalytic biofilm growth on these sulphonated polyHIPE material with *Shewanella Oneidensis MR-1*.

- **Chapter 5** presents the experimental results and discussion from synthesis of hypercrosslinked polyHIPEs. Preliminary studies of polyHIPEs prepared using a novel approach of depositing a metal catalyst at the synthesis stage is discussed in detail. Characterization of these hypercrosslinked polyHIPEs is also reported.
- **Chapter 6** presents the discussion and experimental outputs from the application of sulphonated polyHIPE polymers in sandy loam and clay loam soils. The study reports the investigation of water absorption capacity of these hydrophilic sulphonated polyHIPEs and their effect on soil properties.
- **Chapter 7** gives the overall observation and results achieved in this study and makes suggestions for future work.

Chapter 2 Literature Review

2.1 Emulsions

An emulsion may be defined as the mixture of two immiscible liquids, (typically oil and water) with one of the liquids is dispersed as small droplets in the other. Depending on which phase comprises the drops, the emulsions are categorized as oil in water (o/w) and water in oil (w/o) (Binks, 1998). Clayton (1928) states, in an emulsion the liquid phase which is broken up into globules is termed the dispersed phase, whilst the liquid surrounding the globules is known as the continuous phase. Thus in emulsion terminology, the dispersed phase is frequently referred to as the internal phase and the dispersion medium is the external or continuous phase.

If the dispersed or internal phase is oil, then the emulsion can be termed as o/w emulsion. Alternatively, if the continuous or the external phase is oil, then the emulsion is termed as w/o emulsion. Multiple emulsions can also be produced where both oil-in-water-in-oil (o/w/o) and water-in-oil-in-water (w/o/w) emulsion exists simultaneously. In w/o/w emulsion, water droplets are entrapped inside oil droplets which are in turn dispersed in the continuous water phase, whereas in case of o/w/o emulsions the emulsion is produced by the dispersion of water droplets, where the oil droplets are contained in the oil, hence the water phase separates internal and external oil phase (Lissant, 1988). Emulsions made by mixing pure immiscible liquids are very unstable and break rapidly causing the liquids to separate (Binks, 1998). The process of mixing immiscible liquids together in order to prepare emulsions is called emulsification. When the droplets in an emulsion come in contact with each other, they exhibit attractive forces such as van-der-Waals forces and repulsive forces mainly electrostatic forces on each other (Walstra, 1993). Such emulsions needs to be stabilized by the addition of stabilizing agent (surface active material/ surfactant) which protects the newly formed droplets to merge with each other. Figure 2-1 illustrates the schematic of emulsion formation in the presence of surface active material or surfactant.

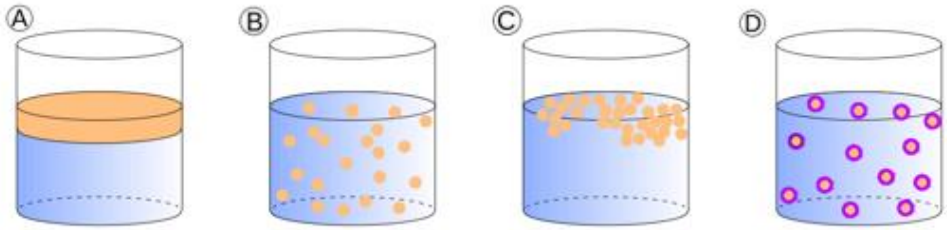

Figure 2-1 Schematic representation of emulsion formation in the presence of a surfactant. [A] - represents two immiscible liquids, not emulsified. [B] - represents emulsion of Phase II dispersed in Phase I. [C] - represents the unstable emulsion progressively separates. [D] represents stable emulsion where the surfactant (purple outline around particles) positions itself on the interfaces between Phase II and Phase I.

In a stable emulsion, the surfactant molecules used consist of two parts, one with affinity to water and other to oil. When added to the mixture of oil and water, they assemble in such a position that the hydrophilic head stays in the water and the hydrophobic tail remains in the oil. Milk can be referred as a classic example of oil in water emulsion where fat globules remain suspended in a continuous phase, stabilized by milk phospholipids. Diagram of a stable emulsion is shown schematically in Figure 2-2.

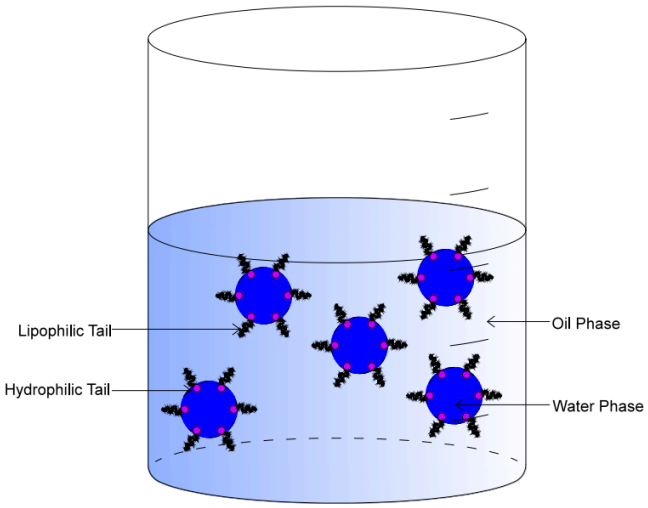

Figure 2-2 Schematic representation of a stabilized emulsion –Not to scale

Emulsions are distinguished in three types according to their droplet sizes and stability to phase separation. Macro emulsions, are those with generally

larger droplet size (droplets > 400 nm) (Anderson and Daniels, 2003). Macro emulsions are inherently thermodynamically unstable systems because the contact between the oil and the water droplet is unfavorable and phase separation occurs over a period of time. The emulsion appear opaque or milky. Miniemulsion can be defined as an emulsion with droplets size between 100 and 400 nm (Anderson and Daniels, 2003). They are obtained by shearing a mixture comprising two immiscible liquid phases and surfactant. Due to the droplet size the emulsion may appear translucent or semi opaque. Microemulsions are thermodynamically stable liquid dispersions of water and oil which usually require the presence of an appropriate surfactant or a surfactant mixture (Becher, 2001). The diameter of the droplets is less than 100 nm. Microemulsions form spontaneously and may not require any agitation (although in practice a small amount of mixing is required). The droplets exhibit low interfacial tension due no direct oil/water contact at the interface (Goodwin, 2004). Micro emulsion droplets appear transparent to an eye as small fraction of the wavelength of natural light penetrates through them.

The properties of the emulsion depends on which phase is used as the dispersed phase. Emulsions can be further classified as Low, Medium and High internal phase emulsions depending on the volume phase ratio. Emulsions are classified as low internal phase emulsions (LIPEs) when the internal phase volume is less than 30% of the emulsion volume, whereas in medium internal phase emulsions (MIPEs), the internal phase volume varies between 30 to 70% of the emulsion volume (Menner *et al.*, 2006; Manley *et al.*, 2009). High internal phase emulsions (HIPEs) are concentrated emulsions in which the internal phase volume occupies more than 74% of the emulsion volume. In this study, materials based on High Internal Phase Emulsion (HIPE) were prepared, which is detailed in Section 2.2

2.1.1 Emulsion Polymerisation

Polymerization is a process through which polymers can be produced from monomers. According to the International Union of Pure and Applied Chemistry (IUPAC), polymerization is classified as either addition polymerization or

condensation polymerization. Emulsion polymerization is essentially a complex process which involves conversion of monomers or a mixture of monomers into a stable dispersion of polymer particles (Blackley, 1975). This process can be explained with free radical polymerization which involves emulsification of a relatively hydrophobic monomer in water by an oil-in-water emulsifier followed by the initiation reaction. The free radical initiator can be either water or oil soluble initiator. In brief, according to the theory proposed by Harkins the conventional emulsion polymerisation comprises of namely water, monomer, initiator and emulsifier (Harkins, 1947). The monomer is emulsified in presence of the aqueous solution and these emulsion droplets remain dispersed in the water. The initiator causes the monomer molecules to polymerize within a certain temperature range. When the polymerization is complete, the resultant emulsion is a stable dispersion of polymer particles in an aqueous medium.

During formation of an emulsion, if monomer mixture is the continuous phase, which is then polymerized, the water droplets are then suspended in an enclosed polymer structure. Thus emulsion polymerization requires free radical polymerizable monomers which build the polymer structure (Yamak, 2013). Some of the factors which affects the kinetics of emulsion polymerization are initiator decomposition, dispersion of the monomer, emulsifier re-distribution between phases, formation of interfacial adsorption layer, initiation of polymerization and diffusion of monomer into polymeric monomeric particles (Khaddazh *et al.*, 2012).

The general theory of the mechanism of emulsion polymerization as proposed by Harkins and Smith and Ewart, can be explained in three stages; the initial stage called particle formation or nucleation, the particle growth stage and lastly the completion stage (Harkins, 1947; Smith and Ewart, 1948).

2.1.1.1 The initial stage (Particle formation or Nucleation)

The initial or nucleation period is relatively short. Monomer molecules are dispersed in the aqueous phase to form the reaction mixture. Free radicals formed by the addition of an initiator, induces polymerisation. These free radicals diffuse into monomer swollen micelles. Micelles are known as an aggregate of the surfactant molecules, and then continue to propagate by reacting with those monomer molecules therein. The monomer in the micelle is polymerised whereby

the micelle is transformed into a polymer particle. Thus new particles are generated as micelles are consumed. Micelles that do not contribute to particle nucleation disperse to supply the increasing demand of emulsifier, thereby maintaining the stability of the growing particle nuclei (Yamak, 2013).

Nucleation becomes less significant as the amount of micellar emulsifier in the system increases. The micelles start to disappear, with the continued adsorption of micellar emulsifier on to the growing particles. Disappearance of micelles of the emulsifier in the aqueous phase indicate the end of polymer-monomer particles, after which the number of particles remains constant (Chern, 2006). Schematic representation of stage one- particle formation is as shown in Figure 2-3a

2.1.1.2 The particle growth stage

During this stage there is no more surfactant to generate new particles. The polymer particles contain considerable amount of monomer by rapid diffusion of monomer from the monomer droplets (Yamak, 2013). The monomer reservoir droplets get slowly consumed. The rate of polymerization at this stage is constant and the monomer/polymer ratio remains constant. The particle growth stage ends, when the monomer droplets are exhausted and completely disappear in the polymerization system. Figure 2-3c illustrates end of particle growth stage.

2.1.1.3 Completion stage

In this final stage, polymerization continues within the monomer swollen polymer particles as seen in Figure 2-3d. The monomer droplets are exhausted and polymerization rate continues to decrease towards the end of polymerization (Blackley, 1975). Polymer particle size is constant and polymerization is complete. Conversion rate can reach up to 80-100%. The final reaction mixture obtained comprises a dispersion of polymeric particles stabilized with emulsifier as illustrated in Figure 2-3e. The main features of different stages in emulsion polymerization are illustrated diagrammatically in Figure 2-3 (a-e).

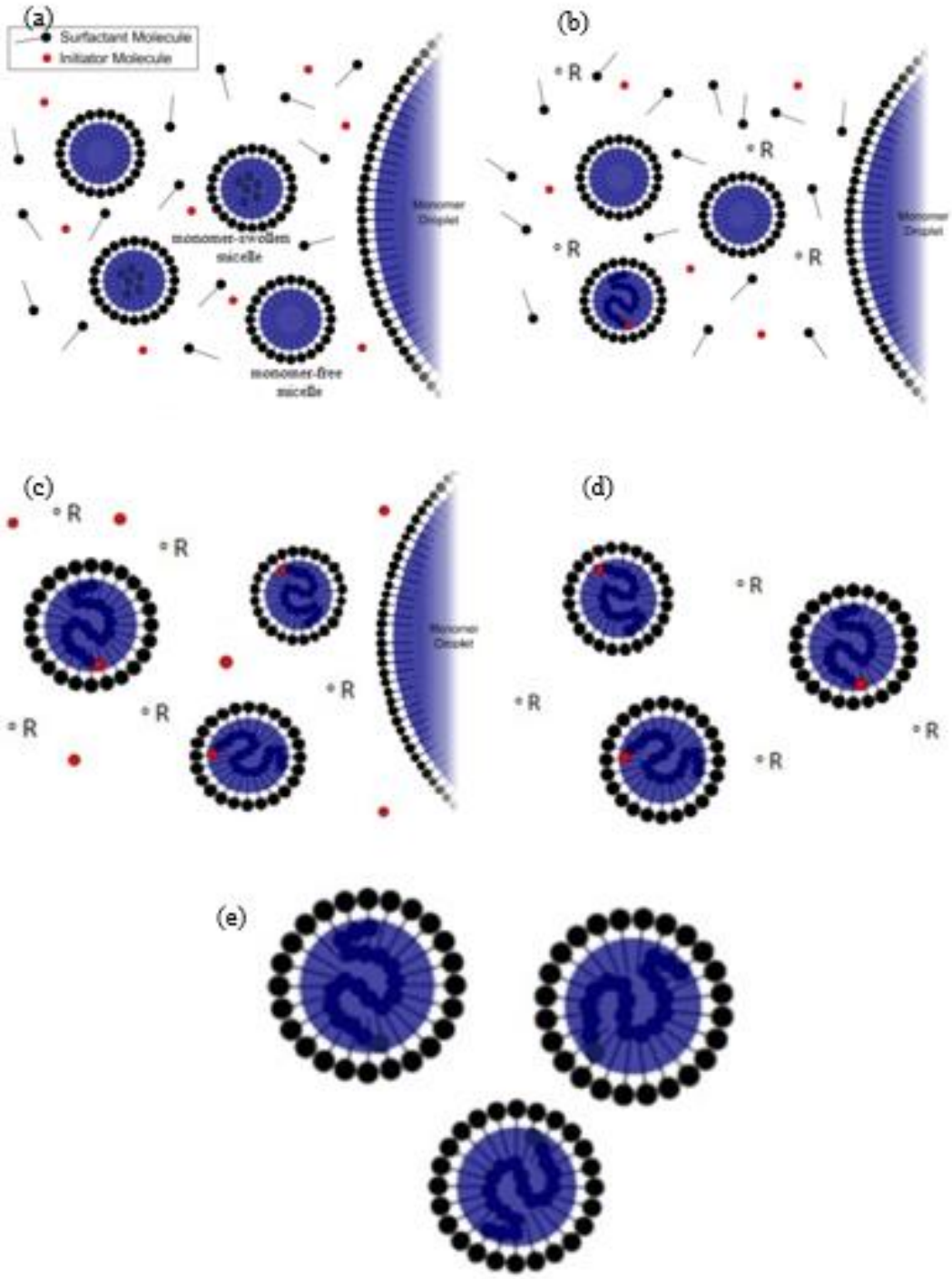

Figure 2-3 Schematic representation of the different stages in emulsion polymerization [Adapted from Yamak (2013)] (a) Presence of surfactant, initiator, monomer free micelle which diffuse into monomer swollen micelle. (b) Disappearance of micelles – End of particle nucleation stage. (c) End of particle growth stage. (d) Completion stage where polymerization continues within monomer swollen polymer particles. (e) Polymeric particles stabilized with emulsifier

2.1.2 Mechanism of Radical polymerisation

In order to understand the relationship between the polymerization parameters and the resulting polyHIPEs properties a brief description into the radical chain reaction is given. Free radicals are atoms or group of atoms with an unpaired number of electrons. The monomers are polymerized via a free radical process in which a macromolecular chain is produced by a single chain reaction, where the chain grows by the addition of a monomer to the terminal free radical reactive site called active center. The four distinct processes which take place during free radical polymerization compromises of initiation, propagation, monomer transfer and termination. These four fundamental steps are described in the following sections.

2.1.2.1 Initiation

Polymerization is initiated during this process. Initiation is decomposition of the initiator by thermolysis or by radiation that splits the original initiator compound into one or more radicals. Thus, initiation involves formation of reactive site where free radicals are generated by added initiator compound via decomposition (Anderson and Daniels, 2003). The free radical then adds on to the monomer molecule 'M' producing a propagating radical chain represented in Figure 2-4. It indicates that the growing polymer radical includes the original monomer.

$$I \longrightarrow 2R\bullet \qquad \text{Initiation}$$

$$R'\bullet + M \longrightarrow MR\bullet \qquad \text{Chain Initiation}$$

Figure 2-4 Basic Schematic reaction for free radical polymerization (Initiation) where R• = free radical, M = molecule of the monomer.

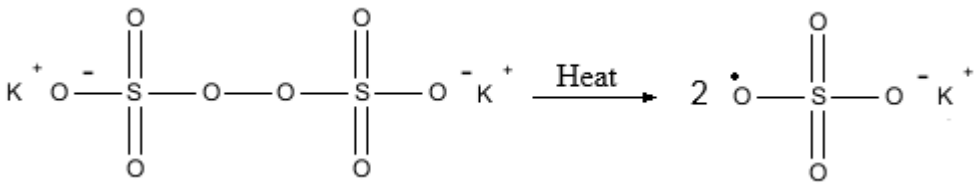

Figure 2-5 Reaction for decomposition of potassium persulphate ($K_2S_2O_8$)

Figure 2.5 illustrates the initiation of polymerization by water soluble initiator potassium persulphate which decomposes into two free radical anions.

2.1.2.2 Propagation

Monomer is consumed and a chain carrier is formed from the reaction of the free radical and the new monomer unit and propagation occurs. During this stage, growth of the monomer molecule takes place by successive addition of monomer molecules 'M' to the primary radical $R'\bullet$ as shown in Figure 2.6. As the monomer molecules gets added to the active chain end, the growing polymer chain continue to develop in molecular weight and reactive site is regenerated after each addition of monomer (Anderson and Daniels, 2003).

$$R'\bullet + nM \longrightarrow R_n\bullet \qquad \text{Propagation}$$

Figure 2-6 Basic Schematic reaction for free radical polymerization (Propagation)

2.1.2.3 Monomer Transfer

At a certain stage, the propagating polymer chain stops growing and transfer occurs when an active radical is transferred to another molecule which can be monomer, initiator or polymer (Yamak, 2013). This event results in termination of the growing polymer chain.

$$R_n\bullet + ZY \longrightarrow R_nZ + Y\bullet \qquad \text{Transfer to monomer}$$

Figure 2-7 Basic Schematic reaction for free radical polymerization (Transfer of monomer) where; ZY = chain transfer agent

2.1.2.4 Termination

In this final stage of polymerization, active chain center is destroyed and growth of the polymer chain is terminated irreversibly. The termination stage can occur showing two main mechanisms. Firstly, combination, in which two active radical end group meet resulting in a single polymer molecule and the second is disproportionation, in which the growing chain detaches an hydrogen atom from another growing chain leaving it with an unsaturated end (Yamak, 2013). Combination and disproportionation mechanism is demonstrated schematically in the following Figure 2-8.

$$R_n\bullet + R_m\bullet \longrightarrow P_{n+m} \qquad \text{Combination}$$

$$R_n\bullet + R_m\bullet \longrightarrow P_n + P_m \qquad \text{Disproportionation}$$

Figure 2-8 Basic Schematic reaction for free radical polymerization (Termination) where; $R_m\bullet$ = propagating radical chains with degrees of polymerisation of m and $P_n + P_m$ = terminated macromolecules

Therefore, under the steady state conditions, the concentration of active growing chains remains constant, i.e. the rates of initiation and termination are equal. It is assumed that the active growing chains are independent of the chain length of the polymer chain.

2.1.3 Surface Chemical Factors in Emulsion Stability

The term “emulsion stability” refers to the ability of an emulsion to keep its properties unchanged over certain period of time and resists the reformation of the bulk fluids from which it was made (Binks, 1998). However, as emulsions are thermodynamically unstable changes do occur. Interfacial tension plays a crucial role in emulsion stability. Reducing the interfacial area and the free energy of the system, results in phase separation. The more slowly the properties change, the more stable the emulsion is. Emulsions may be stabilized by the presence of

emulsifier/ surface active material which acts at the interface delaying the tendency of the liquid to separate. Thus, their presence extends the life span of an emulsion. Emulsion properties may alter in a number of phenomena. They are named as Creaming, Sedimentation, Flocculation, Coalescence and Ostwald Ripening. These different mechanisms which causes destabilization are described in the following section. In some emulsions, phase inversion can also create instability.

2.1.3.1 Creaming and Sedimentation

This process occurs due to external forces usually gravitational or centrifugal. When the density of the droplets in the dispersed phase and the continuous phase are not equal, a concentration gradient builds up in the system (Binks, 1998). When the density of the disperse phase is less, the globules rise to form a concentrated layer at the surface. This phenomenon is known as creaming. On the contrary, if the density of the disperse phase is greater than the continuous phase, dispersed droplets tend to descend and form a concentrated layer at the bottom of the emulsion. This phenomenon is termed as sedimentation. A schematic representation of creaming and sedimentation is shown in Figure 2.9 a&b. Generally, the density of oil is lower than the density of water, thus droplets of o/w emulsions tend to cream. On the other hand, w/o emulsions tend to sediment.

2.1.3.2 Flocculation

In an emulsion, due to Brownian motion or mechanical agitation droplets frequently collide with each other. This causes the droplets to either aggregate or move apart. Flocculation process refers to aggregation of droplets into larger units, without any change in their physical properties (Sherman, 1968). Flocculation occurs when there is net attractive force between the dispersed phase droplet allowing collision and growth of floc. Depending on the magnitude of the attractive energy involved, flocculation may be either weak (reversible) or strong (irreversible). Emulsion flocculation is shown schematically in Figure 2-9c.

2.1.3.3 Coalescence

Coalescence is an irreversible process in which two or more droplets of an emulsion merge together to form a larger single droplet (Marrucci, 1969). This may lead to complete separation of the two immiscible phases. Marrucci (1969) proposed that coalescence occurs when the droplets are in close proximity and the force between them is such that the thin film separating the droplets is ruptured. The film rupture mechanism is largely dependent on the continuous phase properties and on the properties of emulsifier adsorbed at the droplets. Altering the viscosity and using emulsifier forming a strong interfacial film can stabilize coalescence.

2.1.3.4 Ostwald Ripening

Ostwald ripening is a process in which gradual growth of the larger droplets occurs at the expense of smaller ones due to mass transport of dispersed phase through the continuous phase (Taylor, 1995). Ostwald ripening occurs even when the droplets are not in direct contact, high solubility of the smaller droplets and molecular diffusion through the continuous phase causes the larger droplets to grow at the expense of smaller ones. Thus smaller particles continue to shrink until they disappear and large particles grow even larger. Overtime this may even lead to phase separation. To reduce the rate of Ostwald ripening and stabilize the emulsion, high molecular weight compounds can be added that reduce the rate of diffusion of molecules within the dispersed phase.

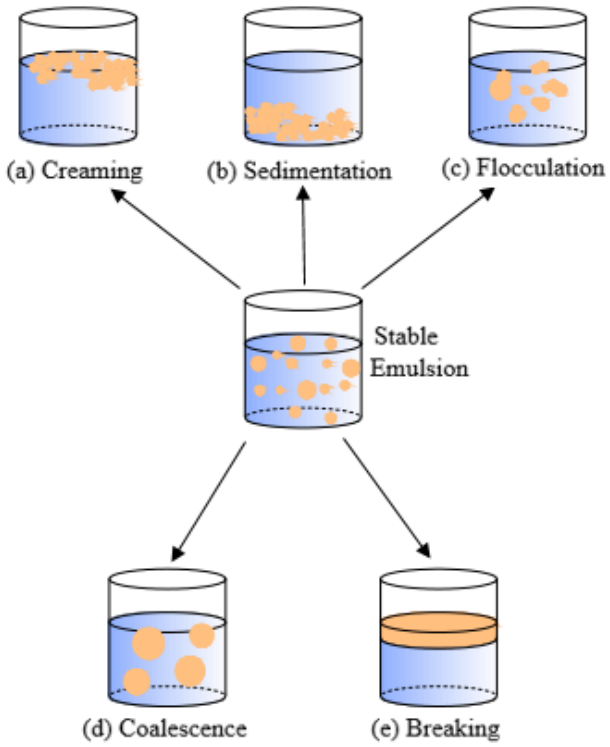

Figure 2-9: Diagrammatic representation of types of instability in emulsions

2.1.3.5 Phase inversion

The instability caused in emulsion where they can invert from an o/w to a w/o emulsion or vice versa is termed as phase inversion. This creates instability within the emulsion which can lead to its separation. Phase inversion occurs under conditions determined by the system properties, phase volume ratio and energy input where the dispersed phase is spontaneously inverted to become continuous phase or vice versa (Yeo *et al.*, 2000). The inversion mechanism is schematically shown in Figure 2-10.

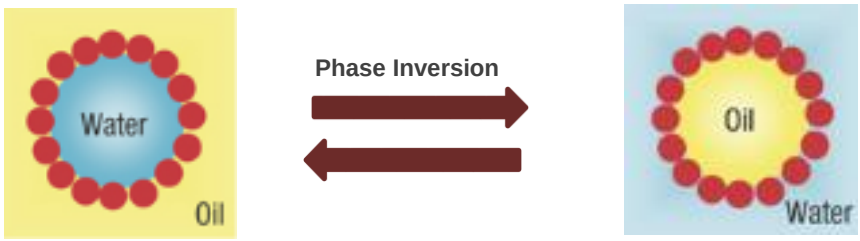

Water-in-oil emulsion **Oil-in-water emulsion**

Figure 2-10 Emulsion droplet showing the inversion mechanism

2.2 High Internal Phase Emulsions (HIPEs)

High internal phase emulsions (HIPEs) are concentrated emulsions in which the internal phase volume occupies more than 74% of the emulsion volume (Pulko and Krajnc, 2012). Lissant (1966) was the first to classify HIPEs as emulsion with over 70% or greater internal phase volume. 74% denotes the most efficient packing arrangement for regular monodispersed spheres. This number represents the maximum packing fraction occupied by uniform spheres, which remain undistorted. HIPEs exceed this maximum packing and hence the spherical droplets are deformed via compression. With further increase in internal phase (74-94%), the droplets distort and arrange in rhomboidal decahedral shape separated by a thin continuous film (Menner and Bismarck, 2006). Exceeding 94%, the interfacial area between the droplets become larger and they take the geometric configuration of truncated octahedrons (Lissant, 1966; Lissant *et al.*, 1974). This method of obtaining a highly porous structure is also referred to as emulsion templating. Figure 2-11 shows the schematic diagram of the packing arrangement of droplet phase in an emulsion and HIPEs.

HIPEs can thus attain internal phase volume up to 99% and adjusting this phase volume can modify morphology creating a highly porous structure. HIPEs are generally formed by constant agitation/stirring with controlled addition of the internal phase to the external phase in presence of a surfactant. Depending on the surfactant properties, HIPEs tend to be viscous (Princen, 1983). Increasing the viscosity of the continuous phase may also cause a major problem as it can impede the dispersion of the internal phase, leading to inadequate mixing of the phase consequently lowering the amount of distributed droplets in HIPEs (Barbetta *et al.*, 2005). Unilever scientists Barby and Haq (1985), successfully pioneered porous polymer structure formed by HIPE and subsequent polymerization of the continuous phase, which is often referred to as ‘poly(HIPE)’. HIPEs have potential applications in varied discipline such as petroleum (fuels), oil exploration, food industry (mayonnaise), agricultural sprays (pesticides), cosmetics and many more.

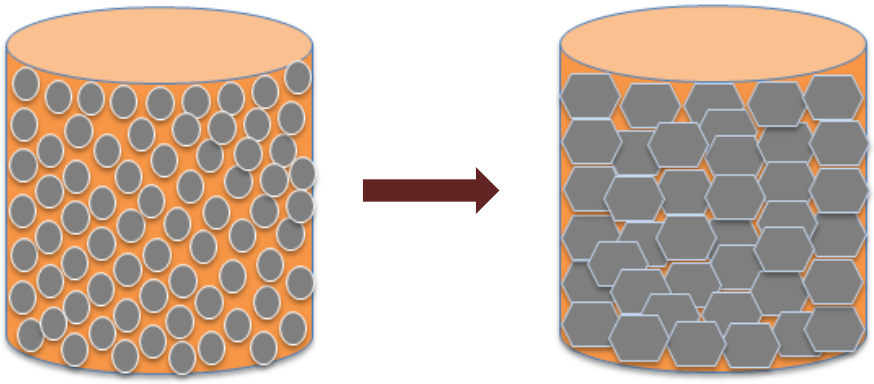

Figure 2-11 Schematic representation of packing arrangement of droplet phase in an emulsion and HIPE

2.3 Preparation of PolyHIPEs from HIPEs

One of the most important and widely used applications of HIPEs is as template for the preparation of a novel type of highly porous polymeric material. This polymerised HIPE is referred to as PolyHIPE following the Unilever patents by Barby and Haq (1982). On a laboratory scale, HIPEs are formed by slow drop wise addition of internal phase to continuous phase under constant agitation with the use of overhead stirrers. Continuous phase (oil phase) is a solution of monomer, surfactant, crosslinker and initiator. The resultant morphology and the size of the interconnecting pores is also affected by the nature and the concentration of the surfactant used (Williams, 1991). The addition of surfactant causes thinning of the monomer film which separates each droplet in the emulsion. The phase volume ratio along with the type and amount of surfactant used determines the open pore morphology of the resultant polymer. (Cameron, 2005). Constant stirring produces a homogenous emulsion. Another factor that impacts the size of the pores and interconnects is the temperature of the aqueous phase. Increasing the temperature causes increase in the mobility of the droplets and also the solubility of the surfactant in the aqueous phase which reduces the stability of the HIPE. Carnachan *et al.* (2006) demonstrated that these two

prominent factors promotes droplet coalescence, leading to an increase in pore diameter. Ostwald ripening and droplet coalescence are the two main factors that affect the HIPE stability. Mixing of the two phases with constant stirring causes the large droplets to break up suppressing Ostwald ripening and droplet coalescence. The resulting HIPE obtained is poured in suitable size/shape mould and is then subjected to polymerisation, where the continuous phase is cured around the internal phase droplets. Thus HIPE can be moulded, dispersed in immiscible solvents or cast to form monoliths, beads or even films (Bhumgara, 1995; Desforges *et al.*, 2002; Menner *et al.*, 2006; Pulko and Krajnc, 2008)

Polymerization of HIPE can be thermal, ultraviolet light (UV), redox or catalytic method which converts (polymerises) the liquid monomer to solid polymer. Polymerisation is followed by washing with water and a lower alcohol via soxhlet extraction. This results in removal of droplet phase along with any unreacted monomeric components. The solid polymer is finally vacuum dried. Thus the resulting polymeric material is highly porous with a well-defined internal structure known as polyHIPE as shown in Figure 2-12.

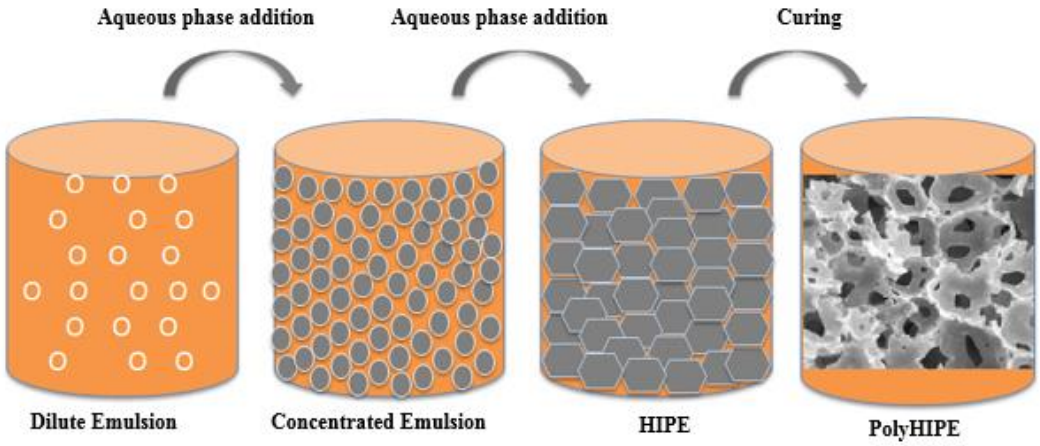

Figure 2-12 Schematic of PolyHIPE preparation

Therefore, the final structure of the polymer has a unique morphology and a hierarchical pore distribution which depends upon the parent HIPE and parameters such as polymerisation time and temperature. The occurrence of droplet coalescence is due to the thinning and subsequent rupture of the interfacial layer (Freire *et al.*, 2005). The holes formed by the removal of the

droplet phase are termed as pores or voids or cavities shown in Figure 2.13 and these are interconnected generating an open, porous permeable structure. The larger pores in the range of 10-100 µm are interconnected with smaller pores (Pulko and Krajnc, 2012). This porous and highly interconnected pore network as illustrated in Figure 2-14.

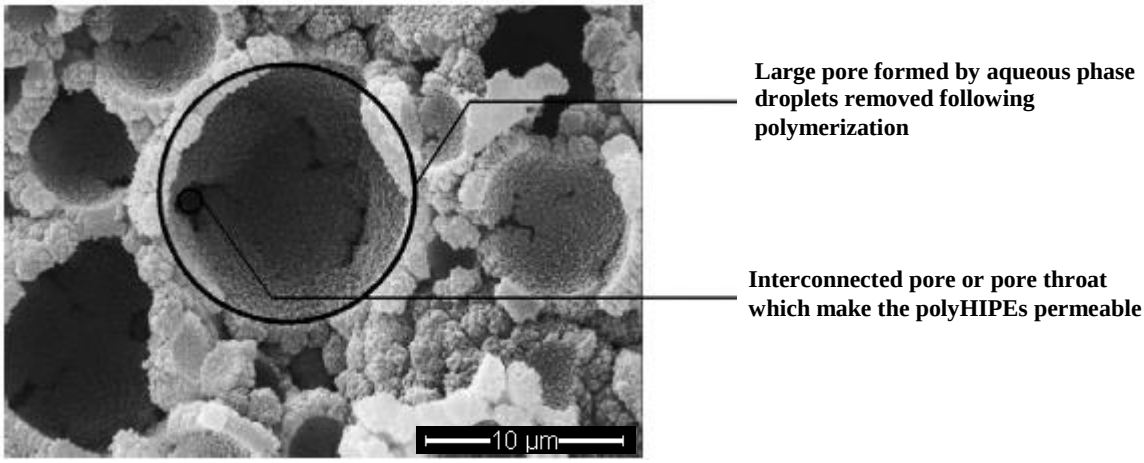

Figure 2-13 SEM showing porous structure of typical PolyHIPE (Junkar *et al.*, 2007)

Figure 2-14 depicts SEM images of a polyHIPE with formation of coalescence pores. Highly porous and highly interconnected morphologies are as seen in SEM images in Figure 2-15. The large pores are termed as cages, voids, cells or pores, while the smaller pores have been termed as interconnects, windows or pore throats in most of the literature on polyHIPEs. In this study, the terms pores and interconnects will be used. Mostly researched polyHIPEs are based on styrene and divinylbenzene (Sty-DVB) monomers due to the emulsion stabilities and ease of polymerization (Barby and Haq, 1985; Williams and Wrobleski, 1988). However, polyHIPEs developed from Sty-DVB demonstrate hydrophobic and brittle properties which may not be desired for many applications (Menner *et al.*, 2006). Furthermore, polyHIPEs have porosity which can reach over 90% and a non-modified polyHIPE has a relatively small surface area between 3 – 20 m^2/g. Deleuze *et al.* (2005) in their research efforts demonstrated densities of polyHIPE as low as 0.040 g/cm^3 and pore size about 4-9 µm. Thus, numerous researches were carried out to improve the properties of polyHIPEs and its applications in various fields. Addition of porogenic solvents

into the continuous phase during synthesis leads to enhancement of polyHIPE surface area.

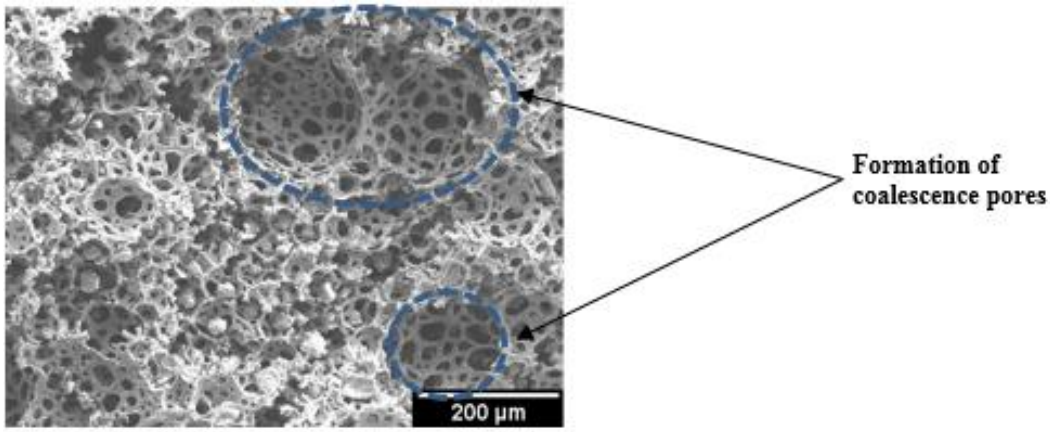

Figure 2-14 SEM showing coalescence pores formed due to emulsion instability

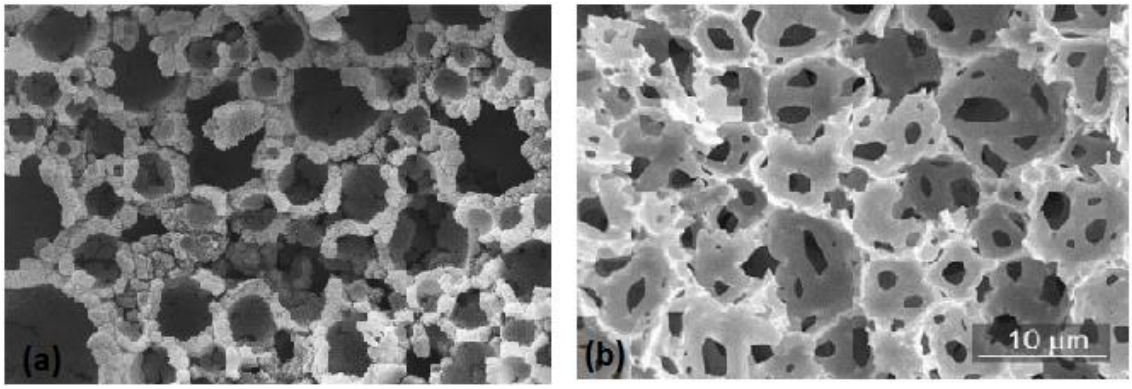

Figure 2-15 (a) Highly porous PHP and (b) highly interconnected PHP (Akay *et al.*, 2005a)

Depending on its application, various chemistries can be employed from a wide variety of monomers for preparation of the polyHIPE. PolyHIPEs were originally developed as carriers and absorbents for liquid by Unilever scientists (Barby and Haq, 1982). Akay *et al.* (2004) developed highly porous scaffold polyHIPE modified with hydroxyapatite which has a potential for bone tissue engineering. Cooper *et al.* (2001) synthesized polyHIPEs with an alternative approach which did not involve usage of organic solvent either in synthesis or purification. Supercritical carbon dioxide was used in templating high internal phase emulsions. This novel approach is particularly suitable in certain

biomedical applications where use of organic solvent is not desired and removal of residual traces is more problematic. Barbetta *et al.* (2000) demonstrated polyHIPEs prepared from vinylbenzyl chloride (VBC) which altered the properties of the resultant foam. PolyHIPEs prepared with VBC were used in many studies for producing hypercrosslinked materials due to the presence of the benzyl chloride group suitable for post-polymerization functionalization (Liu *et al.*, 2008; Liu *et al.*, 2010).

In this study, water in oil HIPE is used, as the production of polyHIPE involves using hydrophobic monomer. The monomers are oil soluble and the aqueous phase functions as the porosity template (Pulko and Krajnc, 2012).

2.4 PolyHIPE Surfactants and Electrolytes

Surfactants also termed as surface active agents are molecules which exhibit the property of absorbing onto the interface and modifying the interfacial free energy of these interfaces. Surfactants are essential to stabilize an emulsion. They achieve this by lowering the surface tension between the two phases and forming a rigid film at the interface, thus holding the two phases together. Surfactants molecules possess both hydrophilic and hydrophobic group and these two moieties of the surfactant are called heads and tails respectively as shown in Figure 2-16. Surfactants can be classified based on the hydrophilic group type. When the head moiety bears a negative charge the surfactant is called anionic whereas cationic surfactants have head moiety with positive charge. If the head moiety bears no apparent charge the surfactant is termed as non-ionic. Lastly, zwitterionic surfactants are head moiety bearing both positive and negative charges. The two major roles played by the surfactant are lowering the interfacial tension and facilitating droplet break up to prevent re-coalescence (Walstra, 1993). Re-coalescence is also governed by the surfactant concentration in the emulsion. Low surfactant concentration may cause the droplets to coalesce when they collide due to insufficient protective layer around them.

Walstra (1993) outlined that depending upon the type of surfactant used the interfacial tension is lowered to a different degree consequently affecting the

final droplet size. Moreover, type of surfactant and surfactant concentration used also help to determine formation of open or closed cell HIPEs. Williams and Wrobleski (1988) demonstrated 20% to 50% surfactant relative to the total oil phase is an optimum surfactant level producing interconnecting, porous foams. They observed below 5% surfactant levels polymer showed closed cell, whereas 7-10% surfactant level produced open cell, interconnected polymer structure. Their study also indicated above 80% surfactant level, the polymer was no longer connected. Thus Williams and co-workers discovered that the surfactant concentration has a profound effect on final cellular structure of polyHIPE; HIPEs prepared with almost 97% internal phase volume and 5% surfactant still produced closed cell polymer (Williams and Wrobleski, 1988). Furthermore, Cameron *et al.* (1996a) proposed that higher surfactant concentration lead to the formation of thinner films separating the emulsion droplets. Their investigation suggested interconnecting pores are formed during polymerisation when shrinkage occurs resulting in the rupture of the polymer film at its thinnest point.

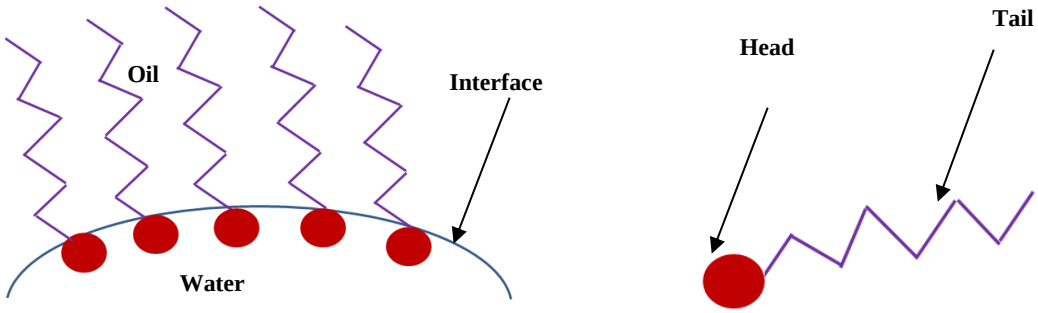

Figure 2-16 (a) Surfactant molecules at the interface **(b) Structure of surfactant**

Sorbitan monooleate, also known as 'Span 80' (Figure 2-17), is the commonly used non-ionic surfactant for stabilization of w/o HIPEs. Morphological features such as pore size and openness are not only affected by the surfactant concentration, but also by its structure (Pulko and Krajnc, 2012). Their studies demonstrated that the surfactant results in thinning of the polymer film of the continuous phase which is then more likely to break or rupture either during the polymerization or post polymerization treatment. Krajnc (2002) observed if a

mixture of Span 80 and Span 85 was used instead of using only Span 80, the polyHIPE obtained had significantly reduced pore sizes. Studies conducted by Barbetta and Cameron (2004) using three component surfactant composed of Span 20 (sorbitan monolaurate), cetyltrimethylammonium bromide, and sodium salt of dodecylbenzenesulfonic acid efficiently stabilised HIPEs as compared with solely Span 80. They also found that the resulting polyHIPE had smaller pores and higher surface areas. Cameron *et al.* (1996a) suggested that the interconnecting pores are formed due to volume shrinkage during conversion of monomers to polymers, whilst studies by Menner and Bismarck (2006) proposed that the pore sizes are affected due to the phase separation of surfactant from the polymerizing organic phase into the contact areas between droplets during polymerization forming surfactant rich and polymer poor regions. These regions rupture when the surfactant is removed during the purification and drying process.

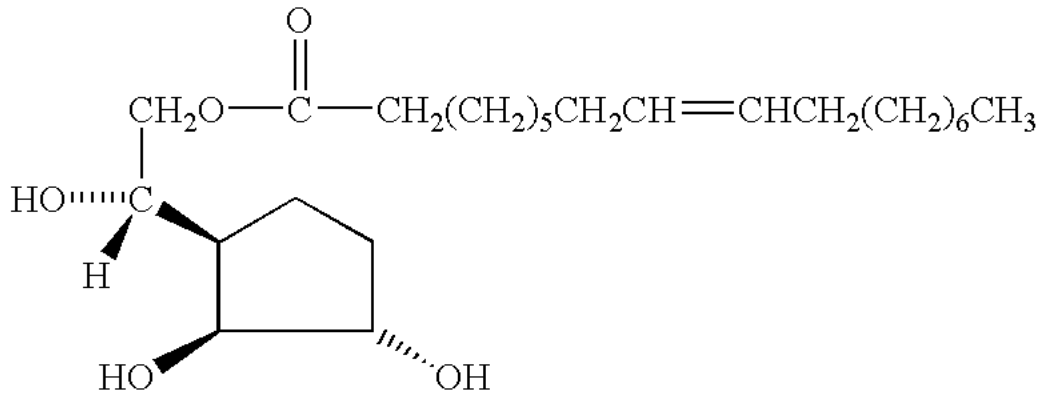

Figure 2-17 Sorbitan Monooleate (Span 80)

According to work conducted by Aronson and Petko (1993), electrolytes such as sodium chloride improved w/o emulsion stability. Furthermore, their studies on incorporation of electrolyte such as potassium chloride (KCl) and potassium sulphate (K_2SO_4) in the aqueous phase not only affected the viscosity and yield stress but also reduced the average droplet size stabilizing the emulsion. Their work concluded that the presence of electrolytes retard processes like Ostwald ripening and coalescence of droplets which were the major causes of emulsion instability. Similarly, Williams *et al.* (1990) reported

potassium persulphate and calcium chloride produce smaller pore size polymer as compared to oil initiator such as lauryl peroxide. Their research revealed pore sizes in the polyHIPE were inversely related to the surfactant level, but are greatly affected by salt concentrations. Thus presence of electrolytes, reduces the interfacial tension of the two immiscible phases due to the stronger adsorption of the surfactant molecules at the interface. Thus, if the surfactant is adsorbed more strongly at the w/o interface a high resistance to droplet coalescence is observed Similarly, Marquez *et al.* (2010) revealed that the presence of calcium chloride dihydrate causes stronger adsorption of the surfactant molecules at the interface of the two immiscible phases as the interfacial tension between the phases reduces. Reynolds *et al.* (2000) demonstrated that higher resistance to droplet coalescence is observed due to strong adsorption of the surfactant at the liquid-liquid interface.

In contrast to these studies, Opawale and Burgess (1998) pointed out too much of electrolyte can be unfavorable to emulsion stability. Their study demonstrated high salt concentration reduces the interaction between the surfactant and water molecules thereby decreasing the interfacial elasticity and therefore emulsion stability. Their research concluded the interfacial film strength in w/o emulsion using Spans 20, 80, and 83 is maximized by using salt in the aqueous phase.

2.5 The Hydrophile –Lipophile Balance (HLB) Concept

The choice of a surfactant for a given system as an emulsifying agent can be complicated as both oil and water phases are of variable compositions. Griffin (1949) first introduced the hydrophilic-lipophilic balance method which assigns a number to the surfactant between 0 and 20, depending on the balance between their hydrophilic and lipophilic moieties. Hydrophile (water loving or polar) refers to surfactant moiety soluble in water whereas, lipophile (oil-loving or non-polar) refers to oil soluble/ hydrophobic moiety of the surfactant molecule. According to Bancroft's rule, surfactants with low HLB values exhibit a lipophilic tendency and stabilizes w/o emulsions on the other hand, those with higher HLB values are hydrophilic and stabilizes o/w emulsions (Bancroft, 1913).

Table 2-1 illustrates the classification of surfactants according to their HLB values and ability to stabilize emulsions

Table 2-1 Surfactant classification by HLB (Bancroft, 1913)

HLB Range	Application
4-6	W/O emulsifier
7-9	Wetting agents
8-18	O/W emulsifiers
13-15	Detergents
15-18	Solubilizing

Thus, the Table 2-1 shows that surfactant having more active hydrophilic group is assigned a high HLB number and will produce an o/w emulsion while surfactant with more active lipophilic group and oil soluble is assigned a low HLB number (4-6) producing w/o emulsions. Thus, according to Griffin (1954) the balance between the size and the strength of the hydrophilic and lipophilic moieties of a surfactant molecule determines its HLB number. This means it is based on the weight fractions of hydrophobic and hydrophilic groups present in the molecule. The HLB number of a surfactant can be calculated based on the surfactant's molecular geometry and is represented by the following equation used for polyoxyethylene type nonionic surfactants (Dechant, 1987). Hence, the HLB value is a function of the weight percentage of the hydrophilic portion of the molecule of a non-ionic surfactant.

Equation 2-1

$$\mathbf{HLB} = (\mathbf{mole}\%\ \mathbf{hydrophilic\ group})/\mathbf{5}$$

For non-ionic surfactant, Griffin used the general formula as represented in **Equation 2-2,** where HLB value is an indication of the solubility of the surfactant.

Equation 2-2

$$\mathbf{HLB = 20\ X\ \left(\frac{M_h}{M_h + M_l}\right)}$$

Where;

M_h = Molecular weights of the hydrophilic moieties of the molecule

M_l = Molecular weights of the lipophilic moieties of the molecule

Sherman (1968) introduced HLB method in a more quantitative basis by assigning numbers to specific molecular groups. The HLB value for the surfactant was calculated as per Equation 2-3

Equation 2-3

$$\mathbf{HLB = \Sigma(hydrophilic\ group\ numbers) - \Sigma(lipophilic\ group\ numbers) + 7}$$

Table 2-2 includes a list of HLB group values of some structural groups (Zatz, 1987)

Table 2-2 HLB Group Values for some common groups (Zatz, 1987)

HLB Groups	Group Number
Hydrophilic	
$-SO_4^-Na^+$	38.7
$-COO^-K^+$	21.1
$-COO^-NA^+$	19.1
-COOH	2.1
-OH(free)	1.9
Lipophilic	
$-CH_3^-$	0.475
$-CH_2-$	0.475
=Ch-	0.475
$-(CH_2-CH_2-O)O$	0.33

2.6 Functionalization of PolyHIPEs

Different strategies and routes can be employed for polyHIPE functionalization according to its diverse applications. Due to recent interest in chemical functionalization of polyHIPEs new functional porous polymer can be obtained. With the addition of monomers, co-monomers and surfactants polyHIPE materials with a wide range of mechanical, chemical and degradation properties can be developed. Kircher *et al.* (2013) explained that the functionalization methods can be divided into two types: (1) HIPE is added with the co-monomer bearing the desired functional group; (2) post-polymerisation modification of a previously prepared polyHIPE grafted with functionalized organic molecules or macromolecules. Although the first method is convenient it has major limitations where the emulsion is destabilised when hydrophilic functional group are used with co-monomers. Moreover, Kircher *et al.* (2013) mentions the first method may also lead to phase separation and even if phase separation does not occur, the polyHIPE formed from the less stable HIPE has poorly defined morphology. Hence second method is preferred for the addition of the functional group, where polyHIPE of desired morphology is prepared by varying factors such as surfactant concentration, stirring rate and temperature. Subsequently, the functional group is grafted on this polyHIPE. However, work by Cummins *et al.* (2007) demonstrated a polymerisable initiator for atom transfer radical polymerization (ATRP) can be incorporated in HIPE without compromising the emulsion stability. Their work showed surface functionalization with poly methyl-methacrylate (PMMA) and re-initiation of hydroxyethyl methacrylate (HEMA) forming a grafted block co-polymer. Moreover, grafting of glycidyl methacrylate (GMA) resulted in polyHIPE with high density of reactive surface functionalities. Although ATRP indicates good approach for surface functionalization, it may have limited biological applications due to incorporation of copper in the polymer.

The porous nature of the polymer can be characterized by surface area, total pore volume and pore size distribution (Gokmen and Du Prez, 2012). According to Wu *et al.* (2012) porous polymers are easy to process and can be moulded in monolithic form, thin films or membranes. Moreover, the synthesis of

porous polymer with high surface area also enables in incorporating multiple chemical functionalities into the porous network. High porosity coupled with interconnectivity make it critically important in tissue engineering, where Akay *et al.* (2004) developed a well-defined highly porous scaffold polyHIPE with a potential for bone tissue engineering. In a following work, Bokhari *et al.* (2005) successfully developed microcellular polymer to enhance cell biomaterial interactions and promote osteoblast growth in vitro. PolyHIPEs were modified with hydroxyapatite which showed good cellular attachment, proliferation and ingrowth resulting in an osteoblastic phenotype support material. They demonstrated the incorporation of hydroxyapatite encourage the penetration of the cells, however the pore sizes of the polymeric material had no effect on the movement of the cells. Busby *et al.* (2001) demonstrated poly(epsilon-caprolactone) based polyHIPE foams exhibited hydrophilicity as they swelled in polar solvents highlighting their potential use in tissue engineering. Pulko and Krajnc (2012) pointed out high degree of control over the pore size using a variety of polymerisation mechanism resulted in many applications which include organic synthesis, separation, hydrogen storage, tissue culturing, catalysis, water purification and enzyme immobilization.

Cameron *et al.* (1996b) demonstrated HIPEs made from styrene/ divinylbenzene (STY/DVB) can be functionalised by bromination, sulfonation and nitration. STY/DVB polyHIPEs were modified via post polymerization by electrophilic aromatic substitution to yield bromo-, nitro-, and sulfonic acid substituted polyHIPE materials. However there was higher degree of functionalization on the surface than in the center due to the relatively low hydrophobicity of the electrophilic reagents as compared with the STY-DVB polymers. This problem was addressed by using reagents with higher hydrophobicity, such as lauroyl sulphate in cyclohexane which resulted in uniform functionalization throughout the polyHIPE polymer. Akay *et al.* (2010) exhibited the process for preparing functionalised nano-structured sulphonated polyHIPE polymer via intensified internal heating. The major advantage of this process is that it allows a high rate of functionalization of the polymer without the need for excessive washing or separation of residue, thereby making it economically viable. Another method of chemical functionalization reported was by the addition of VBC monomer, which introduces the benzyl chloride group in the polymer

structure. This method allows functionalization of the polyHIPEs via post polymerization with nucleophilic amines, such as morpholine and tris(2-aminoethyl)amine (Krajnc *et al.*, 2002). In a similar manner, Mercier *et al.* (2000) demonstrated preparation and post-functionalisation of polyHIPEs bearing pendant vinyl functionalities. The pendant vinyl groups can undergo both bromination and thiol addition via the batch and continuous flow methods, thus introducing routes to binding functional groups through a dimethylene spacer within the polymer network. Therefore, a wide range of functional polyHIPEs can be prepared via addition of thiols (Mercier *et al.*, 2001; Deleuze *et al.*, 2002). Deleuze *et al.* (2002) showed thiol added polyHIPEs can be used as support in organic synthesis.

Theato (2008) revealed monomer bearing an activated ester group can be polymerised via ATRP, Nitroxide mediated radical polymerisation (NMP), reversible addition-fragmentation chain transfer (RAFT) polymerization or Ring opening metathesis polymerisation (ROMP) techniques generating highly functionalised polymer with distinct architecture. Their study reported activated esters covalently links amines with carboxylic acids to yield amides, where the reaction is quantitative and under mild conditions such as stirring at room temperature usually proceeds without any side reactions. Similarly multifunctional well defined polymers and block copolymers were successfully synthesised using active ester monomer pentaflurophenylmethacrylate (PFMA) under RAFT polymerization (Eberhardt and Theato, 2005). However, Kircher *et al.* (2013) reported although pentafluorophenyl groups were reactive towards range of amines, the extent of functionalization was around 50% determined by elemental analysis. Access of the reagent to the reactive sites within the polymer is critical and in some cases sites are accessible when the polymer is swollen in suitable solvent. Kita *et al.* (2001) demonstrated polymer beads allowed to swell extensively in solvents with a wide range of polarities from dicholoromethane, tetrahydrofuran, and water to dimethylformamide also enable high functional loadings. They used hydrophilic polymer for solid phase synthesis where the degree of swelling was expressed either in volume or weight expansion. Gokmen and Du Prez (2012) pointed out high crosslinking densities limit the degree of swelling in porous polymers.

The surface charge in polymers becomes an important criterion in terms of its applicability in environmental and agricultural processes. Excess of adsorbed ions may make the polymer cationic or anionic in nature. Using acid or base monomers, results in positive or negative charge to the polymeric material. It may be also possible to induce surface charge by adding cationic or anionic surfactants during the preparation of polyHIPEs which can result in formation of charged polymer layer around the particles. PolyHIPEs with the ability to swell can be an important feature that determines their applicability in biological and agricultural processes. Burke *et al.* (2010) investigated the potential uses of hydrophilic micro structured polyHIPE in agricultural as soil additives. They demonstrated microwave sulphonated polyHIPEs exhibited water adsorption capacities of 10 fold and 18 fold with nominal pore sizes of 20 and 150 µm respectively. Their study concluded addition of hydrophilic polyHIPEs as soil additives results in enhancement of plant yield under water stress conditions. Akay *et al.* (2010) demonstrated that microwave sulphonation is basically an intensification of the thermal sulphonation treatment method. Their studies revealed that when polyHIPE polymer containing a functional material (in the dispersed phase) is subjected to microwave irradiation, a chemical reaction on the walls of the polymer or within the pores is started and rapidly propagated. This technique not only increases the overall efficiency of the sulphonation process but also decreases the time required for the process from few hours to few minutes. Cation exchange polyHIPEs have been used successfully in agriculture and separation processes (Akay *et al.*, 2005a; Akay, 2006; Akay *et al.*, 2010; Burke *et al.*, 2010; Marques and Fernandes, 2011; Akay and Burke, 2012; Akay *et al.*, 2012).

Thus recent research have focused on different strategies for polyHIPE functionalization determining its potential and efficiency in diverse applications. A range of different functional monomer such as vinyl benzene chloride (VBC), GMA, nitrophenyl acrylate (NPA) can be incorporated in polyHIPE which play an important role in applications like enzyme immobilization or water purification (Kimmins and Cameron, 2011). Due to its high value and performance, functional polyHIPEs can be tailored for their specific properties and therefore specialty applications.

2.7 Hypercrosslinking of PolyHIPEs

The hypercrosslinking reaction involves swelling the polymer in a good solvent such as dichloroethane (DCE) which causes the space formation between the monomers. It is followed by crosslinking the polymer using the Friedel-Crafts reaction, which results in connection of the neighbouring polymer chain. The swollen or the expanded state of the polymer is retained on hypercrosslinking even after removal of the solvent, thus enhancing its surface area and increasing its free volume (Veverka and Jerabek, 1999). The aim of these crosslinking reaction is to create micro pores, making the pores more rigid and stopping them from collapsing due to the crosslinking, thus forming smaller pores in the scaffold of the larger pores. A typical polyHIPE has a modest surface area between 2- 20 m^2/g although they may have high porosity. Jerabek *et al.* (2008) reported introduction of porogenic solvents into the continuous phase during the preparation of polyHIPE can yield material with surface area upto 720 m^2/g. However, for applications such as heterogeneous catalysis, chromatography and gas storage requires polymers with very high surface areas up to 2000 m^2/g. This can be achieved by hypercrosslinking aromatic monomers to form secondary pore structure having high microporous volume. During the last few decades, hypercrosslinked polymers have attracted considerable attention mainly due to their lightweight properties, permanent porosity, microporous network and high thermal stability along with high specific surface area (Xu *et al.*, 2013).

Davankov *et al.* (1973) carried out pioneering work on hypercrosslinked resins with high microporosity. Although hypercrosslinked polystyrene was the first hypercrosslinked polymeric material, many other polymer networks such as styrene-DVB copolymers, polyxylylene, polysulphone, polyarylates can form highly crosslinked network (Tsyurupa and Davankov, 2002). The key approach by Davankov *et al.* (1973) was to maintain the enhanced distance between the neighbouring chain units and to transfer this spatial distribution from the liquid to dry state. Ahn *et al.* (2006) investigated the synthesis parameters such as vinylbenzene chloride monomers, catalyst, and solvent on the pore properties of the resulting polymeric network. They observed ferric chloride ($FeCl_3$) was the most effective catalyst as compared to aluminum chloride ($AlCl_3$) and stannic

chloride ($SnCl_4$). Aluminum chloride and stannic chloride both had poorer solubility as compared to $FeCl_3$ and hence they concluded that ferric chloride catalyst was more effective due to its solubility and molecular size. Their work demonstrated that in gel type 2 mol% DVB-VBC porous precursors, showed extensive microporosity within only 15 minutes of initiating the cross linking reaction yielding a surface area of approximately 1200 m^2/g which enhanced steadily in 18 hours to approximately 2000 m^2/g. These hypercrosslinked polymers with small pore size have potential application in gas adsorption and separation processes. Figure 2-8 illustrates schematic representation of the hypercrosslinking process.

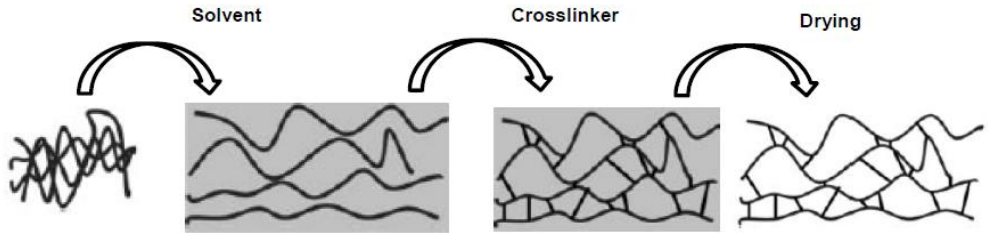

Figure 2-18 Schematic representation of hypercrosslinking process (Germain *et al.*, 2007)

Hypercrosslinked polymers were initially obtained by an extensive post crosslinking of vinylbenzyl chloride and divinylbenzene (VBC-DVB) using internal electrophile as a crosslinking mechanism created by Friedel-Crafts catalyst. Using the Davankov's approach, Schwab *et al.* (2009) demonstrated synthesis of polyHIPE with bimodal pore size distribution and very high surface areas up to 1210 m^2/g. Their research also showed VBC based hypercrosslinked polyHIPE promoted heat and material transport through the microporous pore system thus illustrating efficient use in diffusion controlled processes such as gas purification and separation. Germain *et al.* (2007) exhibited method for the preparation of hypercrosslinked polyaniline which showed remarkably high affinity for hydrogen adsorption. Their research indicated enthalpies of hydrogen adsorption on hypercrosslinked polyaniline was as high as 9.3 kJ/mol in contrast with hypercrosslinked polystyrenes for which significantly lower enthalpies of about 4-7 kJ/mol were measured.

Recently, a new approach to prepare hypercrosslinked monoliths with functional group has been developed (Maya and Svec, 2013). Their work demonstrated addition of acetoxystyrene to styrene based monolith preparation, leads to polymeric materials containing reactive phenolic hydroxyl functionalities and enhanced surface area. These polymers having specific application in liquid chromatography, the addition of acetoxstyrene modulates the hydrophobicity of the stationary phase for reverse phase liquid chromatography, whereas introduction of the phenolic groups made the columns suitable for separating small molecules under normal phase conditions. This may eventually lead to formation of new types of stationary phases for liquid chromatography.

2.8 PolyHIPE Science: Applications

Currently, polyHIPE is one of the most rapidly expanding areas of polymer science. Due to their controlled morphologies and chemistry of the materials, polyHIPEs have found applications in a wide range of areas. Barby and Haq (1985) prepared porous polymers with styrene-DVB through a high internal phase emulsion polymerisation route and created the trade name polyHIPE. They demonstrated polyHIPE can be dried and refilled with selected liquids and can act as an excellent adsorbent.

2.8.1 PolyHIPEs for tissue engineering

The hierarchical structure and tuneable porosities suggests application of these polymeric foams as matrices for cell growth. Hayman *et al.* (2005) compared the cell growth on 2D and 3D polyHIPE scaffolds prepared from STY-DVB based polyHIPEs. They reported addition of tetrahydrofuran to the aqueous phase resulted in polyHIPE foam with enlarged in the range of 50-100 µm. These scaffolds provided an enhanced surface area supporting the growth and differentiation of the cells. The growth on the 2D scaffolds promoted stability of the cells whereas 3D scaffolds enhanced the differentiation where cells formed complex network suitable for neural cell culturing. Results from their research suggest 3D cell culturing can play an important role on cell functional activity and have potential therapeutic applications. Moglia *et al.* (2011) demonstrated synthesis of fully biodegradable polyHIPEs without a toxic diluent that could cure

at physiological temperatures. They reported HIPE stability could be modulated by changing the surfactant concentration to achieve range of pore sizes and open pore network. These rigid, high porosity polyHIPEs showed potential application as an injectable, tissue engineered bone graft. Biodegradable scaffolds are desirable as the need for follow-on surgery and complications to remove the scaffold can be eliminated. Akay *et al.* (2004) developed micro porous polyHIPE as a three-dimensional support matrix for in vitro tissue engineering applications. The authors reported polyHIPE modified with hydroxyapatite showed a significant increase in osteoblast numbers penetrating into the polymer discussed in the earlier section 2.7.

2.8.2 PolyHIPEs for enzyme immobilization

Akay *et al.* (2005b) states that bio intensification can be explained with the development of novel micro porous polyHIPEs which produces dramatic process improvements related to the diffusion path for the reactants and products, and environment to intensify bio-chemical reactions. Akay *et al.* (2005a) mentions bio intensification can be achieved through the reduction of diffusion path for the reactants and products via creation of suitable environment for the bio catalysts and microorganisms which can enhance selectivity, consequently resulting in phenomenon based intensification. Moreover, 3- dimensional architecture of the cell support and its distribution is also important in cell viability and cell function. Akay and collaborators addressed this issue by designing micro cellular polymers of controlled and uniform micro architecture to immobilize bacteria, employing a novel seeding method (Akay *et al.*, 2002a; Akay and Vickers, 2003). Bio intensification was demonstrated by phenol degradation studies using immobilized *Pseudomonas syringae* on micro porous polyHIPE (Erhan *et al.*, 2004). Immobilization of the cells is one of the techniques to increase the productivity of bioreactors. Their study involved continuous micro-bioreactor experiments where bacteria were immobilized on polyHIPE beads and degradation was carried out in a packed bed. Their study revealed immobilized cell systems permit the operation of bioreactors at flow rates that are independent of the growth rate of the microorganism employed. Thus, polyHIPE as micro

reactor exhibit low resistance to flow making them beneficial for low pressure and continuous flow applications.

The two main techniques used to immobilize enzymes are adsorption and covalent attachment. Dizge *et al.* (2008) study showed a lipase from *Thermomyces Lanuginosus* was covalently immobilised onto polyglutaraldehyde (PGA) grafted styrene-DVB based polyHIPE polymer. In their work, PGA attached lipase maintained 100% of the initial activity after the support was reused 15 times and on storing for 30 days in acetate buffer, whereas lipase adsorbed on polyHIPE without PGA grafting showed complete loss of enzyme activity after reusing the support only 5 times. Therefore, immobilizing the enzymes on solid support ensures their reusability. Fernandez-Lafuente *et al.* (1998) reported that the hydrophobicity of the polymeric material has a desirable impact on the activity of the enzymes. They reported that the hydrophobic area around the active site of the open structure of lipase is very strongly adsorbed on octyl agarose solid support. Octyl Agarose is used in protein chromatography and hydrophobic interaction. Both the activity of the lipases and enantioselectivity was improved using the hydrophobic supports. For the production of biodiesel from sunflower, canola, soyabean and waste cooking oils, glutaraldehyde immobilized lipase onto microporous polyHIPEs was found to be an effective catalyst (Dizge *et al.*, 2009a; Dizge *et al.*, 2009b).

2.8.3 PolyHIPEs for catalyst support

Lucchesi *et al.* (2008) demonstrated incorporation of azlactone groups in polyHIPEs synthesized by direct co-polymerization of DVB and N-(p-vinylbenzyl)-4, 4-dimethylazlactone (VBM). The resultant polyHIPEs showed capability of amine scavengers in batch and flow-through processes. These azlactone functionalized polyHIPEs showed scavenging efficiency was better in batch flow as compared to that in flow through process. Mercier *et al.* (2002) reported synthesis of polyHIPEs with styrene, DVB and 4-Ethyl-(2-dibutylchlorostannyl) styrene to produce polymer supporting organotin chloride catalyst. The polyHIPEs incorporated with organotin chloride functioned as a catalyst exhibiting good stability and activity for the reduction of 1-bromoadamantane and the radical cyclisation of 1-Bromo-2-(prop-2-enyloxy) benzene. Schoo *et al.* (1992) produced VBC based polyHIPEs with 90% pore volume which were used for the

immobilization of Flavin catalyst. The highly porous crosslinked polyHIPE matrix proved to be an ideal support resulting in an optimum activity of the catalyst.

2.8.4 PolyHIPEs for Agro-process applications

In another study, polyHIPE polymers were used as soil additives where they function as biomicroreactor and associate with the plant roots, resulting in biomass and crop enhancement (Burke *et al.*, 2010; Akay and Fleming, 2012). Akay and Fleming (2012) reported polyHIPE promotes the interaction between water, nutrients and bacteria at the plant roots at a microscopic scale acting as a synthetic rhizosphere which benefitted the plant in three ways. Firstly, efficient water utilization and conservation by the plant roots (supplemented with hydrophilic polyHIPEs) allows the plants to grow in dry environments. Secondly, enriching the soil with polyHIPEs containing fertilizers (ammonium sulphate) aids in releasing the fertilizer in close proximity to the plant roots, hence larger proportion is utilized by the plant rather than being leached away. Lastly, by modifying the polyHIPEs with beneficial bacteria in particular nitrogen fixing bacteria offers a protective environment for the organisms within the soil, thus enabling them to make a significant contribution to the nutrient requirements of the plants. This technique termed as Agro-process intensification utilized sulphonated, hydrophilic micro porous polyHIPEs. Hydrophobic STY-DVB polyHIPEs were converted into hydrophilic forms via microwave sulphonation. Presence of atrazine in soil or drinking water can be toxic and cause contamination which is detrimental for regions having high agricultural activities. Pulko *et al.* (2007) study of piperazine derivatized polyHIPEs proved effective in removal of atrazine from aqueous solutions with very low concentrations. They incorporated 4-nitrophenylacrylate during polyHIPE synthesis and the resulting piperazine functionalized material covalently bonds with atrazine assisting its removal. Researchers at Unilever, revealed effective removal of Polio type I virus from contaminated water supply using aminated, sulphonated and betainated styrene-DVB polyHIPEs (Bellamy *et al.*, 2008). Their work reported 99.99% reduction in polio virus from contaminated water supply.

Therefore, polyHIPEs due to its tailored morphology and well defined architecture has attracted much attention resulting in its diverse application in

many areas of advanced material science such as catalyst (Ottens *et al.*, 2000; Mercier *et al.*, 2002), tissue engineering (Akay *et al.*, 2004; Bokhari *et al.*, 2005), separation processes (Bhumgara, 1995), agro process intensification (Akay and Burke, 2010; Burke *et al.*, 2010; Akay and Burke, 2012; Akay and Fleming, 2012), energy and environmental process intensification (Akay and Jordan, 2011; Dogru and Akay, 2011), water purification (Pulko *et al.*, 2007), immobilization of enzymes (Pierre *et al.*, 2006; Kimmins *et al.*, 2014), organic synthesis (Kovacic and Krajnc, 2009).

2.9 Introduction: Polymers in Agriculture

The greatest challenge to agriculture is water scarcity and the demand to feed the rapid growing global population has put immense pressure of the freshwater resources (Wallace, 2000). Though freshwater is renewable, it is finite. According to Shiklomanov (1991) irrigated agriculture consumes around three quarters of the annual renewable fresh water resources used by human population. Hence improving the efficiency of irrigation may prove beneficial to look for possible ways to mitigate water consumption in agriculture. McCornick *et al.* (2013) reports by 2050 the agriculture and food security to feed the global population will have a profound effect on water resources. Water scarcity in agriculture will have overall impact on soil fertility, seed germination, plant growth and plant nutrition. Due to this water resource crisis, sustainable agricultural production is of great importance for global food security and development of human societies. Hence finding modes of water management will prove beneficial for sustainable use of water resources in agriculture. One such possible means is to alter the water retention capacity of the soils. This can be achieved by amending the soils with super absorbent / hydrophilic polymers.

Hydrophilic polymers can provide an alternative water saving measures in agriculture by increasing the water retention property of the soils. Andry *et al.* (2009) conducted experiments to study the effects of hydrophilic polymers on the water holding capacity and saturated hydraulic conductivity of a sandy soil at varying soil temperature and water quality. Their results highlighted that applying irrigation in the early morning could help save more water on a sandy soil treated

with hydrophilic polymer by reducing percolation loss. Mixing hydrophilic polymers with the soil helps in building an additional water reservoir for the plant-soil system. Yu *et al.* (2011) demonstrated that the amount of water absorbed by the superabsorbent polymers increased with the increasing polymer cation exchange capacity. Their study exhibited, with increase in soil clay content, water absorbance by the superabsorbent polymers decreased. They observed a continuous increase in the quantity of water absorbed to a steady state level during the first 50 to 60 minutes of wetting with mixing the superabsorbent polymers having large grains (3-4mm) with the soil. Amount of water absorbed also depended on the type of superabsorbent polymers and the soil texture. Their studies indicated that the mechanisms controlling the amount of water absorbed during the wetting procedure might depend on an interaction between the soil and super absorbent polymer that develops during the wetting process. They suggested that the low amount of water adsorbed by the super absorbent polymers with small grains (0.2 – 1.5mm) was probably related to a gradual change in the composition of the exchangeable cations in the super absorbent polymers during the water absorption process. Islam *et al.* (2011) showed that plant growth and different physiological activities are restricted by drought stress. Their results suggested that application of super absorbent polymers could retain the soil water thus making it available to plants when it is under severe water stress. Their studies reported that the growth and water use efficiency of corn treated with super absorbent polymers under deficit conditions favored different physiological activities like net photosynthesis and transpiration rate. Hence under deficit irrigation, corn plants showed enhanced drought tolerance, and their superior growth was attributed to high relative water content in leaves thus effecting the photosynthesis and transpiration rate. This resulted in increasing the survivability of corn plant under drought condition.

More recent Li *et al.* (2014) studies investigated the effect of superabsorbent polymers on soil's physical properties and microbial activity. They found that the addition of super absorbent polymers helped the formation of macro soil aggregated with particle size greater than 0.25mm and soil bacterial abundance under winter wheat cultivation. These polymers also significantly increased the soil water content and soil maximum hygroscopic moisture. Hygroscopic water is on the surface of the soil grains and does not move by the

action of gravity or capillary forces. However, these polymers had no effects on the soil available water holding capacity. The results from their studies indicated that the application of super absorbent polymers assist in the control of water loss and improved the soil physical properties.

Most of the studies are carried out with hydrophilic polymers and their capacity to hold water, thus reducing soil water loss. These hydrophilic polymers are mainly hydrogels. However, one of the major drawbacks using hydrogels is lack of mechanical strength and can be hard to handle or transport. The main benefit of using hydrophilic polymers in agriculture is their properties can be tailored to meet specific needs. To understand the application and potential of hydrophilic polymers in agriculture, we need a better understanding of soil characteristics and its effects on the hydrophilic polymers. The following section describes some of the soil characteristics which will help in understanding the usage and limitations of hydrophilic polymers in agriculture.

2.10 Soil Characteristics

2.10.1 Soil Physical Properties

The physical properties of the soil have direct influence on the productivity of the soil and the level of biological activity sustained within the soil. It plays a major role in determining the soil water retention and air supply capacity to plants. The key aspects that contribute to the soil physical characteristics are its texture, structure, bulk density and porosity

2.10.2 Soil Texture

The texture of the soil is determined by the mineral matter from its parent rock and organic matter from its living organism (Troeh and Thompson, 2005). Hence soil texture refers to the percentage of sand, silt and clay particles found in the soil. These particles differ amongst each other in terms of their size. Sand particles range from 0.05 – 0.2 mm, whereas particles that fall between 0.002 – 0.05 mm are considered silt. Clay form the smallest particles and are less than 0.002 mm in size (Weil, 2016). These three materials constitute the solid portion of soil and determines the amount of pores and the pore size distribution (Brady and Weil, 2008). These pore spaces in between the grains have a large influence

on the water holding capacity, drainage and aeration of the soil in variable proportions. Soil texture and its textural class can be determined by various ways. The following Figure 2-19 shows the soil textural triangle which can help in determining the soil textural class, if the percentage of soil particles is known.

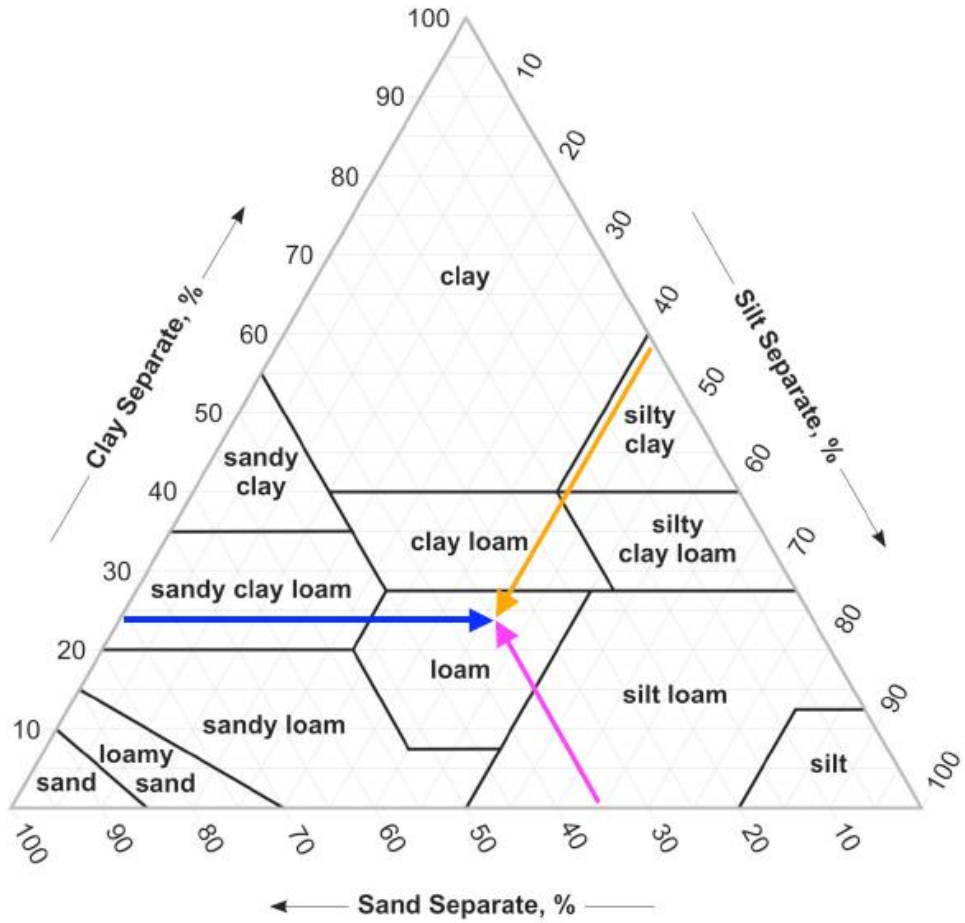

Figure 2-19 Soil textural triangle with each side corresponding to a percentage of soil particles. [Adapted from: Brady and Weil (2008)]

Thus, soil texture influences the amount of air and water it holds and the rate at which the water can enter and move through the soil. Sandy soils have large pores so that infiltration rates and permeabilities to water are high, and they retain little water. In contrast, clays have low infiltration rates, low permeability, retain much water in available as well as in unavailable forms, and may be poorly drained. Soils of intermediate textures such as loams are intermediate in porosity, water retention, and drainage.

2.10.3 Soil bulk density and total porosity

Soil bulk density is defined as the mass of a unit volume of dry soil (Brady and Weil, 2008). It is an indicator of soil compaction and soil health and affects available water capacity, soil porosity and plant nutrient availability. Since subsurface layers in soil are more compacted and have less root penetration as compared to the surface layers, bulk density usually increases with soil depth. According to Batey (2009), an increase in soil bulk density is a major threat to the agriculture and environmental productivity of soils as its adverse effects are linked to depletion of air , water and nutrients to the roots. Bulk density is dependent on soil organic matter, soil texture, and the density of soil mineral (sand, silt and clay). Agricultural practices involving soil tillage also affects its bulk density. The packing arrangement of the soil minerals plays an integral part on the bulk density. In general, well aggregated, porous soils which are rich in organic matter content have lower bulk density. Sandy soils have relatively high bulk density since total pore space in sand is less than silt or clay soils.

The soil total porosity is a function of the total volume of the soil and the volume of pore spaces. Since the soil fluid movement occurs in the pore, their size distribution is of major importance in defining the soil characteristics and in prediction of soil hydraulic properties (Nimmo, 2004). Coarse textured soils have higher average size of individual pores than fine-textured soils, although the first one tend to be less porous than the second one (Brady and Weil, 2008).

2.10.4 Soil moisture and water characteristics

Some of the factors that influence the extent of moisture in the soil are the type of soil, soil depth and the amount of organic matter in the soil. The process where the rain or the irrigation water seeps into the soil is referred to as infiltration. Permeability is the physical capacity of the soil to allow water to move readily through its profile, whereas the capacity to store the assimilated moisture in the rooting zone for plants is referred to as water holding capacity (Troeh and Thompson, 2005). The water holding capacity of a soil depends on the pore size and its distribution. Interconnection and continuity of pores of varied sizes at the soil surface will maximize infiltration and reduce water drainage, thus increasing

the available soil water. Thus the number, size and connectivity of pore spaces have a crucial role in determining the amount of water that a soil can absorb, hold and supply to the root zone (Brady and Weil, 2008).

According to Chesworth (2008) much of the water freely drains from the soil under the influence of gravity after the source of water ceases, provided the drainage of the water is not restricted by compacted or impermeable layers. Rapid drainage occurs in coarse textured soils, whereas fine textured soils drain gradually. Hence clayey soils can hold more water than for instance sandy soils. Hamblin (1985) studies demonstrated that pore sizes from 0.0002 to 0.05mm diameter retain water that can be absorbed by the crops and are referred to as storage pores. Smaller pores where termed as residual pores which hold water too tightly for plants to able to extract. Transmission pores were characterized as pores larger than 0.05 mm diameter which allowed water to drain through the soil and permitted air to enter the pores as the water drains out. Table 2-3 shows the functions of the pores of different size ranges.

Table 2-3 Functions and sizes of soil pores (Hamblin, 1985)

Pores Size (mm diameter)	Description of pores	Function of pores
<0.0002	Residual	Retain water that plant cannot use
0.002-0.05	Storage	Retain water that plants can use
>0.05	Transmission	Allow water to drain out and air to enter
>0.1-0.3	Rooting	Allow plant roots to penetrate freely
0.5-3.5	Worm Holes	Allow water to drain out and air to enter
2-50	Ant nests and channels	Allow water to drain out and air to enter

During rainfall or irrigation applications, when the soil pores are completely filled with water, there is no air left in the soil. The soil water content at this stage where no air is present in the soil, is called saturation point. At saturation, the plant may suffer because it needs both air and water in the soil. When the rain or irrigation has stopped, water from the larger pores in the soil will move downwards. This process is called drainage. When the free drainage has ceased, the soil water content of the wetted soil is termed as the field capacity. Thus value of field capacity assumes that the water removed from the soils is only removed by gravity, not through plants or evaporation. Field capacity is not the same as saturation. Hence when the soil is at field capacity, the pores in between the soil particles contain both air and water. Field capacity is considered the upper limit of a soils capacity to store water for plant use (Troeh, 1993). On the other hand, when the water stored in the soil is used by the plant roots or evaporated into the atmosphere, the soil gradually dries out if no additional water is supplied to the soil. The remaining water in the soil is trapped in smaller pores and is difficult for the plant roots to extract this tightly held water. This stage is called permanent wilting point which occurs when the volumetric water content is very low for the plant to remove water from the soil. The plant wilts and fails to recover even after rewetting the soil. Hence the lower limit of available water is at permanent wilting point. However, soil at permanent wilting point is not completely dry. When the water content of the soil is below the permanent wilting point, water is still present in the soil, but it may be held too tightly in smaller pores and does not readily flow making it inaccessible to plant roots (Troeh and Thompson, 2005).

Available soil water is the amount of water that can be absorbed by the plant roots and is called the total available water capacity. The water content above field capacity cannot be held against the forces of gravity and will drain whereas, on the other hand water content below the wilting point cannot be extracted by the plant roots. Hence the total available water is the difference between water content at field capacity and permanent wilting point. In general, soil types with greater total available water content are more favorable to high biomass productivity due to the main reason that they can supply adequate moisture to plants during times of water scarcity or no rainfall. Williams *et al.* (1983) demonstrated available soil water of 244 soil samples of well-structured

soil was one third to twice as large as that in compared to poorly structured or degraded soils.

2.10.5 Soil hydraulic conductivity

The rate at which water can pass through the soil profile is known as its hydraulic conductivity. Hydraulic conductivity depends on the soil structure and on number, size and continuity of pores. High values of hydraulic conductivity indicate that the soil is permeable through which water can pass easily; low values indicate less permeable soil profile. In saturated soils, the hydraulic conductivity is represented as K_{sat} whereas in unsaturated soil it is represented as K. The hydraulic conductivity is described by Darcy's law, which for one-dimensional vertical flow can be represented as seen in Equation 2-4 (Brown, 2002).

Equation 2-4

$$\boldsymbol{Q = -K\frac{dh}{dz}}$$

Where, *Q* is Darcy's velocity (m/s) or the average velocity of the fluid through a geometric cross-sectional area within the soil, *h* is the hydraulic head (m), and *z* is the vertical distance (m) in the soil. The term dh/dz is called the hydraulic gradient and is a measure of how rapidly the potential changes with distance. The coefficient of proportionality, *K,* as seen in Equation 2-4 is called the hydraulic conductivity (m/s). Therefore, from the above Equation 2-4, hydraulic conductivity can be defined as the ratio of Darcy's velocity to the applied hydraulic gradient.

In laboratories, the constant-head method is commonly used for determining the saturated hydraulic conductivity of coarse-grained soils. In constant-head method, hydraulic conductivity of saturated soils is measured by applying Darcy's equation to a saturated soil column of uniform cross- sectional area. In this method, water is moved through the soil under a constant head condition. A cylindrical soil sample of cross-sectional area *A* and length *L* is

placed between two porous plates. $H_2 - H_1$ is the hydraulic head difference across the sample of length *L*. By measuring the volume *V*, of water that flows through the sample of cross-sectional area *A* for time *t*, the saturated hydraulic conductivity *K* of the soil can be determined by the following Equation 2-5

Equation 2-5

$$\mathrm{K} = \frac{\boldsymbol{VL}}{[\boldsymbol{At}(\boldsymbol{H_2} - \boldsymbol{H_1})]}$$

Similarly to evaluate the hydraulic conductivity of fine-grained soils in the laboratory, falling head test is primarily used. In the falling head test method, a cylindrical soil sample of cross-sectional area *A* and length *L* is placed between the porous plates. The soil sample is first saturated under a specific head condition. The sample column is connected to a standpipe of cross-sectional area *a*, which provides the water head and also allows measuring the volume of water passing through the sample. The water is allowed to flow through the soil without maintaining a constant pressure head. Thus, by measuring the change in the head in the standpipe from H_2 to H_1 during a specified interval of time *t*, the saturated hydraulic conductivity can be determined by Equation 2-6 (Klute and Dirksen, 1986).

Equation 2-6

$$\boldsymbol{K} = \left(\frac{\boldsymbol{aL}}{\boldsymbol{At}}\right) \boldsymbol{ln}\left(\frac{\boldsymbol{H_1}}{\boldsymbol{H_2}}\right)$$

Constant-head test is a direct measure of permeability using Darcy's law, whereas falling-head test is an indirect measurement of permeability using time of flow.

2.10.6 Hydraulic conductivity and hydrophilic polymers

In agriculture, hydrophilic polymers are not only used to enhance the water uptake in plants but they also provide with nutritional benefits (Andry *et al.*, 2009). Due to their high porosity and interconnectivity, these polymers facilitates the transport of water and nutrients through the soil. Hydrophilic polymers have potential of altering the hydraulic conductivity of soil due to their capability of swelling and retaining water up to 500 times of their weight (Kazanskii and Dubrovskii, 1992). Several studies have reported that the use of hydrophilic polymers increases the amount of available moisture in the root zone, thus allowing longer intervals between irrigations (Flannery and Busscher, 1982; Johnson, 1984; Abedi-Koupai and Asadkazemi, 2006)

Bhardwaj *et al.* (2007) demonstrated that the water retention and hydraulic conductivity of sandy soils mixed with water absorbing polymers were found to be affected by both electrolyte concentration in the water and polymer properties. Tap water (presence of electrolytes) and distilled water (absence of electrolytes in the water) was used to evaluate the effect of water retention and hydraulic conductivity on super absorbent polymers. They observed that, when percolated with tap water, the hydraulic conductivity of the sandy soil mixed with polymers initially decreased. This was attributed to the fact that in the presence of electrolytes in the solution (i.e tap water), superabsorbent tend to absorb less water and thus exhibit lesser swelling than in distilled water. However as the polymer content was increased the hydraulic conductivity increased. The more pronounced swelling of the polymer with distilled water exhibited the following two effects. Firstly, greater swelling increased the pore space between the sand particles thus increasing the volume of the mixture. Secondly, narrowing or blocking the water conducting pores by the swollen polymer, decreases the hydraulic conductivity of the mixture. The greater reduction in the hydraulic conductivity in the polymers used was attributed to their smaller average granule size and higher relative swelling capacity. Similarly Huttermann *et al.* (2009) studies illustrated that the effectiveness of adding polymers to soil depends on the soil and super absorbent polymer properties and the soil solution concentration and composition. Their studies concluded that differences in the

chemical composition of the soil and the liquid interact with hierarchical polymer morphology to produce different rates of water absorption.

Many studies indicate that the addition of hydrophilic polymers alters the physical properties of the soil, thus affecting its hydraulic conductivity. Hence, the objective of this study was to examine the effect of polyHIPEs on hydraulic conductivity of soils when applied in varying concentration affecting water absorption.

2.10.7 Soil Chemical Properties

Chemical properties of the soil are the driving factor in determining the nutrient availability within the soil supplied to the plants and the microbes. Different chemical reaction not only affects the soil quality but also affects its fertility. The following section indicates few factors responsible for the soil chemical properties and productivity.

2.10.7.1 Soil Organic Matter (SOM)

Soil organic matter is the most important and most misunderstood indicator of soil quality. Soil organic matter is that fraction of the soil that consists of plant and animal residues, microorganisms at various stages of decomposition (Troeh, 1993). It serves as a reservoir of nutrients and water in the soil, helps in reducing soil compaction and surface crusting and increases water infiltration. Most of the productive agricultural soils have between 3 and 6% organic matter (Hudson, 1994). Lal (2001) reported organic matter improves soil aggregates, which in turn improves the soil structure and porosity. Soil organic components together with the microorganisms (especially fungi) help in binding small soil particles into larger aggregates. This aids in infiltration of the water through the soil increasing the soils ability to take up and hold water. Soil aggregation also offers resistance to erosion and crusting. Plants are benefitted by the water holding capacity of organic matter as it will release most of the water that it absorbs. In contrast, clay holds greater quantity of water, but much of it is not available to the plant root zone. Another important aspect stated by Hudson

(1994), increasing the soil organic matter can reduce erosion because of increased water infiltration and stable soil aggregates formation caused by organic matter.

2.10.7.2 Soil reaction (pH)

Soil pH is an indication of acidity or alkalinity of a soil and is also known as soil reaction. Soil reaction is a vital indicator of ion solubility, which in turn affects microbial and plant growth. Soil pH is the measure of active hydrogen ion (H+) concentration, as the amount of hydrogen ions in the soil increases the soil pH decreases, becoming more acidic. According to Brady and Weil (2008), all soils fall in the pH range of very strongly acidic (pH3) to strongly basic (pH9) with rare extremes as low as 2 or as high as 11. A pH range of 6 to 7 stimulates the most ready availability of plant nutrients. Agronomists generally use soil pH as measured in a 2:1 water to soil mixture as an index of the soil's acidity or alkalinity. Shahid *et al.* (2012b) demonstrated that the application of superabsorbent hydrogel nanocomposite alters the soil pH. Soil pH was reduced whereas electrical conductivity was increased with the application of superabsorbent hydrogel nanocomposite material which was used to evaluate the moisture retention properties of sandy loam soil. They linked this effect to the chemical structure of the super absorbent polymers and the characteristics of the soil. Similarly, Bai *et al.* (2010) reported that with the addition of super absorbent polymers, there are many H^+ ions in their hydrogels which can exchange with the H^+, Ca^{2+}, Mg^{2+}, Fe^{2+} and Al^{3+} ions present in the soil and soil colloids which effects the soil pH and electrical conductivity.

Smith *et al.* (1995) points out that climatic conditions play a major role in altering the soil reaction conditions. High precipitation causes the soils to be acidic, which is due to extensive loss of cations such as Ca^{2+}, K^+, Na^+, and Mg^{2+} and accumulation of acidic cations in the soil surface H^+, Al^{3+}. Also carbon dioxide from decomposing organic matter and root respiration may dissolve in soil water to form a weak organic acid resulting in acidic soils. On the other hand, evapo-transpiration exceeding the amount of precipitation can lead to accumulation of salts in the soil thus building up its pH. Troeh and Thompson (2005) mentions that the extreme acidity or alkalinity of the soil can be detrimental affecting the overall physical and chemical properties of the soil. Bacteria that decompose soil

organic matter are hindered in acidic soils. This result in accumulation of organic matter, affecting the activity of beneficial micro-organism and hindering the supply of essential nutrients required for plant growth.

2.10.7.3 Cation exchanging capacity (CEC)

Cation exchange capacity is an inherent soil characteristics to adsorb and exchange cations (Brady and Weil, 2008). Negatively charged clay and organic matter particles in the soil help retain these positively charges ions through electrostatic forces. Since soil does not have any electric charge, the negatively charge clay particles are balanced by the cations in the soil. Therefore the cations are exchangeable and give the indication of the type of clay minerals present in the soil and its capacity to retain nutrients against leaching (Foth and Ellis, 1997). Many clay minerals found in soils have the ability develop a net negative charge which is satisfied through the electrostatic adsorption of cations. In general, high clay and organic matter present in the soil, high is the CEC. Without cation exchange capacity essential nutrient cations such as potassium and calcium would have to be continually supplied as inorganic fertilizers throughout the plant growing season. Cations are adsorbed as essential minerals by the plants, hence CEC is crucial to maintain the soil fertility (Poritchett and Fisher, 1987). Although cations held on the exchangeable sites are easily available for the plants, they do not represent the soils ability to provide the cations (Binkley *et al.*, 1992). Cations removed from the exchange site are often replenished from sources such as organic matter decomposition and mineral weathering, however the true availability of cations is difficult to assess. Yu *et al.* (2011) demonstrated that the amount of water absorbed by the superabsorbent polymers increased with increasing polymer CEC. The authors reported that the ions in the polymer chain attract water molecules.

Buchholz and Graham (1998) states that the ability to absorb water and swell by the hydrophilic polymer network depends on the concentration of ions within the polymer structure, charge repulsion and the amount of cross linkage between the chains. Therefore, the relative concentrations of the cations in the soil help determine the degree of absorption of water. Orikiriza *et al.* (2009a) reported that the CEC of the polymer can alter the ion composition of the soil water. Their studies concluded that the effect of additional cation exchange

system (hydrophilic polymer) that enters the soil resulted in efficient water uptake and increased the biomass of the of the tree species. Therefore, it is essential to study the soil amended with hydrophilic polymers exhibiting good ion exchange capacity and its effect on soil chemical properties.

Chapter 3 Materials and Methods

This chapter details the preparation and characterization of polyHIPE polymers. The methodology for preparation of the polyHIPE polymers with different monomers is described. The polyHIPE samples washing treatment is then explained. Synthesis of hypercrosslinked polyHIPEs is detailed. Sample morphology and structure are characterized using Scanning electron microscopy (SEM), Surface area analysis, Fourier Transform Infrared Spectroscopy (FTIR) and Thermal analysis. Section 3.5 describes the pressure plate extractor methodology used to determine the water retention characteristics of polyHIPEs in sandy loam and clay loam soils. Finally, biocompatibility testing of the polyHIPE is described with the inoculation of *Shewanella Oneidensis* Mr-1 with formation of catalytic biofilms.

3.1 Materials

Styrene (STY) (99% CAS No:100-42-5), divinyl benzene (DVB 80% CAS no: 1321-74-0), vinylbenzyl chloride (VBC CAS No: 30030-25-2), potassium persulphate ($K_2S_2O_8$ CAS No: 7727-21-1), Isopropanol (99.7% CAS No: 67-63-0), ethanol (95% CAS No: 64-17-5), 2-chloroethylbenzene (CEB CAS No: 622-24-2), chlorobenzene (CB CAS No: 108-90-7), ferric chloride ($FeCl_3$ CAS No: 7705-08-0), sorbitan monooleate (Span 80 CAS No: 1338-43-8), 1,2-dichloroethane (DCE CAS No: 107-06-2), p- xylene dichloride (XDC CAS No: 623-25-6), sulphuric acid (H_2SO_4 99.9% CAS No:7664-93-9), methanol (99.8% CAS No: 67-56-1) and acetone (99.9% CAS No: 67-64-1) were purchased from Sigma Aldrich Chemicals, UK. All the chemicals were of analytical grade, unless stated otherwise. Deionized water from the laboratory generator (conductivity of 0.055 microsiemens at 25^0C) was used for the preparation of the aqueous phase of the polyHIPE samples and during its purification. All chemicals were used as received without further purification.

3.2 Methodology:

3.2.1 Preparation of HIPE

Different types of HIPEs were prepared by mixing the aqueous and the oil phase in a stainless steel jacketed reaction vessel. The composition of both the phases were determined according to the desired type of polyHIPEs, is given in Table 3-1. The oil and the aqueous phase composition in HIPE1 was used as per Akay *et al.* (2005b). Polymers obtained from polymerization of HIPE1 was used to compare the structure and morphology against polyHIPEs obtained from various HIPEs. HIPE2 was used to prepare sulphonated polyHIPEs. The aqueous phase contains 5% sulphuric acid (Çalkan, 2007). The polymers from HIPE2 were sulphonated and used for agricultural application Sulphonation via microwave irradiation was used in this study. HIPE3 was used to prepare polyHIPEs with porogens. The method used in this study was compared to Barbetta *et al.* (2000). The composition and the volume of the oil and the aqueous phase was determined according to the desired application in this study. Cameron and Barbetta (2000) studies found that the addition of porogen reduces the physical strength of the polyHIPEs. Hence in this study we decided to investigate the influence of porogens with the current composition of HIPE3, on the morphology of the resultant polyHIPE polymers. HIPE4 was used to prepare hypercrosslinked polyHIPEs and its composition was tried for the first time. The major change was the addition of ferric chloride to the aqueous phase which was carried out to verify the distribution of catalyst particles throughout the polyHIPE samples. However, this requires that the catalyst precursor to be incorporated into the polyHIPE samples which acts as Friedel-Crafts catalyst. In order to obtain various types of polyHIPE materials, the composition of the HIPE and coding is shown in Table 3-1.

The basic styrene divinyl benzene polyHIPE was coded as STY-DVB PHP, whereas the sulphonated samples were coded as SPHPA. The hypercrosslinked samples were coded as HXI-PHP and HX2-PHP due to the addition of $FeCl_3$ in the aqueous phase of the later HIPE. The process for preparation of HIPE4 is mentioned here, whereas the same procedure was repeated while preparing each HIPE. The dispersed aqueous phase in HIPE4

consisting of the initiator potassium persulphate and ferric chloride is mixed in a beaker on a magnetic stirrer till it is completely dissolved in the distilled water. The oil phase composition of VBC, DVB, CEB, CB and emulsifier span 80 was placed in the stainless steel jacketed reaction vessel as shown in Figure 3-1(b).

Table 3-1 Composition of HIPE's

PHP coding system	PHP	Oil Phase		Aqueous Phase	
		Content	% (v/v)	Content	% (w/v)
STY-DVB PHP	HIPE1	Styrene	76	Potassium persulphate	1
		DVB	10		
		Span 80	14		
SPHPA	HIPE2	Styrene	76	Sulphuric acid	5
		DVB	10		
		Span 80	14	Potassium persulphate	1
HX1-PHP	HIPE3	VBC	46	Potassium persulphate	1
		DVB	10		
		CEB	15		
		CB	15		
		Span 80	14		
HX2-PHP		VBC	46	Potassium persulphate	1
		DVB	10		
		CEB	15		
		CB	15	$FeCl_3$	5
		Span 80	14		

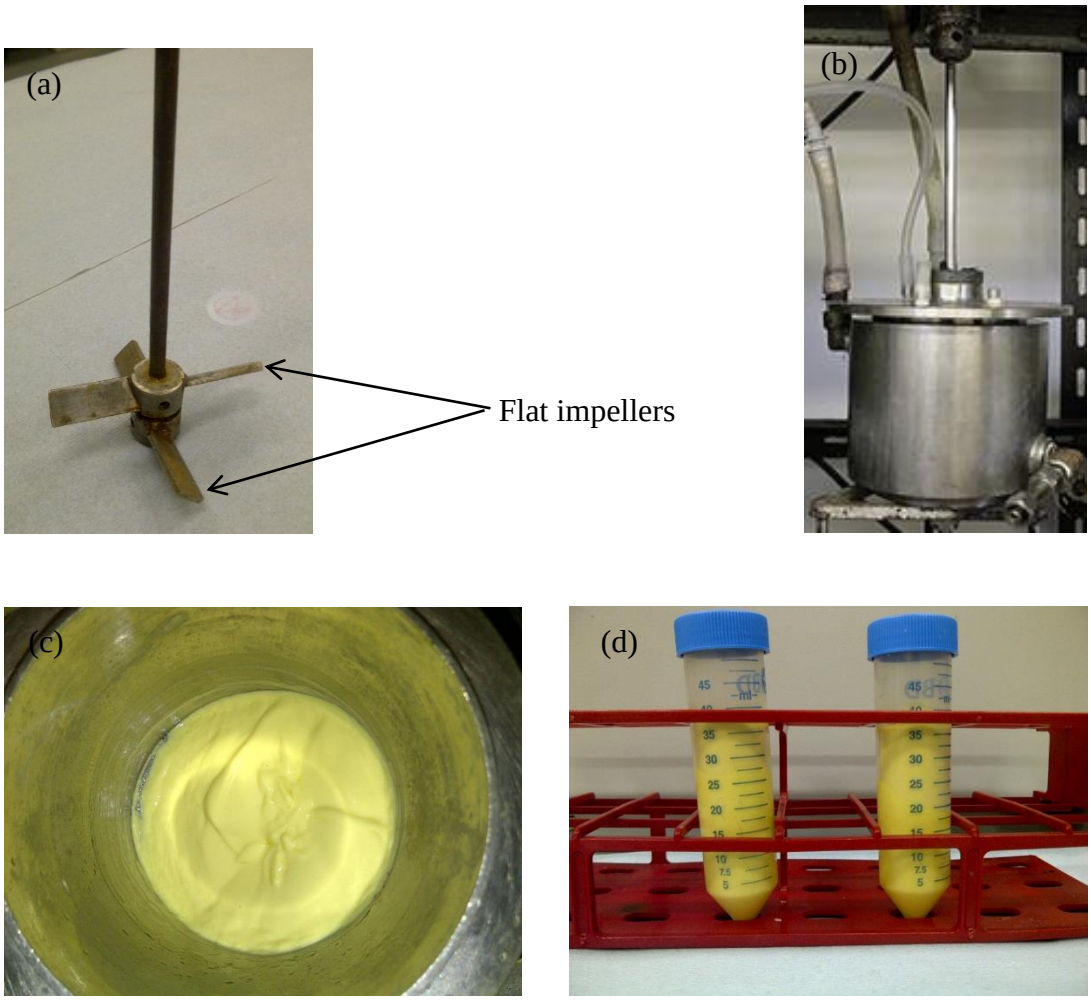

Figure 3-1 (a) Stirrer rod with impellers. (b) Stainless steel jacketed reaction vessel. (c) HIPE. (d) HIPE transferred in Falcon tubes

The experimental rig for the preparation of HIPE's is set up in a fume cupboard. The schematic diagram of the rig is as shown in Figure 3-2. The reaction vessel is fitted with a funnel and a stirrer rod having two flat impellers perpendicular to each other as illustrated in Figure 3-1(a). The impeller rod is connected to an overhead stirrer motor. The reaction vessel is connected to circulating ice water bath at low temperatures maintained around 4-7 ^{0}C, during preparation of HIPE4, since the mixing of the aqueous phase containing ferric chloride with the oil phase is exothermic. The aqueous phase was slowly added to the oil phase with the help of a peristaltic pump. The stirring rate of 300 rpm was kept constant during the preparation of the emulsion.

In order to obtain homogenous mixing, the lower blade of the impeller of the stirrer rod was kept close to the bottom surface of the reaction vessel, while the final level of the emulsion was about 1 cm above the top blade of the impeller. The processing condition included dosing time t_d (time taken to add the aqueous phase) and homogenization time t_h which is the time taken for mixing both the phases. The dosing time for aqueous phase was 5 minutes and homogenization time (t_h) was varied from 10 minutes to 30 minutes as per polyHIPE samples produced. The total polymer volume of both phases is 250 ml of which 90% is aqueous phase and 10% is oil phase. The resulting emulsion in case of HIPE4, a yellow colored mustard sauce like appearance is as seen in figure 3-1(c). The preparation of HIPE1, HIPE2 and HIPE3 was carried out at room temperature and did not involve connecting the reaction vessel to the ice water bath.

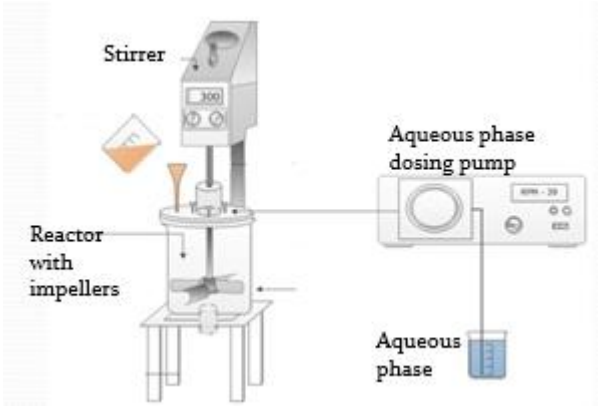

Figure 3-2 Schematic diagram of preparation of polyHIPE polymers (Greco, 2014)

3.2.2 Preparation of PolyHIPE

The resulting HIPE were transferred into 50 ml Flacon tubes and sealed as illustrated in Figure 3-1(d). The Falcon tubes were placed in a conventional oven at 60-70 ^{0}C for 24 to 48 hours for polymerization to take place. The polyHIPEs were then removed from the tubes and cut into 5 mm thickness as represented in Figure 3-4 with the help of a microtome. The polyHIPE sample clamped on the sample holder of the microtome and the desired thickness of the monolith is cut with the blade moving in the perpendicular direction of the sample holder. Since the polyHIPE is still wet, monolith obtained can be easily sliced

without any cracks or fractures. The circular polyHIPE discs then taken for washing in a Soxhlet apparatus.

Figure 3-3 Stages from preparation of HIPE to polymerization

Figure 3-4 PolyHIPE polymer and PolyHIPE discs

3.2.3 PolyHIPE washing

The polyHIPE discs were washed extensively in a Soxhlet apparatus with ethanol/ isopropanol or methanol for 4-5 hours as illustrated in Figure 3-5. This was followed by washing with distilled water overnight. Extracting in a Soxhlet apparatus ensures removal of any impurities, residual surfactants, unreacted monomers or initiator. The polyHIPE discs were dried to constant weight in a vacuum oven at 60 ^{0}C. These discs were further used for functionalization, characterization or hypercrosslinking.

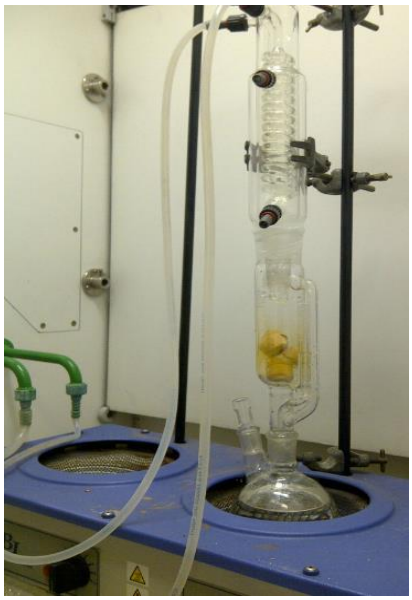

Figure 3-5 Soxhlet extraction

3.3 Hypercrosslinking of polyHIPE

The objective of this process is to enable the hypercrosslinking of the polyHIPE polymer to increase its surface area and facilitate deposition of the Lewis acid catalyst $FeCl_3$ onto their porous structure.

3.3.1 Hypercrosslinking Method

A solution of 10 weight% of hypercrosslinker XDC in DCE was prepared for hypercrosslinking. PolyHIPE discs were weighed and placed in a round bottom flask to which 150 ml of above solution of XDC in DCE was added. $FeCl_3$ was used as Friedel-Crafts catalyst. The amount of $FeCl_3$ used in hypercrosslinking corresponded to a 1:1 weight ratio between the polyHIPE discs and $FeCl_3$ in the experiments. Weight of a typical polyHIPE disc after purification and drying is approximately between 0.2- 0.23 gms. Gentle agitation was provided to enable dispersion and homogeneous mixing of the $FeCl_3$ and the flask was vented. The polymer discs were left soaking in the flask for 2 hours. The flask was then transferred into the oven for curing at 80 ^{0}C overnight for the

hypercrosslinking reaction to take place. The hypercrosslinking reaction allows the introduction of very small pores into the polymer structure. The resulting discs were washed with methanol and then with acetone. The washing of the polymers included soaking and gentle stirring. Each washing lasted for 1 hour, repeated twice. Finally, double distilled water was used to wash all the samples for 1 hour before final drying. They were then dried in the oven for 24 hours until no change in weight was recorded.

3.4 PolyHIPE Characterization

3.4.1 Scanning Electron Microscopy (SEM)

SEM is a powerful and versatile technique for achieving high resolution images of surfaces. It involves scanning a fine beam of high energy electrons over a specimen. Magnetic lenses are used to focus the beam on the surface and electrostatic scan coils are used to deflect the raster scan which controls the magnification of the image produced. The (primary) electrons interact with the specimen surface and generate a range of possible signals which can be used for imaging. The main topographic imaging mode is based on detectors collecting the secondary electrons emitted from the specimen surface after the bombardment by the primary electrons. A schematic diagram of SEM is shown in Figure 3-6.

Electrons emitted by the gun are accelerated by the applied voltage. They pass through the condenser lens and are focused on the sample by the objective lens. Scanning coils then electrostatically scan this beam of electrons on the sample surface. Electrons emitted by the sample are detected and amplified. The signal is then used to produce an image. When the electron beam hits the sample, various signals from the sample can be collected and used to form the images. The signals are secondary electrons, backscattered electrons, electron beam induced current, cathodoluminescence, Auger electrons and X-rays. Auger electrons are emitted from atomic layers very close to the surface and hence give valuable information about the surface chemistry. Secondary electrons originate

from within a few nanometer from the surface. Hence they are sensitive to the surface structure and provide topographic information.

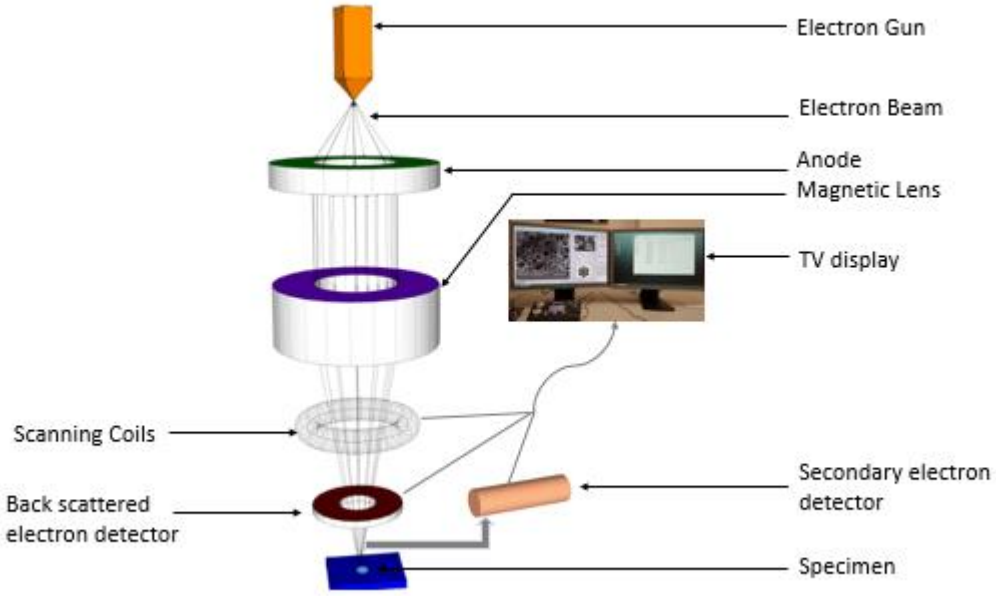

Figure 3-6 Schematic of scanning electron microscope (Vernon-Parry, 2000)

The backscattered electrons originate from much deeper within the sample almost few micrometre below the surface. They interact more strongly with the sample and provide compositional information. However, they produce lower resolution images. X-ray analysis or energy dispersive x-ray (EDX) give the elemental composition measuring the nature and quantity of different elements in the sample (Goldstein *et al.*, 2003).

SEM studies were conducted to observe the surface morphology (porous characteristic and interconnected polymer network) using a Cambridge S240 scanning electron microscope. The surface of the polyHIPE disc to be examined was fractured rather than cut or sawed to avoid any damage to the cellular structure. The sample is then mounted on a stub which consists of a circular disc 2.5mm in diameter with a cylindrical pin of 8mm length coming off the bottom. In this study, aluminum pin stubs where used. Brass and copper pin stubs are also available. A carbon tape is attached to the cylindrical disc of the stub on which the sample is mounted. The carbon tape has an adhesive surface on which the sample remains attached and stable during the analysis.

Samples which are non-conductive can be damaged by the charge which builds up inside the SEM. Hence, the samples must be coated with thin layer of conductive material like carbon or gold. To achieve a fine coating of nanometer thickness, a sputter coater is used which covers the material with conductive material on the surface through a cold plasma process. This process aids in retaining the morphology of the samples. The fractured samples in this study, were gold coated using the Polaron E1500 Sputter Coater before analysis and then examined under SEM.

3.4.2 Surface Area Analysis

Brunauer-Emmet-Teller (BET) is an important analysis technique for the measurement of the specific surface area of a material.

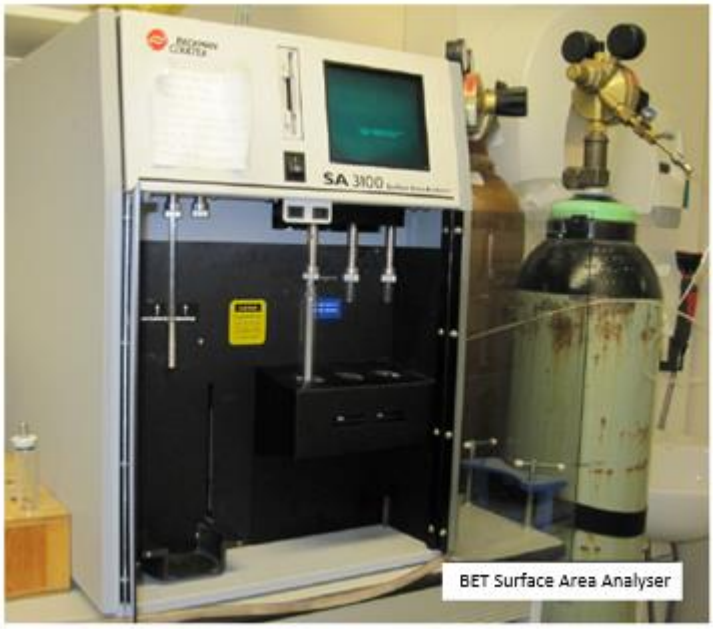

Figure 3-7 BET Surface Area Analyser

The theory explains physical adsorption of gas molecules, mostly nitrogen, on the surface of solid material. The gas molecules are adsorbed on the surface of the sample and the micropores are filled up forming a monolayer. The amount of adsorbate gas corresponding to the monolayer formation on the sample surface is used to determine the specific surface area. Alternatively, capillary condensation process in which multilayer adsorption from the vapor phase into a

porous medium proceeds to a point where the condensed liquid from the vapor phase fills up the pores spaces on the sample. This method can be applied to assess the presence of pores, pore volume and pore size distribution. Therefore the surface area and pore size distribution of the samples can be calculated from the adsorption and desorption isotherms. In this study, BET model was used to calculate the surface area and Barret, Joyner and Halenda (BJH) model was used to measure the pore size distribution. All the calculation models were based on physisorption process and not on chemisorption process.

Polymer surface areas were measured using the Brunauer-Emmet-Teller (BET) method with SA3100 Gas Adsorption Surface Area Analyser (Palo Alto, CA) shown in Figure 3-7. The dried polymer discs obtained after the purification step is crushed, weighed and transferred to the sampling tube. Samples were outgassed for 5 hours at 200 ^{0}C under nitrogen and helium flow before analysis to remove any contaminants. The samples were then analysed in an evacuated sample port while the tube immersed in liquid nitrogen to provide a constant temperature. The processing time for a single sample tube for complete analysis was approximately 6-8 hours.

3.4.3 Fourier Transform Infrared Spectroscopy (FT-IR)

Fourier Transform Infrared Spectroscopy is a qualitative analysis which is used to obtain an infrared spectrum of adsorption or emission for analysis of solid, liquid or gases. It gives direct information about the existence of the different functional groups and elucidates the structure of matter at the molecular state. An infrared spectrum is obtained by passing IR radiation through a sample. Some of the infrared is absorbed by the sample and some transmitted through it. The resulting spectrum characterizes the molecular absorption and transmission, creating a unique molecular fingerprint of the sample. Figure 3-8 illustrates the schematic diagram of working principle of FTIR spectrometer.

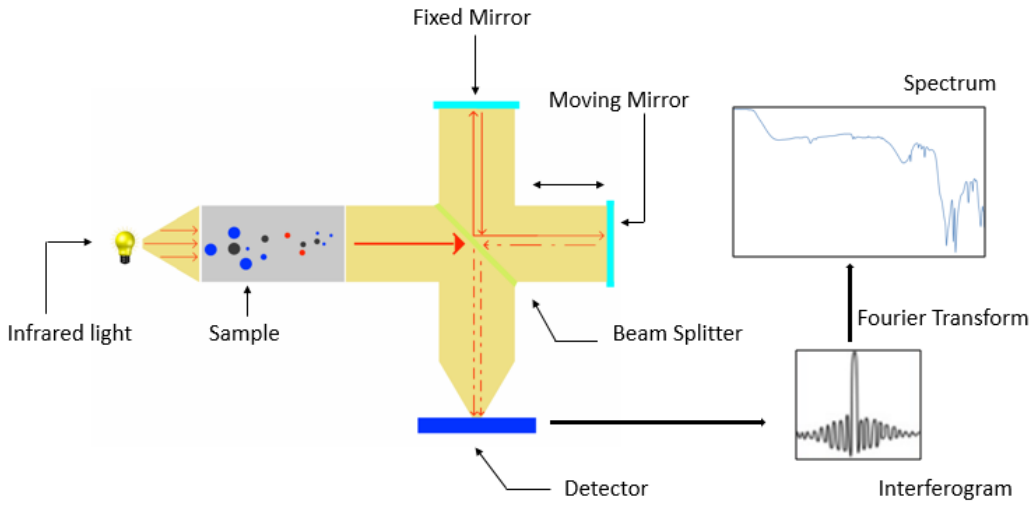

Figure 3-8 Schematic diagram of FTIR

Infrared energy is emitted from a source and this beam passes through an aperture which controls the amount of energy presented to the sample. The beam then enters the sample compartment. Depending on the type of analysis, IR is transmitted or absorbed at a particular energy. The energy at which any peak appears in the spectrum corresponds to the frequency of vibration of the sample. The beam enters the interferometer where the spectral encoding takes place. The beam finally passes through the detector, which is designed to measure the special interferogram signal. The measured signal is then digitized and sent to computer where the Fourier transformation takes place. Finally, the infrared spectrum is available for interpretation (Barrios *et al.*, 2012).

In this study, the polyHIPE samples were analysed by a Varian 800 FT-IR spectrometer system which produces spectra between 4000 cm^{-1} and 400 cm^{-1} from solid, liquid and oil samples using the Pike technologies diamond crystal plate attenuated total reflection (ATR) immersion probe.

3.4.4 Thermogravimetric analysis (TGA) of polyHIPES

In this work, thermogravimetric analysis was carried out with the use of Perkin Elmer simultaneous thermal analyser (STA 6000). Thermogravimetry measures the amount and rate of change in mass of sample as a function of

temperature or time in a controlled atmosphere. Figure 3-9 depicts the schematic of a TGA instrument.

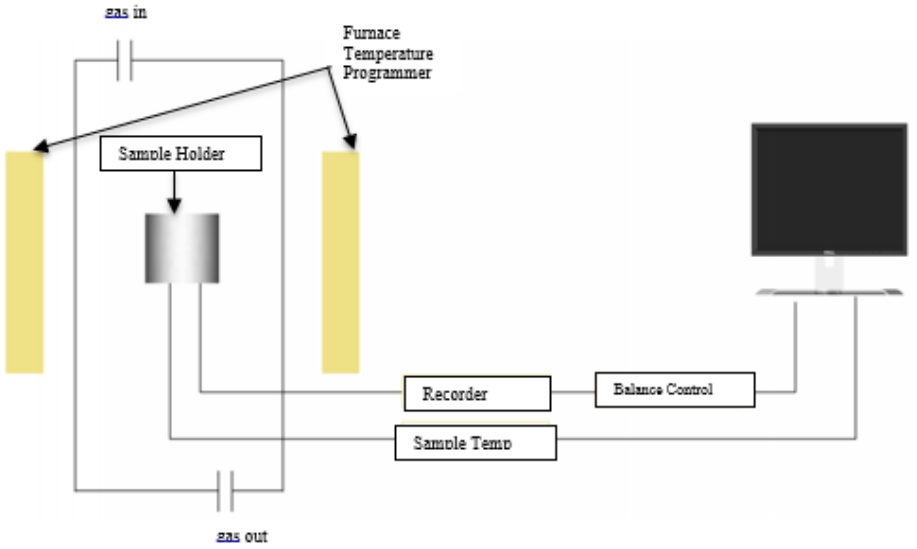

Figure 3-9 Schematic diagram of TGA instrument

The thermogravimetric instrument consists of a microbalance surrounded by a furnace. A computer records the sample mass loss or gain due to decomposition, oxidation or loss of volatiles. Weight is plotted against time for isothermal studies and as a function of temperature for experiments at constant heating rate. The rate of heating the sample and the ambient atmosphere during analysis are important factors to be controlled during thermal analysis. The maximum temperature is selected so that the sample weight is stable at the end of the experiment, implying that all chemical reactions are completed.

Figure 3-10 shows a thermogravimetric curve of three polymer samples. The x-axis of the thermogram represents the temperature in degree Celsius which is converted to the time scale due to the constant temperature ramp. The y-axis represents the percentage residual mass of the polymers as the temperature was increased at a steady state.

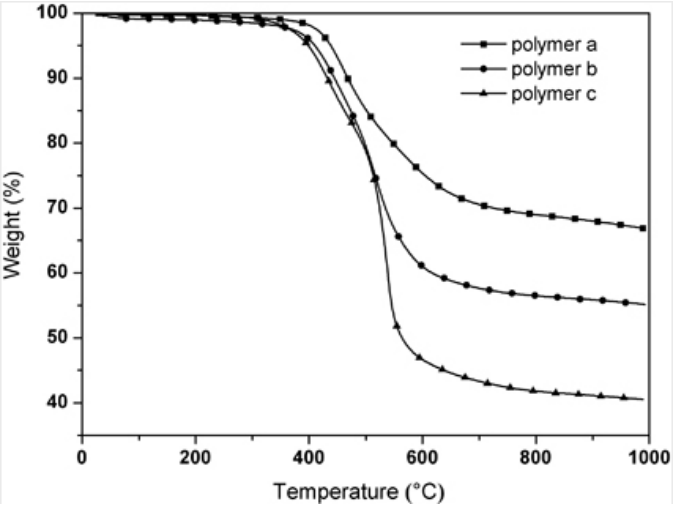

Figure 3-10 TGA curve of 3 polymer samples (Li *et al.*, 2011)

In this study, approximately 14 mg of polyHIPE sample placed in a ceramic sample pan was heated at a scanning rate of 10^0C/min from 40^0C to 950^0C under a nitrogen purge. The continuous recording of weight loss as a function of temperature, helps in determination of the degradation reaction of the polyHIPE sample. The thermogravimetric analysis (TGA) curves and derivative thermogravimetric analysis (DTGA) curves were plotted to study the thermal stability and loss of components in the sample. This procedure was repeated for all the polyHIPE samples.

3.5 Determination of water retention characteristics of sandy loam and clay loam soils

The efficacy of polyHIPE polymers in improving soil moisture content were examined on sandy loam and clay loam soils. Pressure plate extractors described in the following section are used in determining the water holding characteristics of soil samples.

3.5.1 The Pressure Plate Extractor methodology

The sandy loam and clay loam soil samples were obtained from Cockle park farm, one of the Newcastle University agritech research centres located near Morpeth, Northumberland. The soil was air dried and gently passed through a

4mm sieve. Soil fractions of less than 4mm were used for further study. The polyHIPEs were mixed with the soil samples at four different rates (0%, 0.25%, 0.5% & 1% w/w) including control with five replicates. The mixture of soil and polyHIPEs were then filled in stainless steel cores 5.3 cm in diameter and 5 cm in height. The bottom of core was covered with a fine muslin cloth to prevent any loss of soil. The soil samples were then placed in a water tray, where water was added from the bottom to saturate the soil samples and avoid trapping any air. The cores were allowed to saturate for a 2-3 days. Figure 3-11 show the saturated cores for sandy loam and clay loam soil

Figure 3-11 Saturated soil cores for sandy loam and clay loam soils.

The porous ceramic plates were prepared by applying slurry of fine silica sand to allow good hydraulic contact between the cores and the plate. Saturated soil cores were then weighed and placed in the extractor on the porous ceramic plates. Figure 3-12a shows the pressure plate extractor equipment used in this study and Figure 3-12b illustrated the cross section view of the ceramic pressure plate and soil samples in the extractor. Low pressure plate extractor was used to determine the field capacity (0.05 bar) and easily plant available water (0.05 – 2 bar). After placing appropriate bolts and wing nuts on the extractor lid, the pressure in the extractor chamber was set at 0.05 bar forcing any excess water out of the cores through the micropores of the plate.

(a) Pressure plate extractors

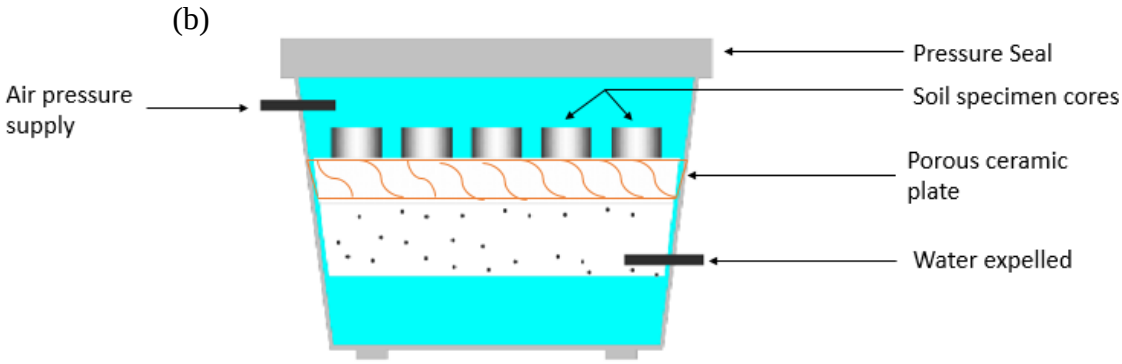

Figure 3-12 (a) Pressure plate extractors and (b) Cross section view of porous ceramic plate and soil samples in the extractor

The chamber is connected to a burette through a small tube where the water collects outside the pressure extractor plates. The cores are considered to be in equilibrium of the specified pressure when no more water is coming out of the cores. This required between 7-10 days. The soil samples were then removed and weighed. The pressure was increased to 2 bar and the process was repeated till second equilibrium was attained (10-12 days). The cores are then transferred to 15bar pressure plate extractor, to determine the wilting point. Once again the samples are allowed to attain equilibrium which takes around 20-25 days. The

sample cores are then removed and weighed and placed in the oven to dry at 105^0C for 24 hours. The water content was determined gravimetrically. By analyzing the core samples at different pressure, the characteristic pressure versus water content relationship can be determined for the soil.

3.6 Biological Works

3.6.1 Strain and culturing condition

Frozen stocks of *Shewanella Oneidensis* Mr-1 were stored in a glycerol solution at -80^0C. Cultures were maintained in Luria broth (LB) flask containing 1% agar by weight to ensure continuity of the stock cultures and incubated for 24 hours at 30^0C. Individual colonies were isolated and inoculated in LB medium and were incubated aerobically at 150 rpm and 30^0C for approximately 36 hours. This time indicates the start of early stationary phase corresponding to an optical density measured at 600 nm.

3.6.2 Biofilm formation

Two sulphonated polyHIPE discs were cut into small $5mm^3$ cubes and autoclaved. They were placed on a Petri dish and wetted with lactate (1 g/L) and left in an oven to dry at 30^0C for 5-6 hours. *Shewanella Oneidensis* MR-1 cells, previously grown in LB broth, was put onto the surface of the cubes and left in the oven for 24 hours. Under sterilized condition, lactate was added every 2 days to enhance the growth of the biofilm. Control experiments were performed previously to identify the appropriate period needed for the biofilm to be developed. Samples were collected every day for scanning electron microscopy. The collected samples were fixed with 2.5% glutaraldehyde solution in phosphate buffer. They were then dehydrated in increasing ethanol solution 20, 40, 60, 80, 100 % and subjected to critical point drying using an automated critical point dryer. The samples were then sputtered with gold for examination under scanning electron microscopy.

Chapter 4 Preparation of Catalytic Sulphonated PolyHIPE materials

This chapter presents the experimental outputs generated from preparation and sulphonation of polyHIPE polymers. The objective of the experiments was to enhance the polyHIPE morphology and investigate its porous characteristics. In addition, increase in the surface area was also investigated. The latter objective aims at augmenting the polyHIPEs for hydrophilic activity and increased water uptake capacity. Variation in the mixing time and its effects on the architectural properties of the polyHIPE were investigated. Microwave irradiation was used for sulphonation of the polyHIPEs, instead of the conventional thermal treatment. Formation of catalytic biofilm was also investigated on these sulphonated polyHIPEs.

As part of this study in preparation of novel polyHIPEs for agricultural application, we required material with high surface area, interconnectivity and good ion exchange capacity. Hence this chapter highlights the production of sulphonated polyHIPE polymers which have good hydrophilicity and bio-compatibility and can be further tested for water absorption capacity in different types of soils for agricultural application.

4.1 Production of polyHIPE polymers

PolyHIPE polymers were produced as described in section 3.2.1 and 3.2.2 of Chapter 3. HIPE 2 formulation was used for the preparation of the polyHIPE polymers and their further sulphonation whereas, HIPE 1 was used to prepare unsulphonated polyHIPE polymers. The following Figure 4-1 shows the SEM micrograph of the structural morphology of unsulphonated polyHIPE polymer (ST-DVBPHP). According to IUPAC recommendations, the pore sizes are categorized as micropores (pore diameter < 2nm), mesopores (pore diameter 2-50 nm) and macropores (pore diameter > 50nm) (Sing *et al.*, 1985).

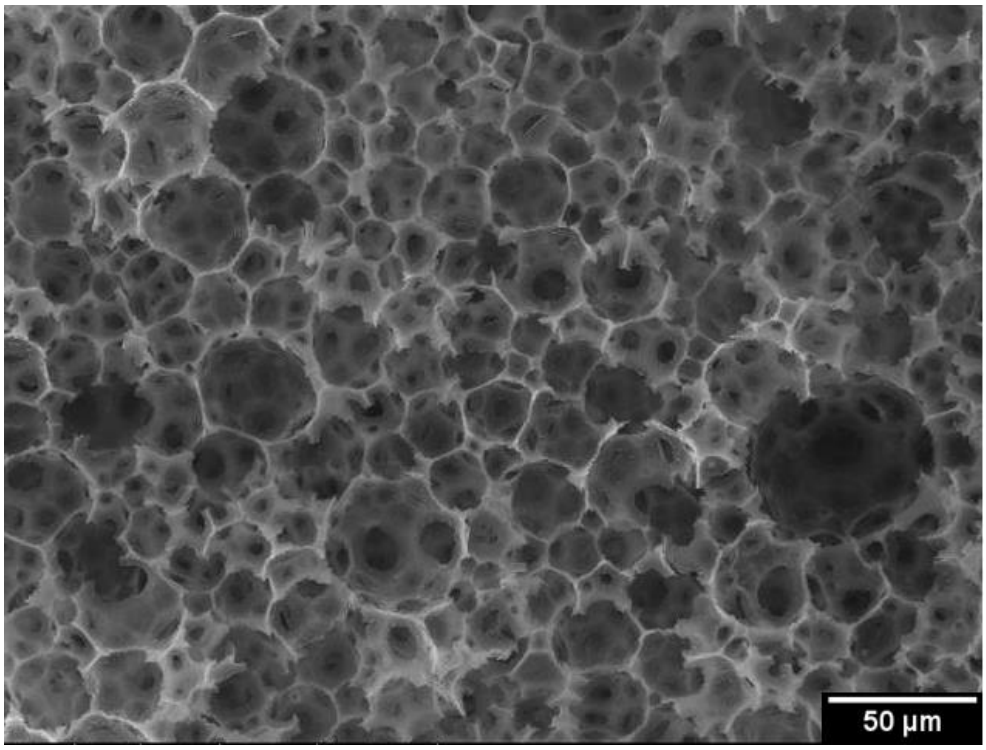

Figure 4-1 SEM image of ST-DVBPHP polyHIPE polymers

As seen from the SEM micrograph Figure 4-1, the morphology of the polyHIPE shows an open pore structure resulting from the oil and water emulsion polymerization. On polymerization the aqueous phase is evaporated forming the pores and interconnects showing a structural hierarchy. Thus the larger pores are interconnected by a series of smaller pores revealing an open porous network. The polyHIPEs obtained are hydrophobic in nature.

4.2 Sulphonation of polyHIPE polymers

The ability of fuctionalise the polyHIPEs for specific applications is of utmost importance. Applications in agriculture not only require hydrophilic polymers but also good ion exchange properties to facilitate nutrient exchange which may enhance the soil productivity. It is also essential to ensure that the materials used and the processes are sustainable and economic. Sulphonation imparts hydrophilicity to the polyHIPEs.

Sulphonation is defined as a substitution reaction used to attach the SO_3^- group on an organic compound. SO_3^- is an aggressive electrophilic reagent that

rapidly reacts with any organic compound containing an electron donor group. Styrene and DVB based polyHIPEs involves chemical modification where the phenyl rings of the styrene-DVB crosslinked polymer are used as reactive sites and the sulphonic acid $SO_3^-H^+$ functional group attaches to the carbon atom. Figure 4-2 shows the sulphonation reaction of polyHIPE polymers.

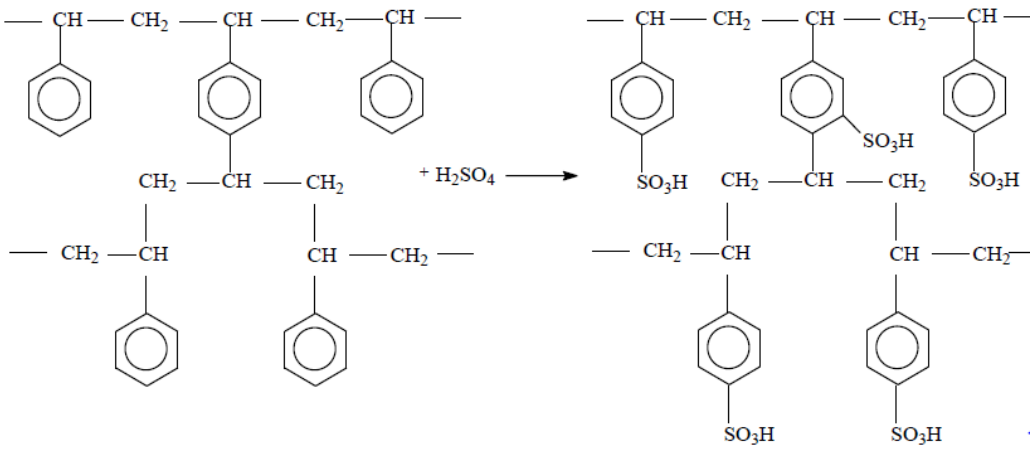

Figure 4-2 Sulphonation of polyHIPE polymers

After sulphonation, the polyHIPE polymers become hydrophilic and also possess high water absorption and ion exchange capacity. The polyHIPEs were prepared using 76wt % styrene, 10wt% divinyl benzene (DVB) and 14wt% non-ionic surfactant span 80 as the oil phase as detailed in section 3.2.1 (Table 3-1). Aqueous phase contained 94wt% deionised water with 5wt% sulphuric acid and 1wt% potassium persulphate. Dosing of the aqueous phase into the stainless steel reactor was 5 min, while the mixing of both the phases was carried out at 300 rpm. Three different sulphonated polyHIPE samples were prepared SPHPA10, SPHPA20 and SPHPA30. Mixing time for SPHPA10 was 10 minutes and for SPHPA20 and SPHPA30 20 minutes and 30 minutes respectively. The effect of mixing time on pore and interconnect sizes is discussed later in section 4.3.3. Volume fraction of the oil and aqueous phases were 0.1 v% and 0.9 v% respectively were kept constant for all samples. Thus, sulphonated polyHIPEs were prepared with HIPE2 formulations as described in section 3.2.1.

The polyHIPE discs were then washed in soxhlet apparatus with mixture of isopropanol and distilled water for 5hours, followed by pure distill water overnight.

The discs were finally dried in the oven at 60^0C for 24-48 hours till no change in the weight was recorded. The dried discs were weighed and then soaked in 98% concentrated sulphuric acid for 4 hours. The white monolith discs changes to yellowish/orange colour after soaking in sulphuric acid. These acid soaked discs were then microwaved for 2 minutes, turning the disc around every 30secs so that both the sides were equally irradiated. A domestic microwave oven (1400watt) was used for microwaving the soaked discs. After every 30sec cycle, the microwave door was left open for 1-2 minutes to vent the fumes. It was observed that the polyHIPE discs were spongy, swollen and exhibited increase in weight. The discs turned black which was more pronounced on the circular edges. The charring at the edges is caused due to microwave irradiation of the excess of the viscous acid concentrated on the surface and the edges. Figure 4-3 shows the polyHIPE discs before and after sulphonation.

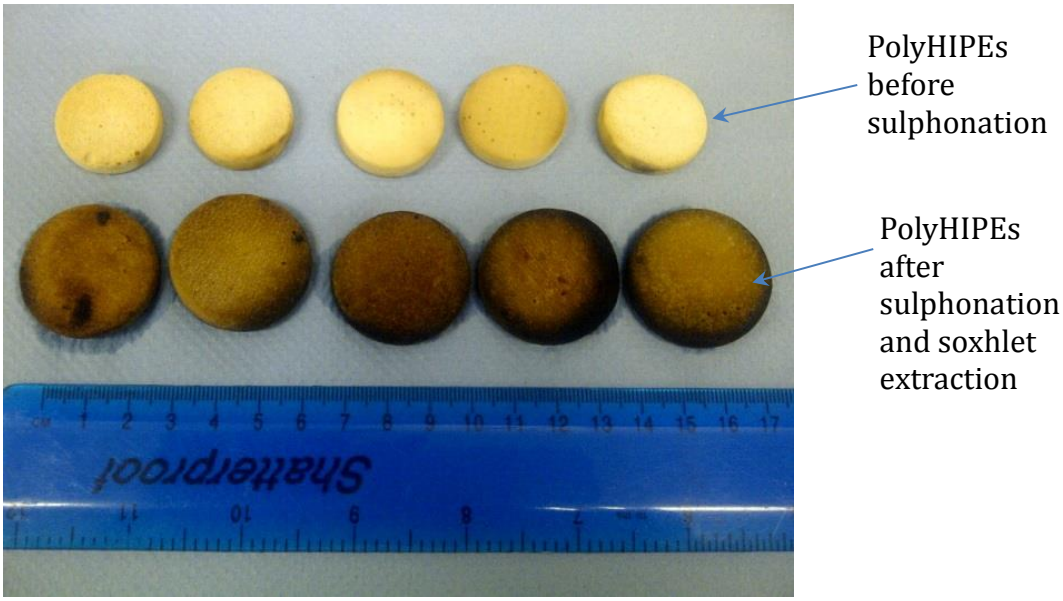

Figure 4-3 PolyHIPE discs before and after sulphonation

In this study, all the polyHIPE polymers were sulphonated with the use of microwave irradiation. Conventional methods for sulphonation requires thermal treatment at elevated temperatures, longer duration for reaction and large amount of sulphuric acid (Regas, 1984; Toro *et al.*, 2008). Moreover, the functionalization is more pronounced on the exterior surface then the interior of the polymer (Cameron *et al.*, 1996b). Microwave irradiation reduces the overall

process duration required for sulphonation, at the same time achieving higher degree of sulphonation. These sulphonated polyHIPEs were further characterized by SEM, FTIR, BET, TGA and IEC analysis.

4.3 Results and Discussion: Sulphonated polyHIPE polymers characterization

4.3.1 Scanning Electron Microscopy (SEM)

Microwave sulphonation resulted in enhancement of the structure of the polyHIPE polymers. SEM images for both unsulphonated and sulphonated polyHIPEs were observed for changes in the morphology. It was observed that the polyHIPEs after microwave sulphonation were spongy and swollen. In this current method of obtaining sulphonated polyHIPEs, sulphuric acid is added directly into the aqueous phase during the emulsification stage. The presence of filler or additives in the aqueous phase results in destabilization of the emulsion. This destabilization of the HIPE causes water droplet coalescence. Such formation of the coalescence pore is seen in the SEM image of unsulphonated polyHIPEs in Figure 4-4(b) evident on the left of the SEM image. All SEM images from Figure 4-4 to Figure 4-7 are for the polyHIPEs prepared with 10 minutes mixing time SPHPA10. The following Figure 4-4 and Figure 4-5 shows the overall appearance and the magnified view of unsulphonated polyHIPE polymer respectively.

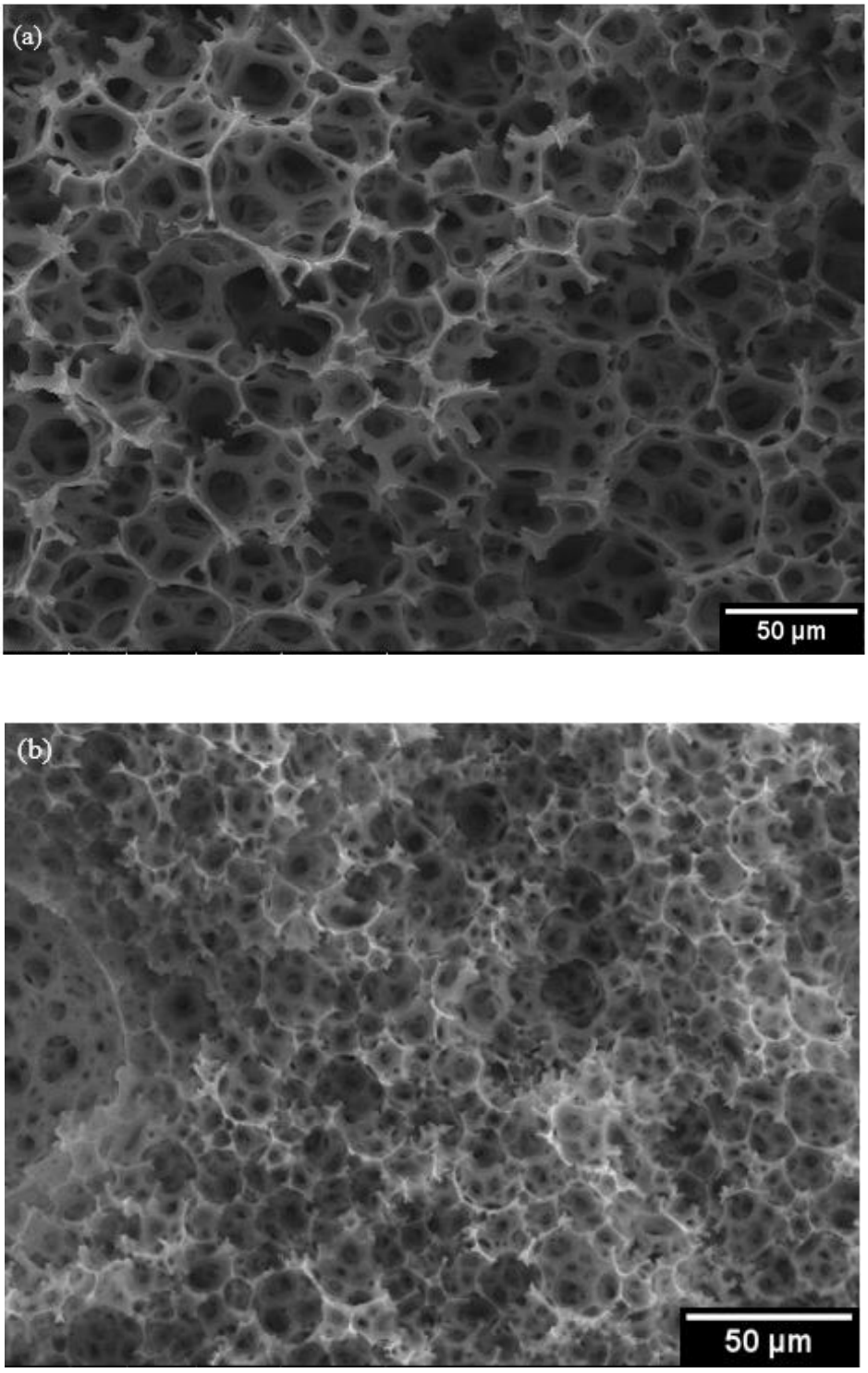

Figure 4-4 (a) Overall SEM image of unsulphonated polyHIPE & (b) Overall SEM image of unsulphonated polyHIPE showing coalescence pore on the left.

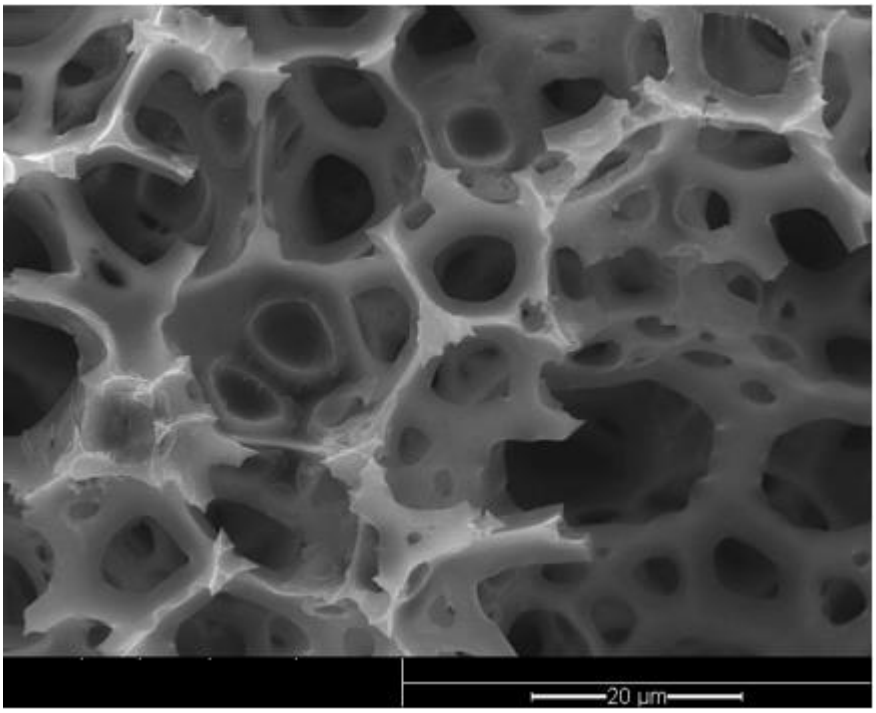

Figure 4-5 Unsulphonated polyHIPE magnified view

If the coalescence droplet size increases, it can result in complete separation of both the phases. However, no evidence of emulsion breakdown indicating separated aqueous phase was observed. Some distinctive changes in the morphology can be observed from the SEM images of the sulphonated polyHIPE polymer as seen in Figure 4-6 (a) & (b) at various magnification.

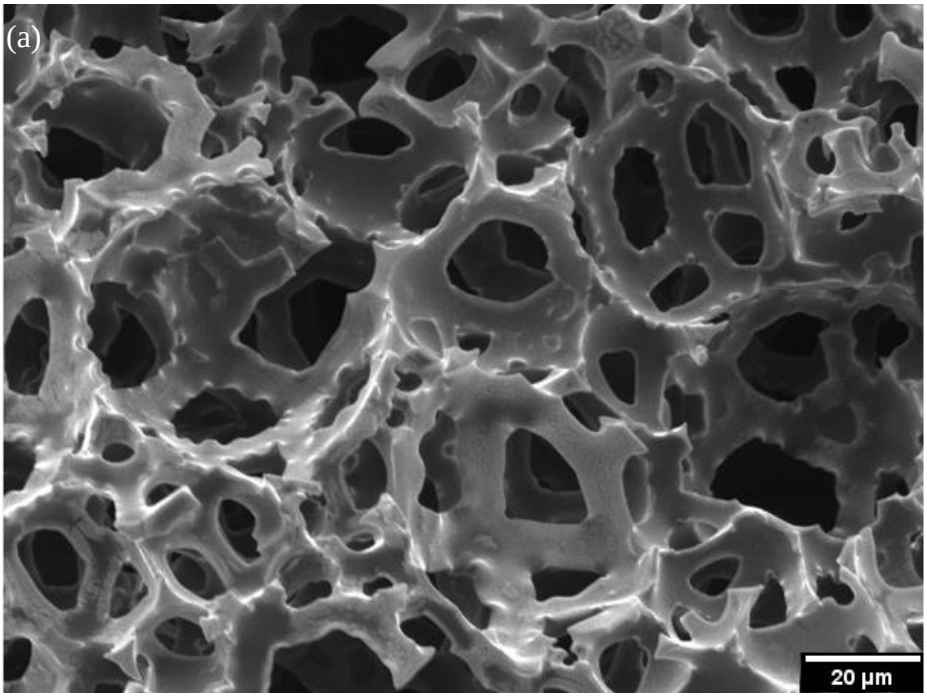

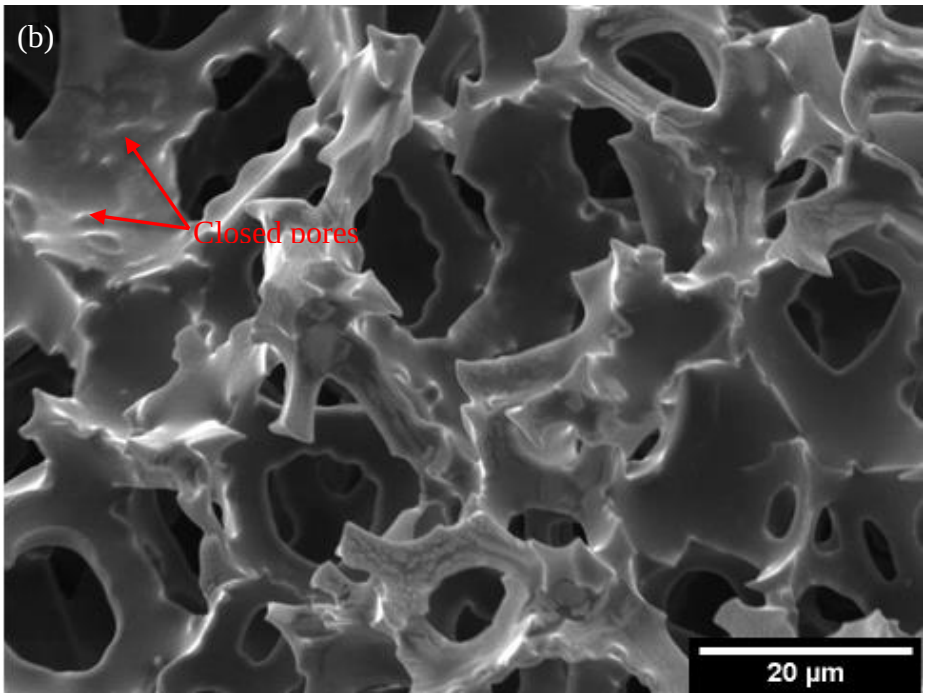

Figure 4-6 (a) & (b) SEM of sulphonated polyHIPE produced by 5% sulphuric acid in the aqueous phase and microwave irradiated for 2 minutes

Some closed pores are also evident in Figure 4-6 (b). Some of the smaller pores were covered with thin polymeric films. These closed pores may be also formed by the surfactant concentration (14% v/v) based on the total amount of styrene and DVB used in the oil phase. The influence of the surfactant concentration on the closed pores, will require a closer study. Zhou *et al.* (2007) reported, when the amount of surfactant (Span 80) was below 30% based on the total amount of styrene and DVB, the resultant polymer has smaller pore sizes. The surfactant concentration may affect the stability of the films separating the emulsion droplets and as the interfacial tension reduces the films get thinner which are more vulnerable to rupture (Ikem *et al.*, 2010). The presence of larger pores due to coalescence and the closed pores in the polymer network indicate emulsion instability. After the microwave irradiation, sulphonated polyHIPEs, along with the coalescence and primary pores also exhibited curvy pore edges. The walls of the primary pores were thicker as seen in Figure 4-6. Good permeability is achieved in polyHIPEs as the primary pores are connected to each other by smaller pores referred as interconnects. Some of the nano-pores formation is also evident.

These nano-pores are formed when the sulphuric acid entrapped in the polyHIPE monolith escapes due to the heat during microwaving

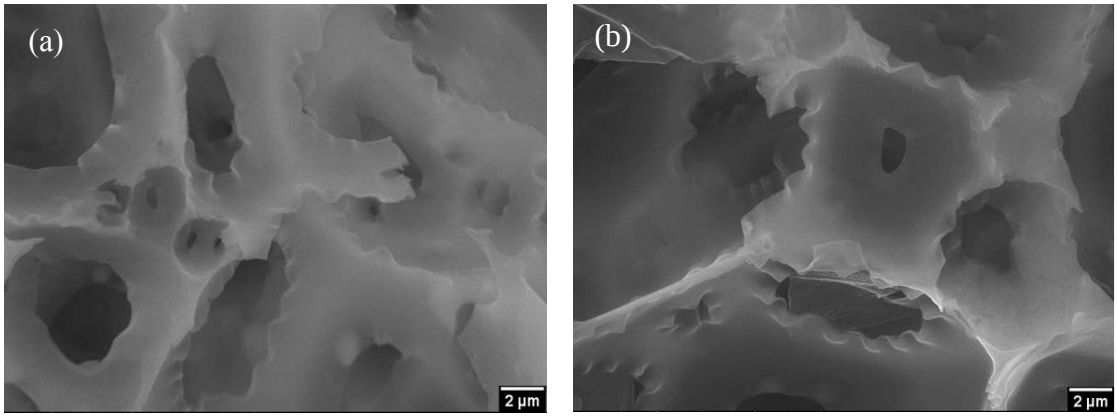

Figure 4-7 SEM of sulphonated polyHIPE showing curvy edges and nano pores formation (Scale bar- 2 µm)

These nano-pores are seen in the Figure 4-7 (a) with distinctive feature of curvy edges of the sulphonated polyHIPEs. Microwave irradiation also causes charring of the polyHIPEs, indicating signs of carbonization which is more pronounced on the circular edges of the monolith. Figure 4-8 depicts microwave irradiated sulphonated polyHIPE monolith.

Figure 4-8 Microwave irradiated sulphonated polyHIPE

This carbonization of the sulphonated polyHIPE make them electrically conductive and they can be examined under the SEM without the application of the conductive coating like carbon or gold. However, since the carbonization is

not uniform throughout the structure of the monolith hence SEM analysis of the polymer samples in this study was carried out with gold coating.

4.3.2 Nano and micro pores formation in sulphonated polyHIPE polymers

PolyHIPE production has the advantage of controlling the morphology of pores and interconnects according to the intended applications. Akay *et al.* (2002b) demonstrated polyHIPEs with pore sizes ranging to 150 µm can be obtained by incorporation of additives or fillers in the emulsion. In the current study, sulphuric acid in the aqueous phase causes the presence of coalescence pores along with the primary pores. The increase in the rate of coalescence pores is due to the thinning of the liquid film whereby the van der Waals forces are strong due to polarizability (Kizling and Kronberg, 1990). These additives or fillers added to the aqueous phase in small quantities do not take part in the polymerization reaction. The main purpose of these fillers is to modify the surface within the polymer. Incorporation of the sulphuric acid, resulted in water droplet coalescence leading to larger pores as seen in Figure 4-4(b), but the cross linking reactions and the competing polymerization prevents emulsion separation. However if their concentration is increased, it may lead to emulsion instability and eventually phase separation.

In this current study, sulphuric acid was used as the internal phase during emulsification, hence excess acid (usually needed in thermal treatment) and its homogenous penetration into the pores is avoided as the acid is already present within the polymer structure. Another feature of the sulphonated polyHIPEs is the formation of blisters within the structure of the polymer. These blisters make the surface irregular and some may even appear to form interconnects. Figure 4-9 illustrates the blister formation on the surface of polyHIPE polymers. Microwave irradiation is carried out immediately after soaking the polyHIPEs in sulphuric acid for the stipulated time. The trapped sulphuric acid within the monolith structure reacts and escapes during the microwaving. This results in formation of blisters, cracks within the walls and formation of micro and nano pores. This results in enhancement of the polyHIPE structure and intensification of the process duration. Formation of micro and nano-pores is seen from the SEM images in Figure 4-10. Fractured surface on the walls is also evident near the blister

formation. Figure 4-10 depicts the formation of blisters appearing to form interconnects maintaining the hierarchical structure of the polyHIPE.

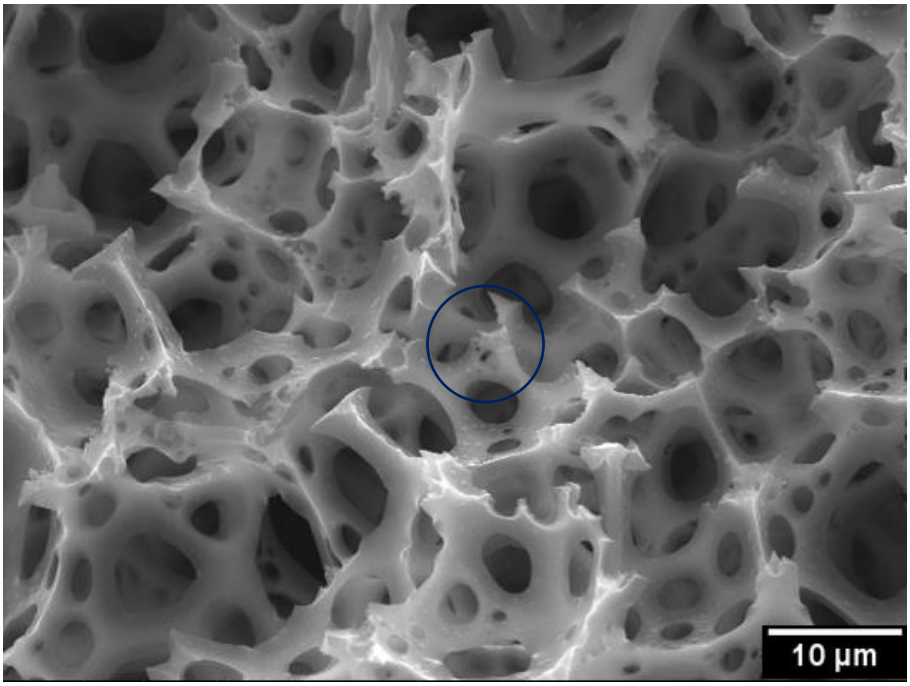

Figure 4-9 SEM of sulphonated polyHIPE showing blister formation

The circled area in Figure 4-9 is magnified and shown in Figure 4-10 highlighting the formation of interconnected pores.

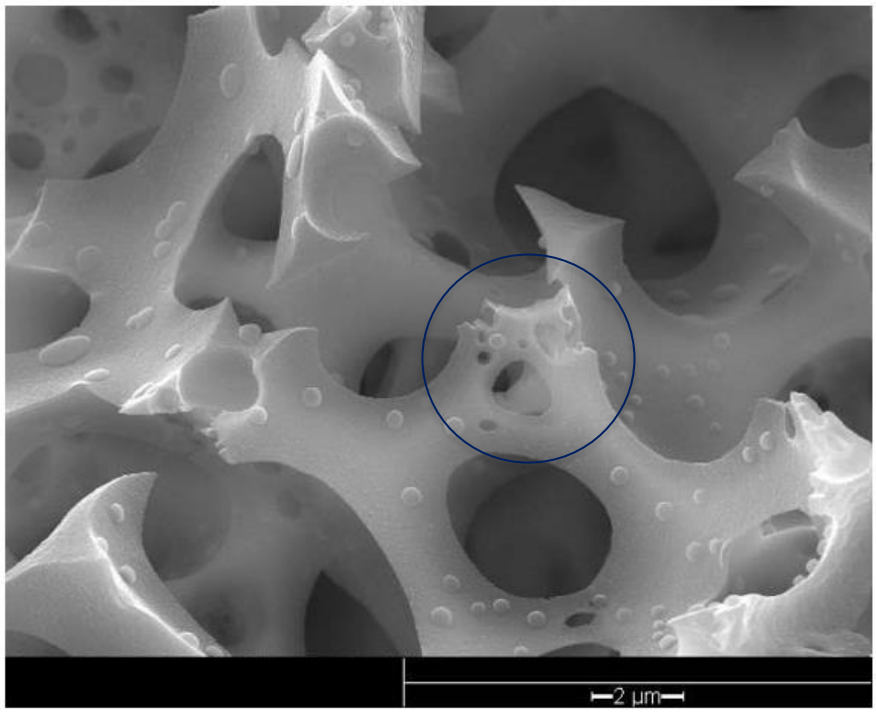

Figure 4-10 Formation of blisters appearing to form interconnects

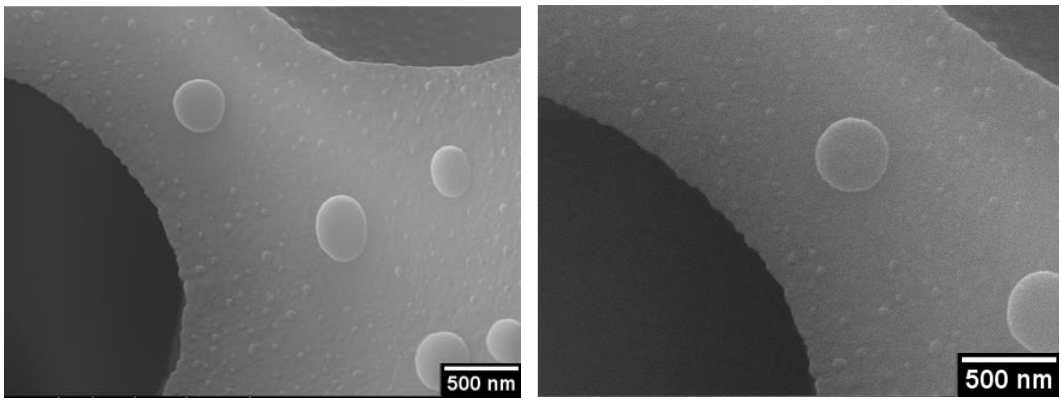

Figure 4-11 Detail of the blister formation at magnification of 35000x and 50000x

Thus it was evident that the blisters created uneven and irregular surface within the polyHIPE structure. This surface roughness can be favorable for the attachment of bacteria and microbes when used in soils for agricultural purposes (Akay and Fleming, 2012). Another important aspect of the sulphonation, is that it imparts hydrophilicity to the polymer. Unsulphonated polyHIPEs are hydrophobic and exhibit very low surface area (2-5 m^2/g). Addition of the sulphonic group to the polyHIPEs not only makes them hydrophilic, but also enhances their surface area. The enhancement of the surface area through sulphonation is discussed in the next section. Small cracks and fractures within the walls of the polymer along with interconnectivity and high degree of crosslinking may increase the ability to absorb water or liquid. The capacity of the polyHIPEs to absorb and retain water is discussed later in the water uptake studies.

4.3.3 BET surface area enhancement and effect of homogenization time on pore and interconnect sizes

Unsulphonated polyHIPE polymers are hydrophobic with a modest surface area between 2-10 m^2/g (Akay, 2006; Burke *et al.*, 2010; Akay and Fleming, 2012). In this study the BET surface area of the polyHIPE samples before sulphonation was between 9-10 m^2/g. The polyHIPE discs were usually soxhleted after the sulphonation procedure in the previous methods used in (Akay *et al.*, 2005a; Burke, 2007; Çalkan, 2007). The modification done in this current study,

was the polyHIPE samples were soxhletted twice. This was done to ensure effective removal of unreacted monomers/ surfactant from the polymers. Firstly, post polymerization the discs were soxhleted with mixture of isopropanol and distilled water for 4-6 hours followed by distilled water overnight. Later the polyHIPE discs were completely dried before carrying out the sulphonation procedure. This ensured that the unreacted monomers were removed and the pores were dried before soaking into the sulphuric acid. The discs were soxhletted again following the same procedure after sulphonation by microwave irradiation was completed. The enhancement in the surface area after sulphonation can be attributed to effective removal of the unreacted monomers and drying the polymers which allows levelled penetration of the sulphuric acid during the soaking period. Along with the hydrophilicity imparted through sulphonation, it was also observed that there was increase in the size of the polyHIPE discs. Sulphonated polyHIPE discs were enlarged by 10-30% from its original size in its dried state. The BET surface area of the three polyHIPE samples prepared with the different mixing time is as shown in Table 4-1.

Table 4-1 BET surface area for polyHIPE samples

PolyHIPE sample code	BET before sulphonation (m^2/g)	BET after sulphonation (m^2/g)	Increase in surface area (m^2/g)
SPHPA10	9.4 ± 0.25	110.3 ± 3	100.6
SPHPA20	9.8 ± 0.18	108.5 ± 6	98.2
SPHPA30	9.23 ± 0.42	112.1 ± 5	102.77

Çalkan (2007) reported similar enhancement in the surface area of the sulphonated polyHIPEs in their study to develop an intensified gasification system which uses the polyHIPE polymers for both gas purification and water treatment. It is clear that surface area does not depend on any variation of the mixing time.

In agricultural application, it is crucial to have good pore distribution and high interconnectivity to allow water movement and nutrient transport through the hydrophilic polymers along with the compatibility of microbial cell attachment within their open structure. Akay *et al.* (2005a) have reported that the morphology of polyHIPEs can be tailored by controlling the dosing and mixing time along with varying the emulsification temperature. Similarly Carnachan *et al.* (2006) demonstrated that increasing the temperature of the aqueous phase in the emulsion leads to an increase in average pore and interconnect sizes in the resultant polyHIPE structure.

In this study, we carried out the mixing of the HIPE at room temperature. Further modification of the porous characteristics of the polymer would be decided according to the morphological structure obtained for our required agricultural application. The calculation of average pores and interconnects diameter was performed using the image analysis software ImageJ. The pore and interconnects sizes may vary throughout the polyHIPE discs, hence SEM images at various locations (top, center, bottom) were used. Thus, the evaluation of the average pore and interconnects diameter was performed by measuring approximately 50 pores with the help of imageJ and the data was then subjected to statistical analysis. Table 4-2 shows the average pore and interconnect size of the three polyHIPE samples prepared.

Table 4-2 Average pore and interconnect size for polyHIPE samples

PolyHIPE sample code	Average pore size (µm)	Average interconnect size (µm)
SPHPA10	46.89 ± 3.1	11.2 ± 2.5
SPHPA20	37.5 ± 4.6	9.1 ± 0.6
SPHPA30	30.8 ± 2.2	7.3 ± 1.2

It is worth nothing that the size of the pores and interconnects reduce with increasing the mixing time from 10 minutes to 30 minutes. The average pore size for the sulphonated polyHIPE was reduced by 34.3% from 46.8 µm to 30.8 µm, whereas the average interconnect size decreased similarly by 34.8% with the increase in mixing time. Thus, our results confirmed that the variation of the average pore diameter can be tuned by the mixing time of the emulsion. The extended mixing time accounts for the input of mechanical energy consequently reducing the emulsion droplet size. Burke *et al.* (2010) demonstrated that hydrophilic sulphonated polyHIPEs obtained with mixing time of 1 min resulted in large pore-size polymers of nearly 150 µm. These polyHIPEs increased the water uptake capacity by 18 fold and resulted in increasing the biomass yields of rye grass by about 140 and 300% under semiarid and arid conditions respectively. Similarly Akay and Fleming (2012), investigated the application of these sulphonated polyHIPEs as soil additive which act as micro-bioreactors within the soil with the aid of nitrogen fixing bacterium *Azopirillum brasilense* to enhance the yield. Both of the studies mentioned above, produced sulphonated polyHIPEs with large pore diameters between 100 to 150 µm. However, for water transmission within the soil and adequate bacterial activity pore sizes ranging from 2 µm to about 50 µm are beneficial (Rowell, 1994; Troeh, 2005). Larger pores and interconnects may allow efficient transfer of the water and nutrients, but may also risk water and essential nutrients being leached out under field conditions. Akay *et al.* (2004) in their study of using polyHIPEs as potential scaffolds for bone tissue engineering demonstrated that pore and interconnect sizes of almost 40 µm were beneficial for cell penetration and showed enhanced migration into the polyHIPE structure.

In this study, considering the application of sulphonated polyHIPEs in clay loam and sandy loam soils the morphological properties of sulphonated polyHIPE SPHPA10 with surface area of 100.6 m^2/g and interconnect and pore sizes ranging from 11.2 µm to 46.8 µm was considered appropriate. Figure 4-12 shows the SEM images for SPHPA10, SPHPA20 and SPHPA30 obtained with varying mixing time of 10, 20 and 30 minutes respectively. It is evident from the SEM images that pore and interconnect sizes are reduced significantly with an increase in mixing time. The SEM image figure 4-12 (c), 30 minutes mixing time also depicts that the pore and interconnect distribution becomes homogeneous

with circular pores, whereas SEM image figure 4-12 (a) with 10 minutes showed irregular pore shapes.

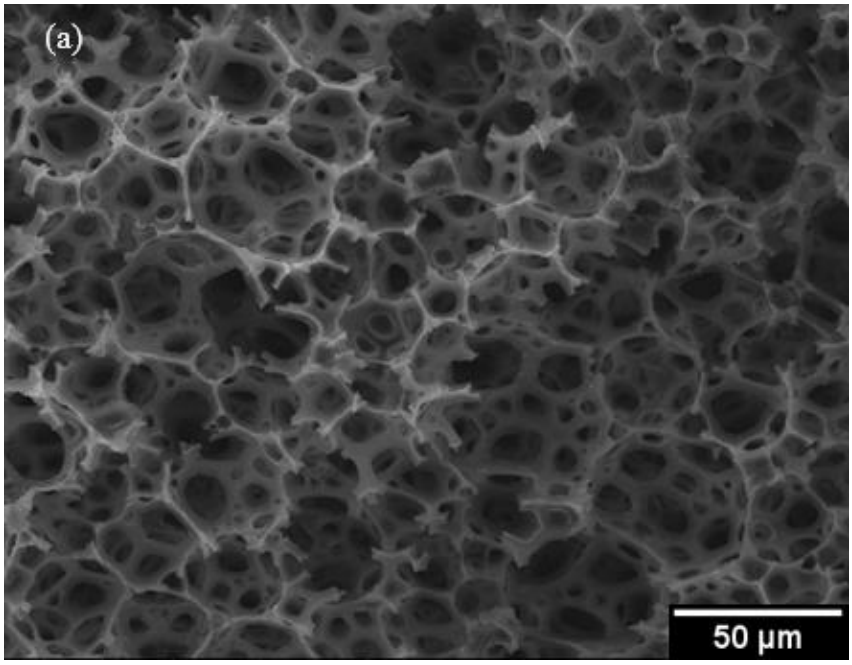

(a) SPHPA10 polyHIPE

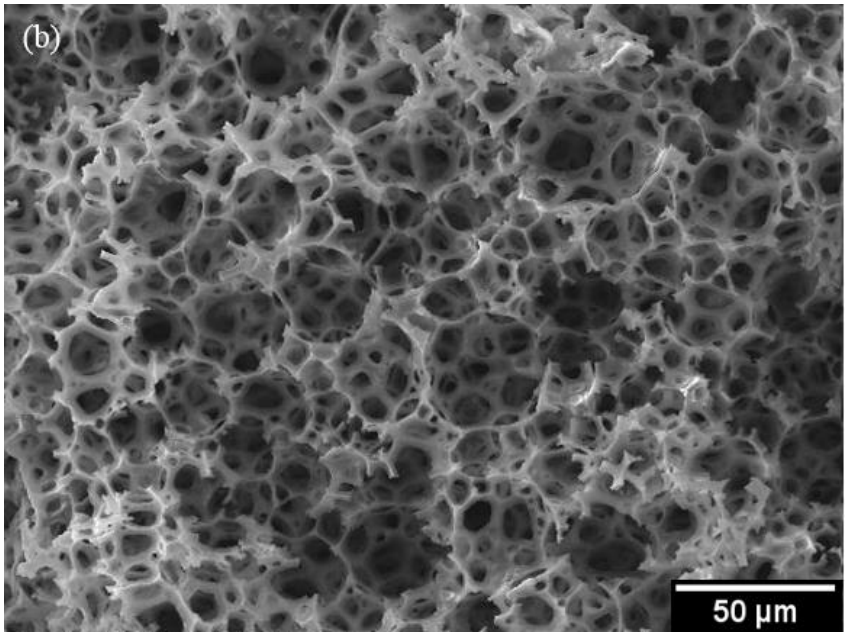

(b) SPHPA20 polyHIPE

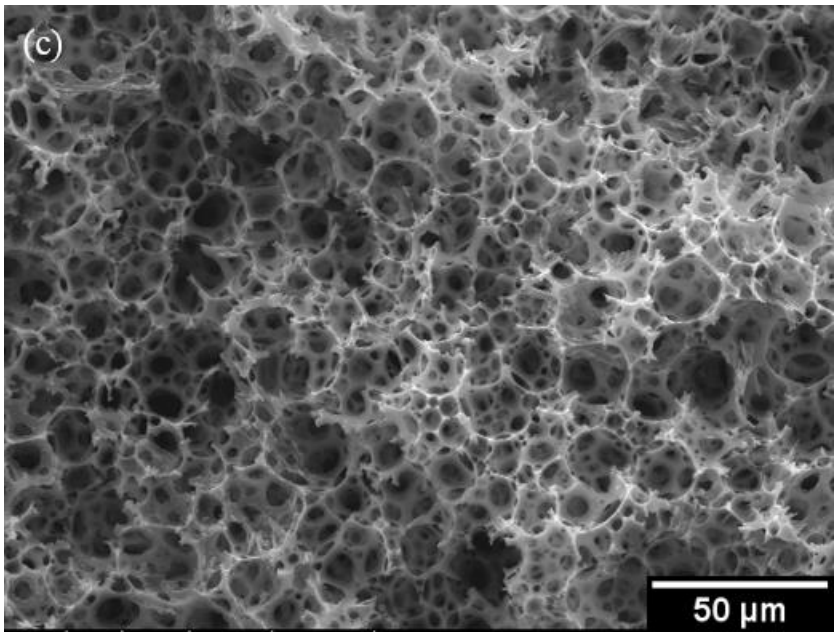

(c) SPHPA30 polyHIPE

Figure 4-12 SEM images magnification 500x of (a) SPHPA10, (b) SPHPA20 & (c) SPHPA30 with varying mixing time of 10 minutes, 20 minutes and 30 minutes respectively (Scale bar: 50µm).

These sulphonated polyHIPEs SPHPA10, SPHPA20 and SPHPA30 were further investigated for their water uptake properties which is an important aspect of agricultural processes and plant growth.

4.3.4 Water uptake studies

The sulphonated polyHIPE polymers were spongy and hydrophilic. The absorption capacity of SPHPA10, SPHPA20 and SPHPA30 was determined by selecting three discs from each sample codes. The discs were weighed before the water uptake test. The whole discs were then immersed in a beaker of distilled water until absorption equilibrium was reached. One of the disc was removed after a minute to check the absorption within the structure. Fracturing the disc, it was observed that most of the disc was swollen except for a small section at the center which remained dry. This implied that the hierarchical network of pores allowed the absorption of water into the structure of the polymer within a small time frame. All the discs achieved equilibrium swelling (no more weight change was observed) after 5 minutes of soaking. Figure 4-13 shows swollen SPHPA10

polyHIPE which had undergone water stress at equilibrium swelling and developed cracks. Figure 4-14 (a) & (b) shows a swollen SPHPA10 disc and the center dry section after 1 minute water uptake test.

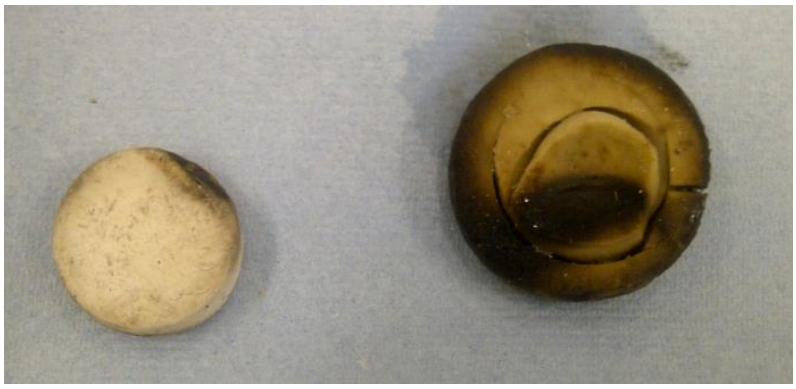

Figure 4-13 SPHPA10 swollen and cracked after water uptake test

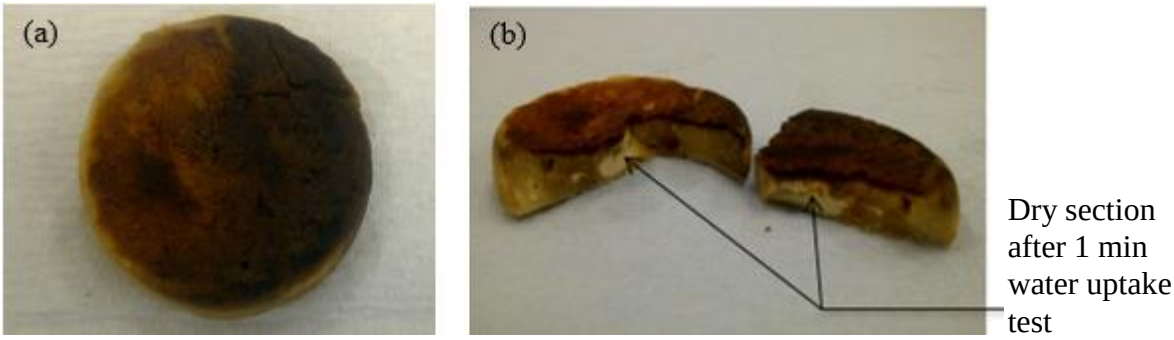

Figure 4-14 (a) Swollen SPHPA10 & (b) SPHPA10 showing the dry section after 1min water uptake test

After equilibrium, the discs were removed from the beaker and excess of water was dabbed with a tissue. The disc were reweighed. The water absorbed by each disc was calculated using Equation 4-1.

Equation 4-1

$$\text{Water uptake} = \frac{w_e - w_d}{w_d}$$

Where,

W_e = weight of the disc recorded at equilibrium (swollen state)

W_d= weight of the disc recorded before soaking in water (dry state)

Thus, the water uptake capacity was calculated as a ratio of the amount of water held by the polymer disc in the equilibrium state to the weight of the disc in dry state. The data for each polyHIPE sample was evaluated as an average of three readings using three discs of the same sample code. PolyHIPE sample SPHPA10 and SPHPA20 demonstrated a maximum of about 17-fold whereas SPHPA30 exhibited 18-fold water uptake capacity respectively. The results were tabulated in Table 4-3.

Table 4-3 Water uptake test for polyHIPE samples

PolyHIPE sample code	Water uptake % (g/g)	Fold increased
SPHPA10	1562	17
SPHPA20	1609	17
SPHPA30	1752	18

The crosslinker concentration plays an important role in the water absorption capacity of the polyHIPEs. In this study, DVB was used as the crosslinking agent to modify the properties of the polymer. The function of the crosslinking agent is to join two or more molecules from a smaller molecule. Hilgen *et al.* (1975) describes that crosslinking increases the rigidity of the structure and thus maintains the conservation of porosity within the structure. Their studies with styrene DVB copolymers prepared with sufficient DVB content maintained the pore stability and retained their pore volume after removal of solvent. Extensive studies done by Burke (2007) on sulphonated polyHIPE polymers with varying concentration of DVB demonstrated that 10% DVB content was optimum with respect to water absorbency and crosslinking density. Their studies concluded 10% DVB content increased the water absorption by 58.4% as compared to the polyHIPE prepared with 8% DVB. Low DVB content (2% DVB) showed low water absorption which gradually increased with the increase

in concentration of DVB. Thus, their study illustrated water absorption capacity increases with increasing crosslinking concentration until it reaches an optimum point and then decreases. They also reported that further increase in the DVB content effected the porosity and caused reduction in the surface area of the polymer. Similarly Li *et al.* (2004) in their study on the synthesis of salt resisting polymeric hydrogel reported that as the amount of crosslinking agent *N,N'*-methylene bisacrylamide is increased, the absorbency of the hydrogel increases, however it decreases if the crosslinking concentration is increased above 0.1%.

In our study, we used 10% DVB for synthesis of our polyHIPEs based on Burke (2007) studies. All three polyHIPE samples showed excellent water absorption capacity as seen from Table 4-3. The water uptake capacity was increased upto 17 to 18 fold in these polymers compared to their dry state. The water uptake results show that the absorption capacity was not affected by the mixing time. However, the amount of time taken to reach equilibrium swelling differed. Nevertheless, all three polyHIPE samples showed rapid water uptake and were saturated and swollen within 5 minutes of the water uptake test. Some of the discs showed signs of water stress and cracks under equilibrium state as shown in Figure 4-13.

Okay (1987) explains that the inhomogeneity of the crosslink distribution play an important role in the swelling behavior. The author demonstrated that the inhomogeneity in the styrene DVB copolymers increases with increasing DVB concentration. These findings were consistent with polymers prepared by Çalkan (2007). The regions that swell less or more are due to the reaction occurred during polymerization between the DVB monomers and the mechanism of the resultant network formed. Later Yan *et al.* (2000) also reported that the unusual swelling were due to the inner strain developed in the less crosslinked domains of the styrene DVB copolymers. Thus the cracks developed in some of our polyHIPEs disc were due to the less crosslinked network formed during the initial polymerization reaction. The structure of the material is critical to explain the water uptake studies. Hence the modification of the polyHIPEs making it hydrophilic for water uptake was further studied with FTIR spectra.

4.3.5 Fourier Transform Infrared (FTIR)

The polyHIPE samples produced were highly hydrophilic as explained in the previous section. The incorporation of the $SO_3^-H^+$ functional group imparting hydrophilicity to the polymer was evaluated through FTIR. It was observed that the spectra for SPHPA10, SPHPA20 and SPHPA30 were almost same overlapping each other. This can be expected as all the three samples were sulphonated for the same time duration. Hence in this section we have compared spectra of SPHPA10 with the unsulphonated polyHIPE sample to understand the changes occurring due to sulphonation reaction. The IR spectra of unsulphonated and sulphonated polyHIPEs (SPHPA10) were compared as shown in Figure 4-15 to study the incorporation of sulphonic acid groups on the aromatic rings.

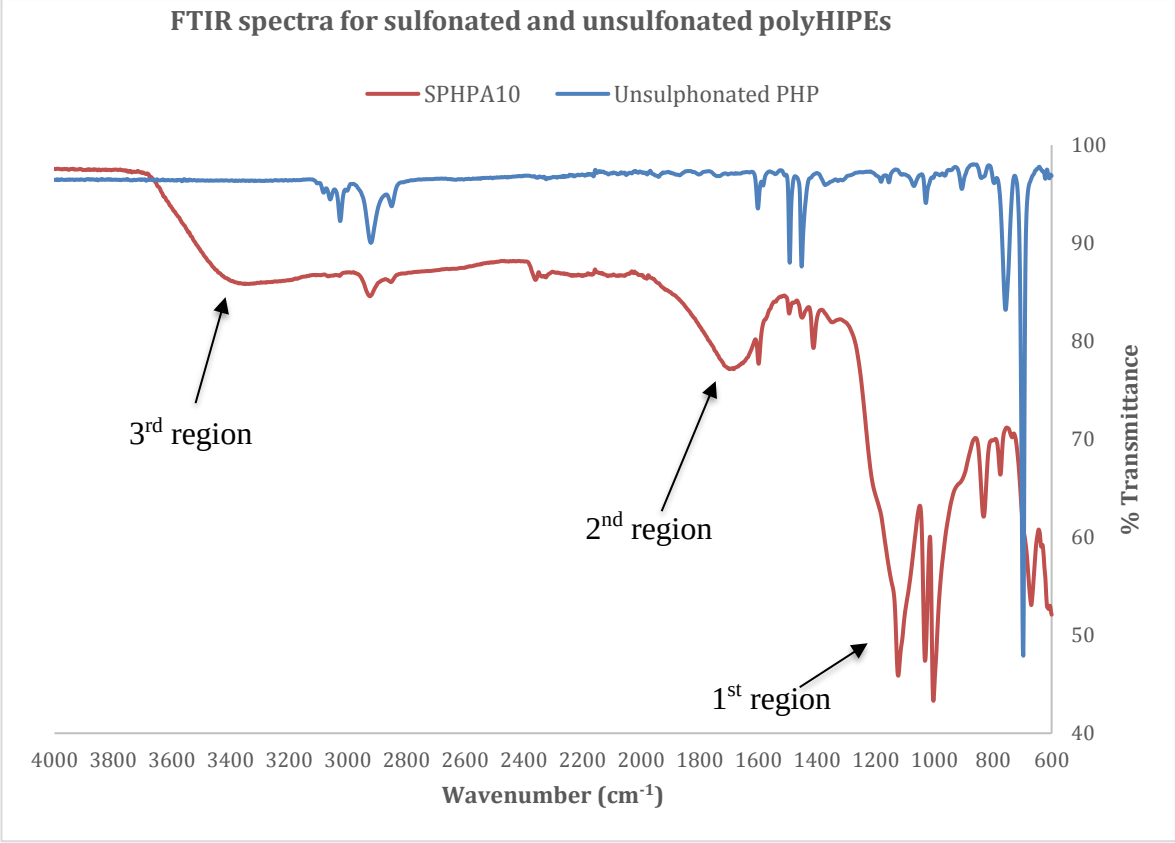

Figure 4-15 FTIR spectra of unsulphonated and sulphonated (SPHPA10) polyHIPEs

Sulphonation results in significant changes in the spectrum as seen for SPHPA10. The appearance of broad and strong peaks at three main regions

confirms the sulphonation of the polymer. The first region in figure 4-15 at the frequency 1000 – 1300 cm^{-1} is assigned to -SO_3H groups. The three prominent bands observed in this region were 830, 1003, 1034 and 1176 cm^{-1} represent characteristics bands associated with the stretching vibrations due sulphonation (Lin-Vien *et al.*, 1991; Elabd and Napadensky, 2004). The presence of bands at 830 and 1003 cm^{-1} is observed due to the in-plane bending vibrations of the aromatic ring in styrene substituted with the sulfonic acid group, whereas the symmetric and asymmetric stretching vibrations of the sulfonate group is represented by bands 1034 and 1176 cm^{-1} respectively.

The second region in the figure 4-15 showing bands at 1485 cm^{-1} and 1590 cm^{-1} were observed due to the aromatic C=C stretching whereas the band at 1412 cm^{-1} is associated to asymmetric C-H bending deformation of methyl group (Lin-Vien *et al.*, 1991). The band between 1600 cm^{-1} and 1800 cm^{-1} is assigned to the generation of carbonyl (-COOH, >C=O, etc) groups during sulphonation which is in agreement with the peaks obtained by Malik (2009) in their studies for sulphonation of styrene divinylbenzene macroporous resins. Finally, the third region showing a broadband between 3200 – 3400 cm^{-1} as seen in Figure 4-15 is associated with the region of OH stretching vibrations which also indicates the formation of acid sites after sulphonation (Ordomsky *et al.*, 2012). This effect is associated with the increase in hydrophilic behavior due to the incorporation of the sulphonate group in the polyHIPE structure. The appearance of bands at 699 and 759 cm^{-1} seen in the unsulphonated polyHIPE spectra in Figure 4-15 is attributed to the out of plain bending band of C-H in the benzene ring. Sulphonation leads to disappearance of these bands. The infrared assignments of SPHPA10 spectra were illustrated in Table 4-4.

In summary, the changes observed in the FTIR spectra of SPHPA10 thus ascertained the presence of -SO_3H groups. The results of FTIR analysis clearly demonstrated the success of sulphonation process and the incorporation of the suphonate groups in the polyHIPE structure. The thermal stability of the modified structure is assessed in the next section.

Table 4-4 Infrared Assignments of SPHPA10

Frequency range (cm^{-1})	Bond Assignments
3200, 3400	OH stretching vibrations
1412	Asymmetric C-H bending deformation of methyl group
1485, 1590	Aromatic C=C stretching
1034, 1176	symmetric and asymmetric stretching vibrations of the sulfonate group
830, 1003	In-plane bending vibrations of the aromatic ring substituted with the sulfonic acid group

4.3.6 Thermogravimetric Analysis (TGA)

To study the degradation of polymers, TGA with linear temperature increase is a very useful tool. The thermal stability of the sulphonated polyHIPE samples was examined by TGA under a nitrogen gas atmosphere. The polyHIPE samples SPHPA10, SPHPA20 and SPHPA30 were thermally analyzed to study the effect of the degree of sulphonation on their thermal properties. The thermogram obtained for all three samples were similar, hence thermogram for SPHPA10 is discussed in this section. The thermogram and differential thermogravimetric trace of unsulphonated polyHIPE and SPHPA10 are shown in Figure 4-16 a & b.

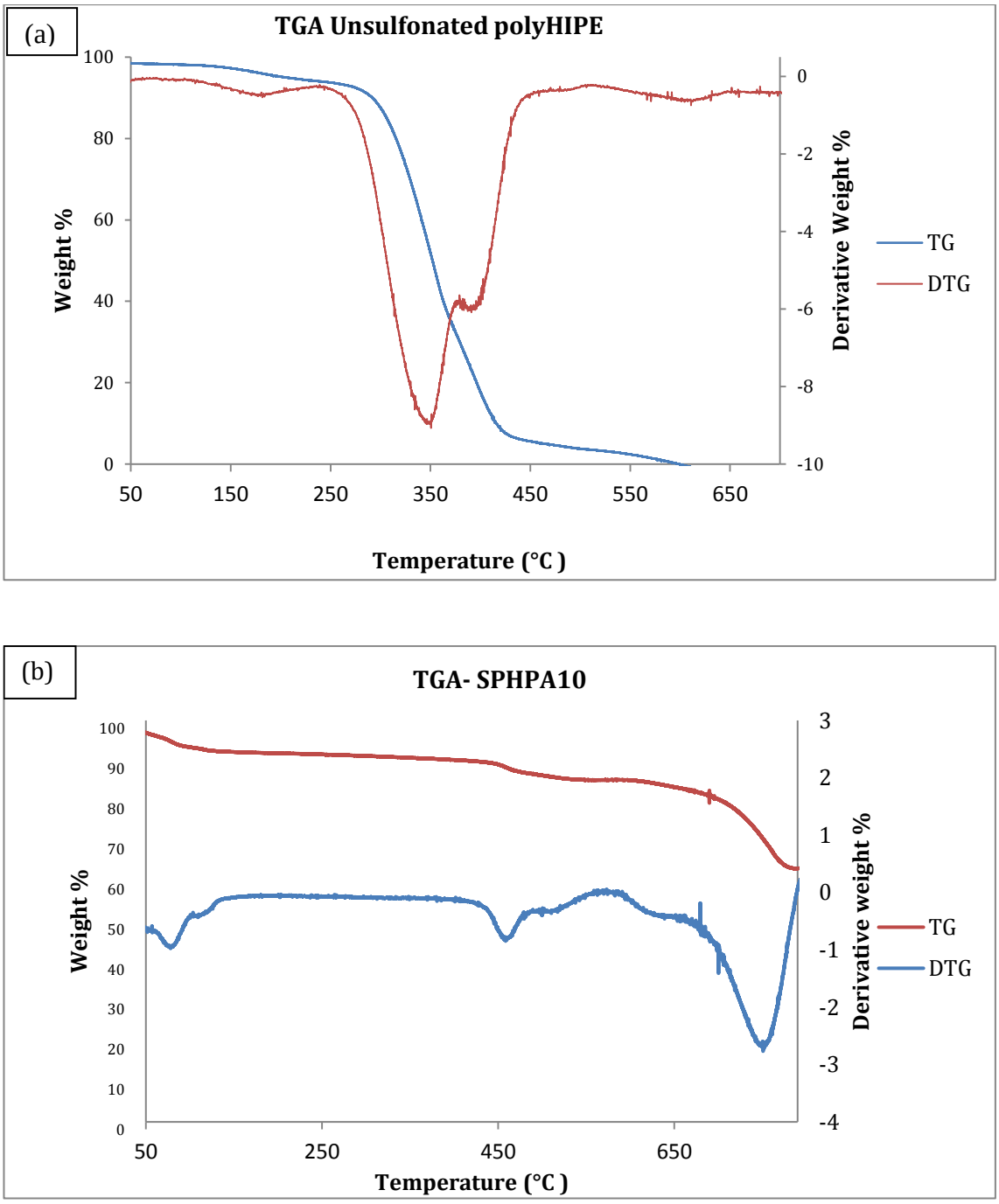

Figure 4-16 TGA trace (a) Unsulphonated PolyHIPE & (b) SPHPA10

Figure 4-16 (a) illustrates that the initial decomposition temperature for unsulphonated polyHIPE is around 250^{0}C. The major weight loss was obtained over the temperature range of 250 to 450^{0}C which corresponds to the structural decomposition of the polyHIPE. The weight loss region around 350^{0}C is attributable polystyrene decomposition. This assignment agrees with the studies

by Kaniappan and Latha (2011) on investigation and characterization of polystyrene/ poly methyl methacrylate blends. Two step degradation behavior was observed by the thermogram of SPHPA10 as seen from Figure 4-16 (b). The initial weight loss observed around 70-80^{0}C attributes to small amount of moisture loss from polyHIPE considering the hygroscopic nature of the monolith. The second weight loss observed around 400-450^{0}C corresponds to the decomposition of the sulphonic acid groups. They represent the breakdown of the sulphonate group attached to the styrene-DVB rings. This finding is consistent with the studies of thermo stability of highly sulfonated polystyrene by Smitha *et al.* (2003). The final weight loss around 650^{0}C corresponds to the polyHIPE backbone/chain degradation with a residual mass of 34.79%. The thermal properties of sulphonated polyHIPEs were similarly to the sulfonic cationites investigated by Singare *et al.* (2011). The authors reported degradation of the sulfonic cationites namely Amberlite IR-120, Indion-223 and Indion-225 at higher temperatures up to 520^{0}C showing decomposition of sulfonic acid functional groups.

Thus, the decomposition temperature of the sulphonated polyHIPE (SPHPA10) is higher as compared to that of unsulphonated polyHIPEs. It indicates that SPHPA10 possess higher thermal stability than the unsulphonated polyHIPE. Our studies conclude that the incorporation of the sulphonic groups thermally stabilize the polymer backbone by shifting the degradation temperature to 650^{0}C.

4.3.7 Ion exchange capacity (IEC)

To determine the ion exchange function of the resulting polyHIPE incorporated with the sulphonic group, titrimetric analysis of the sulphonated polyHIPEs was performed. The ion exchange capacity depends on the presence of number of ion exchange groups occurring in the polyHIPE structure. Hence, the IEC of all the three polyHIPE samples (SPHPA10, SPHPA20, and SPHPA30) was determined by acid-base titration method.

In this study, prior to analysis the sulphonated polyHIPE samples were powdered. This was done to increase the contact area. They were then immersed

with 1 M hydrochloric acid solution for 1 hour. This assured that all the SO_3^- groups were in the H^+ form within the polyHIPE. Excess amount of hydrochloric acid was then eliminated by rinsing the powdered polymer repeatedly with deionized water. The powdered polyHIPE samples were dried in an oven at 60^0C. Subsequently, these dried samples were weighed and immersed in 0.1 M NaOH solution. Thereafter the slurry was swirled for 3 hours to displace H^+ ions. The solution obtained was then titrated against 0.1 M hydrochloric acid solution. All samples were analysed using a Mettler Toledo Excellence Line T90 titrator with a DG111-SC electrode attached. The samples were analysed and processed using LABX 2014 software. The ion-exchange capacity of the polyHIPEs (IEC, meq/g) was calculated with the following Equation 4-2 by Akkaramongkolporn *et al.* (2009)

Equation 4-2

$$\mathbf{IEC} = \frac{\boldsymbol{C} * \boldsymbol{V}}{\boldsymbol{W_{dry}}}$$

Where, C is the standardized concentration used

V is the volume of the titrant

W_{dry} is the mass of the dry polyHIPE sample

The data for IEC and water uptake for each polyHIPE sample was evaluated as an average of three readings using three discs of the same sample code. Table 4-5 represent the experimental (average of three titrations) IEC values for sulphonated polyHIPE samples SPHPA10, SPHPA20, and SPHPA30 and its corresponding weight increase after sulphonation and water uptake.

Table 4-5 Effect of sulphonation and IEC in polyHIPEs

PolyHIPE sample code	%Weight Increase after sulphonation	Water uptake % (g/g)	IEC (meq/g)
SPHPA10	62	1562	3.22
SPHPA20	65.52	1609	3.40
SPHPA30	66.31	1752	3.42

All three polyHIPE samples exhibited good ion exchange capacity. SPHPA10, SPHPA20 and SPHPA30 exhibited IEC of 3.22, 3.40 and 3.42 meq/g respectively. It was observed that there was slight increase in the IEC values with the increase in mixing time. This observation can be attributed to the decrease in pore sizes of the polyHIPE samples with increase in the mixing time. According to Gokmen and Du Prez (2012) micropores less than 2 nm can maximize surface area for ion storage whereas the mass transport to the interior regions of the samples is carried out by mesopores (2 to 50 nm). SPHPA20 and SPHPA30 exhibited average pore sizes in the range of 37.5 µm and 30.8 µm respectively whereas the average interconnects were in the range of 9.1 and 7.3 µm respectively. The hierarchical structure with the decrease in pore size with increase in mixing intensity thus reflect on the higher IEC values seen in SPHPA20 and SPHPA30 samples.

Also, it was found that the weight of the polyHIPE disc increased after sulphonation, hence the percent weight increase was observed in all the samples. The addition of the sulphonic group results in the increase in weight in the resultant polymers. Consequently, this confirms successful sulphonation which was corroborated by the FTIR results obtained in this study. The intensity of the band 830 and 1003 cm^{-1} observed in Figure 4-15 confirms the extent of sulphonation reflecting the substitution of the H atom in an aromatic ring by a sulphonate group (Blanco *et al.*, 2001). However in our study the FTIR spectra for all three samples almost overlapped each other hence we could not study the difference in extent of sulphonation between the samples. Nevertheless, our IEC

data for SPHPA20 and SPHPA30 show a marginal difference which might explain the overlap in the FTIR spectra for these samples. Toro *et al.* (2008) reported in their studies that in case of polystyrene polymer, mono-sulphonation of each benzene ring in the polymer backbone exhibits IEC of about 5.4 meq/g whereas in polystyrene-DVB polymers with 50% crosslinking, IEC decreases to approximately 4.7 meq/g. This effect was observed due to increase in the molecular weight of the resultant polymer structure. In comparison, the IEC of all three polyHIPE samples in our study indicate higher level of sulphonation. The uniqueness of the structural hierarchy with interconnected pores in SPHPA10, SPHPA20 and SPHPA30 provide less tortuous pathways for ion transport.

Recent studies by Barlik *et al.* (2015) in surface modification of monolithic polyHIPE polymers for anionic functionality demonstrated IEC of 3.01 meq/g for styrene-DVB polyHIPEs with 12% degree of crosslinking. The volume fraction of styrene and DVB used by the authors in their study was similar to the polyHIPEs prepared in this research except for the concentration of DVB (23%) which was slightly higher. Although their experimental results effectively demonstrated good IEC for the polyHIPEs, they reported water uptake by polyHIPEs was enhanced only 10 times it's mass. In contrast, the water uptake in our study for all the three polyHIPEs was increased by almost 17-18 fold. Thus, our studies suggest good swelling capacity with lower concentrations of DVB. These results are consistent with the studies by Chakrabarti and Sharma (1993) where they reported that gel type resins made from styrene DVB beads with low content of DVB (12%) exhibit good swelling capacity, however higher percentage of DVB reduces its swelling capacity and hinders the rate of diffusion processes within the polymer structure. Similarly, work reported by Ahmed *et al.* (2004) indicate that the cation exchange capacity of styrene-DVB resins decreases when the beads were manufactured with high proportions of DVB. They also demonstrated that the exchange capacity depends on the porosity of the beads which aids in faster diffusion of the sulphonating agents through the interconnected pores.

Thus, from our results it may in principle be concluded that greater degree of sulphonic groups added to the polyHIPEs, greater was the interchange of counterions which results in higher IEC. There is a definite correlation between the IEC and %DVB added during the synthesis of the polyHIPEs. Studies indicate increasing the concentration may have adverse influence on the ion exchange

capacity although the effect may be controlled by the porosity and interconnected hierarchical structure of the polymer. Overall, it was observed polyHIPEs prepared in our study not only have extended surface area, but the interconnected morphology and good IEC make them attractive as an ion exchange material.

4.4 Sulphonated PolyHIPEs – Investigation of polymer network for biocatalytic film formation

Sulphonated polyHIPEs were tested for catalytic biofilm growth with *Shewanella Oneidensis* MR-1. Shewanella is typically a rod shaped bacterium with 2-3 µm in length and 0.4-0.7 µm in diameter. These bacterium have capacity to respire on various metals and successfully reduce them, resulting in formation of biofilms (Gralnick and Newman, 2007). In agriculture, biofilms can facilitate exchange of nutrients, metabolites and play an important role in rhizosphere which is a critical interface region between the plant roots and soil. Biofilms have also recently been of great commercial concern for their potential use in sustainable production of chemicals (Rosche *et al.*, 2009). Sulphonated polyHIPE sample SPHPA10 was used for the catalytic biofilm formation due its pore sizes and morphology which was found suitable for further testing in sandy and clay loam soils discussed in chapter 6.

Biological work carried on SPHPA10 for the biofilm formation is described in sections 3.6.1 and 3.6.2 included in chapter 3. Control experiments indicated that the appropriate period for the biofilm formation was 12 days. Hence samples of SPHPA10 polyHIPEs were taken for observation from the petri dish collected on the 3rd, 5th, 7th, 10th and the 12th day to monitor the biofilm growth.

4.4.1 Biofilm Growth on SPHPA10

The following SEM images shows the biofilm formation on SPHPA10 polyHIPE samples. Figure 4-17 shows the SEM images of the SPHPA10 polyHIPE (blank) before the biofilm formation.

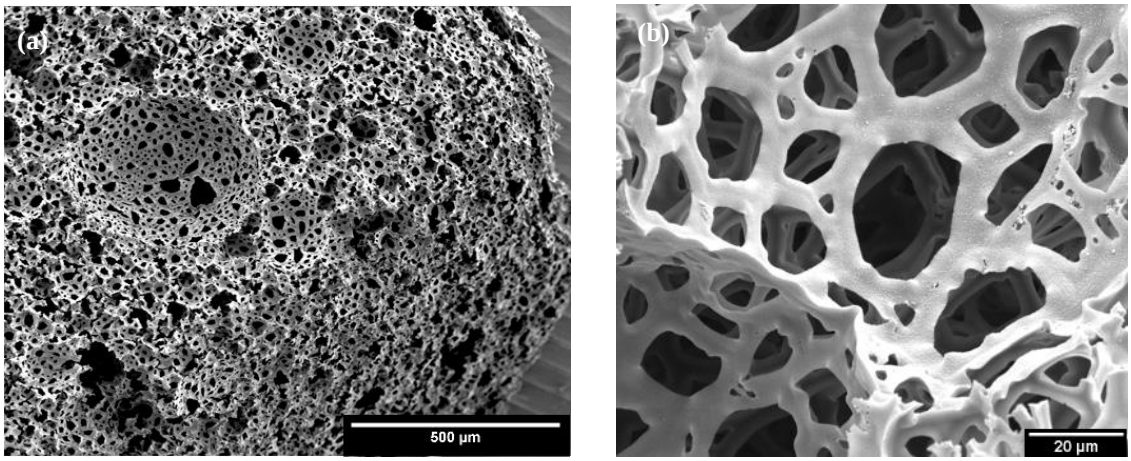

Figure 4-17 SEM images of SPHPA10 (Control) (a) Overall view magnification 500x (b) Blank view magnification 2000x.

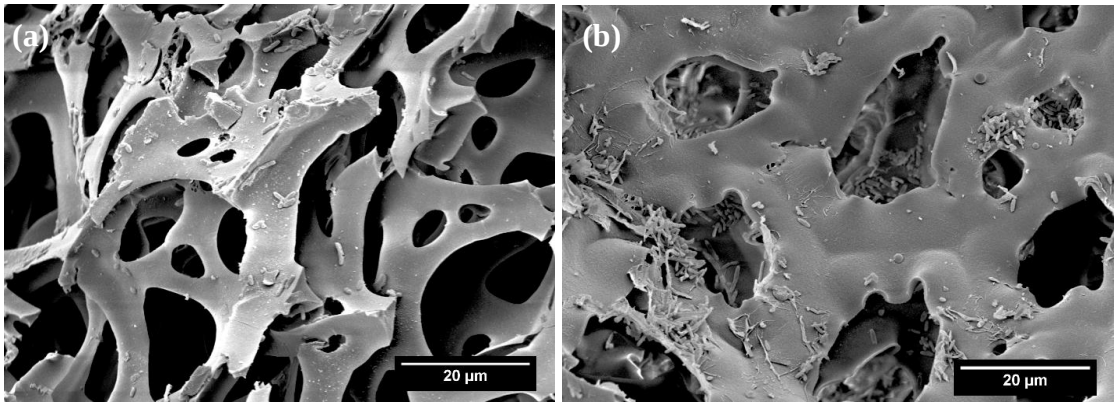

(a) SPHPA10 - Day 3 **(b) SPHPA10 - Day 5**

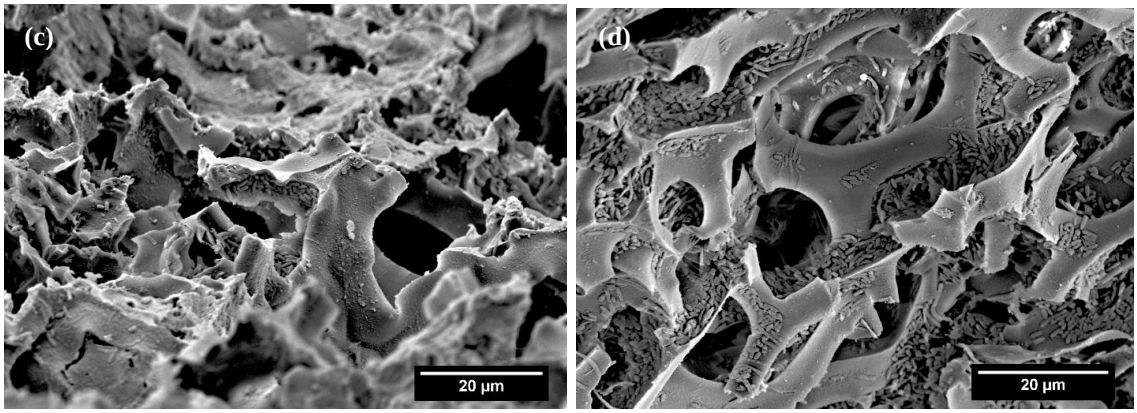

(c) SPHPA10 - Day 7 **(d) SPHPA10 - Day 10**

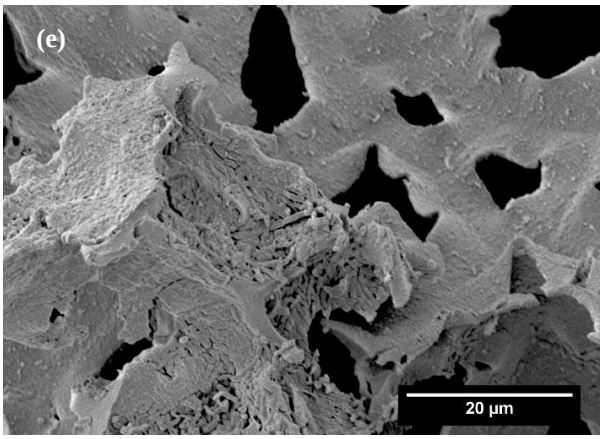

(e) SPHPA10 - Day 12

Figure 4-18 SEM images magnification 1200x Biofilm formation (a) Day 3, (b) Day 5, (c) Day 7, (d) Day 10 & (e) Day 12

From the SEM images, SPHPA10 samples taken on the day 3 shows the rod shaped bacteria attaching to the rough surfaces of the polymer. Day 5 samples clearly show that the bacterium cells have divided rapidly and formed isolated colonies which were found adhering to the uneven curvy structure of the polymer surrounding the pores. The depth formed by the curvy surfaces appear to provide a channels for the biofilm development. Day 7 samples illustrates that the biofilm becomes more established and propagates within the structure. The cells proliferate and grows in thickness along the gaps and fractures on the polymer. Isolated micro-colonies appear on different region of the polymer. They appear to grow laterally covering the surface area available around them. SEM images taken on day 10 show a dense population of the colonies rapidly covering most of the pores and interconnects as seen in Figure 4-18 (d). Day 12 SEM images illustrate fused micro-colonies showing a biofilm formation. The previously isolated colonies completely proliferate over the uncovered polymer surface blocking the pores and interconnects. Figure 4-18 (e) also depicts the fused micro-colonies towering and increasing in thickness over the surface. Thus, a complete biofilm was formed over the SPHPA10 surface as well as within the polymer. It was observed that the pores on the surface were more densely covered with the micro-colonies compared to those inside the structure. The migration of the cells is due to the transport of the nutrients and metabolites by

the concentration gradients and convective forces from fluid flow within the hierarchical structure (Sikavitsas *et al.*, 2002). Similar growth structure for biofilm formation with *S. Oneidensis* MR-1 was reported by Thormann *et al.* (2004), where they demonstrated initial lateral spreading of the biofilm of the surface was followed by extensive vertical growth after the surface was completely covered. This resulted in formation of towering mushroom like structures giving rise to three dimensional architecture. They also reported that *S. Oneidensis* MR-1 grow more robust biofilms, with greater interaction between the surface and the microbes when the nutrients levels are poor. Another study by Akay and Fleming (2012) describes the use of nitrogen fixing bacteria *Azospirillum brasilense* supported on hydrophilic polyHIPEs which aids in nitrogen fixation. These polyHIPEs immobilised with the bacteria act as micro-bioreactors within the soils which facilitate water and nutrients uptake proving a critical interface between plant roots and soil. Their studies demonstrated progressive yield enhancement with the use of these sulphonated polyHIPEs also providing a sustainable alternative to expensive chemical fertilisers.

Hence, our results indicate that the hierarchical structure of the pores and interconnect facilitates the transport of the cells migrating from one region to another within the polymer. The enhanced surface area, along with the surface chemistry, pores and interconnectivity was found suitable for biofilm formation with *S Oneidensis* MR-1. Thus, catalytic biofilm was successfully developed on SPHPA10 sulphonated polyHIPE.

4.5 Conclusions and Outlook

This study outlined the preparation and characterization of sulphonated polyHIPEs. It was observed by varying the mixing time the architectural morphology of the polyHIPEs could be altered as per desired applications. Microwave irradiation significantly reduces the process duration whilst enhancing the polyHIPE structure. It was found that sulphonation through microwave irradiation is more sustainable as it reduces the sulphonation time from several hours to a few minutes with no excess acid wastage. Thus this microwave

treatment for sulphonation achieves process intensification over conventional thermal treatments. Sulphonation also leads to creation of very small pores which not only increases the surface area but also provides accessibility to ion exchange sites.

Sulphonated polyHIPEs exhibited presence of considerable amount of sulphonic groups in the polymer backbone resulting in significant enhancement in polyHIPE hydrophilicity. Thermal stability was also enhanced in these polyHIPEs. These resulting polyHIPEs with high ion exchange capacity, hydrophilicity and thermal stability can be also used as catalyst support or proton exchange membrane. Biological work with *S. Oneidensis* MR-1 confirmed that the polymer proves as a good substrate for the growth of the micro-organisms resulting in biofilm formation. Thus, these highly porous polyHIPEs are easy to synthesize and functionalize, which could become an alternative to conventional hydrogels/ beads in agricultural applications.

Chapter 5 Preparation and functionalization of monolith high surface area hypercrosslinked polyHIPE polymers

This chapter presents the experimental outputs generated from the preparation and functionalization of polyHIPE polymers with porogens chlorobenzene and chloroethylbenzene. Hypercrosslinking process and Friedel-Crafts reaction was used to enhance the surface area. The objective of the experiments was to further enhance the polyHIPE morphology and increase the surface area. Several independent factors such as type and composition of the monomers and initiator significantly affect the formation of pores during synthesis of the monolith. Sulphonated polyHIPEs demonstrated good ion exchange capacity and thermal stability, which can have potential application as catalyst support. However they lacked the adequate surface area required to be used as monolithic catalyst supports. In order to increase the surface area, we investigated addition of porogens and preparation of hypercrosslinked polyHIPE polymers with catalyst precursors.

In this study, we for the first time report the use of $FeCl_3$ in the aqueous phase forming a stable emulsion. There is no reported literature of addition of the Lewis acid catalyst to HIPE prior to polymerisation. The selection of $FeCl_3$ for hypercrosslinking was done based on the studies carried out by Ahn *et al.* (2006) where they demonstrated $FeCl_3$ was the most effective Lewis acid catalyst (compared to $AlCl_3$ and $SnCl_3$) for the hypercrosslinking reaction. Moreover, different studies have reported use of $FeCl_3$ catalyst for synthesis of hypercrosslinked polymers with high surface areas (>1000m^2/g) (Lee *et al.*, 2006; Macintyre *et al.*, 2006; Fontanals *et al.*, 2008). Similarly, Fontanals *et al.* (2015) in their hypercrosslinked materials review states that $FeCl_3$ may be consistently more active due to its solubility and molecular size. In addition $FeCl_3$, being a solid catalyst was preferred in terms of ease of handling.

5.1 Preparation of hypercrosslinked polyHIPE polymers

PolyHIPEs were prepared with porogens as described in section 3.2.1 and 3.2.2 of Chapter 3. HIPE 3 and HIPE 4 formulations were used for the hypercrosslinked polyHIPEs. The polyHIPEs obtained by these formulations were soxhleted and dried for hypercrosslinking process. Hypercrosslinking of the polymers was carried out as described in section 3.3.1 in Chapter 3. We denote hypercrosslinked polyHIPEs prepared with HIPE 3 as HX1-PHP whereas HIPE 4 formulation polyHIPEs were coded as HX2-PHP. Three different hypercrosslinked polyHIPEs were prepared with HIPE 4, HX2-PHP10, HX2-PHP20 and HX2-PHP30 where the homogenization time for the polyHIPEs was varied 10 minutes, 20 minutes and 30 minutes respectively. Sulphonated polyHIPEs (SPHPA10) prepared were also hypercrosslinked post polymerization as described in section 3.3.1 in Chapter 3. Hypercrosslinked sulphonated polyHIPEs were coded as HX-SPHPA10.

5.2 Catalyst insertion in hypercrosslinked polyHIPE polymers

Current technique of catalyst insertion are carried out by impregnation of the hypercrosslinked polymers in swollen state with a suitable catalyst precursor followed by catalyst reduction. However, due to the very small pore sizes of the hypercrosslinked polymer, most of the catalyst would be located on the surface of the polymer rather than at the interior and within the pores. Hence to obtain uniform catalyst distribution throughout the polymer, the following two routes could be attained:

(1) The presence of hierarchic pore structure in the hypercrosslinked polymers which allows catalyst precursor in the solution to penetrate uniformly into the polymer.

(2) The incorporation of the catalyst precursor salt dissolved in the aqueous phase of the HIPE at the emulsification stage. However, this requires that the catalyst precursor to be incorporated into the polymer acts as Friedel-Crafts catalyst.

The latter option restricts the choice of catalyst precursor. However, we hypothesize uniform catalyst distribution throughout the polymer. Hence this second option was investigated to study the distribution of the catalyst in our hypercrosslinked polymers.

5.3 Results and Discussion

5.3.1 Effect of porogens and hypercrosslinking on surface area

The following Figure 5-1 shows the SEM image of the structural morphology of HX1-PHP polyHIPE polymer before and after hypercrosslinking.

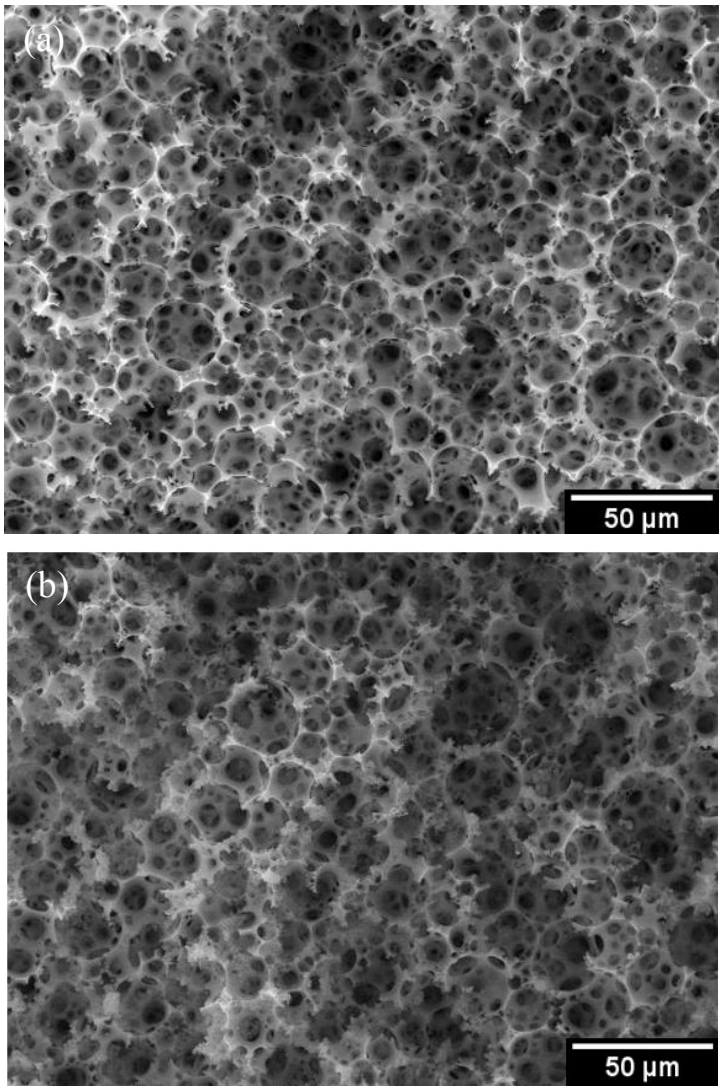

Figure 5-1 SEM images HX1-PHP x500 (a) before (b) after hypercrosslinking

SEMs images obtained for HX1-PHP before the hypercrosslinking reveals the influence of the porogen on the polyHIPE morphology. The overall pore sizes appear smaller as compared to the sulphonated polyHIPEs with the same processing parameters. The SEM investigation reveals that the pores are characterized by many interconnecting holes. The presence of such interconnecting holes, much smaller than the pores is a peculiar feature obtained in polyHIPEs by the addition of the porogens. The number of interconnecting holes per single pore is interestingly higher in HX1-PHP than in sulphonated polyHIPEs. Cameron and Barbetta (2000) studies demonstrated that the decrease in the emulsion droplet size leads to a decrease in the pore sizes, since the polymer morphology reflects the emulsion structure prior to gel formation during the polymerization process. Thus the droplet size decreases with increasing emulsion stability subsequently as the surface energy per unit area is lower. Barbetta and Cameron (2004) reported porogens CB and CEB has the tendency to co-adsorb at the interface together with the surfactant, thus increasing the interface contact and reducing the interfacial tension. Consequently, with the interaction between the porogens and the surfactant due to which the surfactant is adsorbed more strongly at the w/o interface results in resistance to the droplet coalescence. In this respect, CB and CEB influences the surfactant lowering the interfacial tension and enhancing the emulsion stability by preventing the water diffusion through the organic phase to produce larger droplets. Thus, addition of the porogens in our study, resulted in a viscous emulsion, which reflects on the sizes of the pores and interconnecting holes. Butler *et al.* (2003) in their studies of synthesis of highly porous emulsion templated polymers demonstrated that the raised viscosity of the continuous phase, suppresses the tangential interfacial flow of the continuous phase which impedes droplet coalescence. This results in smaller droplets in the emulsion. Thus the SEM images obtained in our study are in agreement with these findings of the above authors.

The polyHIPEs obtained after the hypercrosslinking were fragile and crumbled into fine powder easily on small compression. SEM image in Figure 5-1 shows open celled porous morphology with evidence of broken wall structure at many places. The SEM micrographs also show development of new micropores

on the pore walls. The fragile hypercrosslinked structure is more prominent in Figure 5-2.

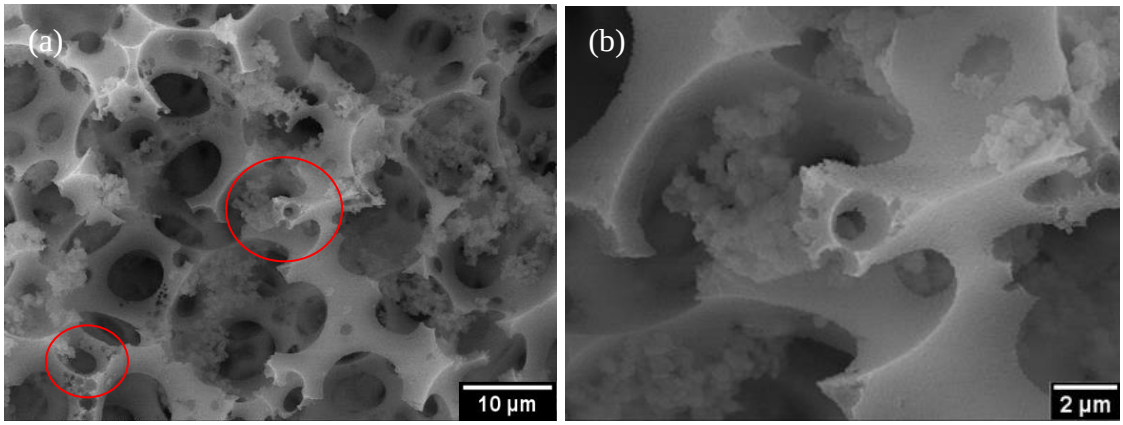

Figure 5-2 Hypercrosslinked HX1-PHP showing fragile structure and nanopores (a)x2000 and (b)x6500 magnifications

The red circled area in the center of Figure 5-2 (a) shows the broken wall structure which has been enlarged in Figure 5-2 (b). The circle at the left bottom corner in Figure 5-2 (a) shows interconnecting pores formed on the walls by hypercrosslinking process are as small as 1 nm. The increase in the micropores and interconnectivity, with the average pore sizes remaining constant weakens the mechanical structure of the hypercrosslinked polyHIPEs (Luo *et al.*, 2012). There was also evidence of sub-micron size agglomerates on the surface. As compared to the sulphonated polyHIPEs, the pore walls and interconnects edges were smooth and distinctively different from the curvy edges seen in SPHPA10. The surface area enhancement and pore size data is reported in Table 5-1 and Table 5-2.

The surface area of HX1-PHP was 164.7 m^2/g which dramatically increased to 802.1 m^2/g on hypercrosslinking. The pore size distribution and the average pore diameter for HX1-PHP showed a less symmetrical distribution with the mean value of 23 µm. More pores in the region of 15 to 25 µm were present, lowering the average value to 23 µm.

Table 5-1 Surface areas before and after hypercrosslinking

PolyHIPE sample code	BET before hypercrosslinking (m^2/g)	BET after hypercrosslinking (m^2/g)	% increase in surface area
HX1-PHP	164.7 ± 3.45	802.1 ± 2.25	387
HX-SPHPA10	110.3 ± 3	421.6 ± 2.4	282.7

Table 5-2 Average pore and interconnect sizes after hypercrosslinking

PolyHIPE sample code	Average pore size (μm)	Average interconnect size (μm)
HX1-PHP	23.35 ± 2.8	5.1 ± 1.43
HX-SPHPA10	46.89 ± 3.1	8.1 ± 1.5

Liu *et al.* (2008) demonstrated that the addition of porogens having good thermodynamic compatibility with the polymer network leads to phase separation at a later stage of polymerization resulting in smaller average pore sizes and large specific surface area. In this study, the porogens CEB and CB may have a similar effect which results in phase separation at a later stage, consequently forming micropores and enhancing the surface area. Along similar lines, Okay (2000) reported that with good solvating power of the diluent, increases the number of micropores. The authors stated that the average pore size becomes smaller and the pore size distribution shifts towards smaller pores due to increase of polymer-diluent interaction. The average interconnect size of 5.1 μm obtained in HX1-PHP reflects the effect of hypercrosslinking on the polyHIPE morphology. Hypercrosslinking of HX1-PHP achieved on treatment with $FeCl_3$ is mainly the

function of the Cl content but also depends on resulting the hierarchical structure obtained by the precursors used. Hypercrosslinking process converts the chloromethyl groups into methylene bridges. Veverka and Jerabek (1999) demonstrated that the conversion of the chloromethyl groups into methylene bridges can progress rapidly if a benzene ring of the neighboring polymer chain was available next to the choromethyl group. Hence the rate of the hypercrosslinking reaction will be strongly impacted by the steric effects and by the mobility of the polymer chains. Thus, the combination of the precursors and the porogens used favors the formation of the micropores during hypercrosslinking process, however makes the structure fragile. The conversion of the $–CH_2Cl$ groups in hypercrosslinked polyHIPEs is confirmed in the FTIR spectra discussed in the next section.

On the other hand, the surface area for HX-SPHPA10 was significantly increased to 421.6 m^2/g on hypercrosslinking. The SPHPA10 polyHIPEs were also swollen in thermodynamically good solvent dichloroethane and $FeCl_3$ catalysed Friedel Crafts crosslinking reaction was carried out. During this process, the polymer chains becomes fixed in their solvated state which results in formation of desired network of nanopores which persevere within the polymer structure even after the solvent is removed (Veverka and Jerabek, 1999). HX-SPHPA10 showed a rather regular distribution, with the mean value of the pore diameter of 46 µm, however there was marked reduction in the average interconnect size from 11.2 to 8.1 µm. This reflects the micropores created during the hypercrosslinking process. This microporosity is the result of the hypercrosslinked matrix high rigidity which prevents collapse of the micropores formed after removal of the solvent. The larger pores facilitates the $FeCl_3$ transport in the polymer network and aids in the conversion of the chloromethyl groups. HX-SPHPA10 polyHIPEs obtained were mechanically more robust than HX1-PHP after the hypercrosslinking. The coalesce pores developed within the morphology exhibited well distributed primary pores with formation of good interconnecting pores throughout the structure. The increase in the proportion of the micropores formed correlates with the increase in the BET surface area for HX-SPHPA10. The following Figure 5-3 shows the pore diameter distribution in HX1-PHP and HX-SPHPA10 polyHIPEs after hypercrosslinking.

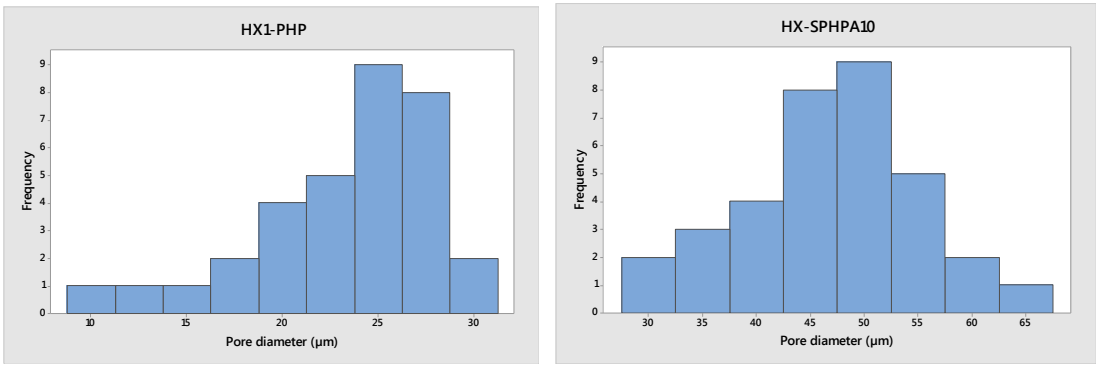

Figure 5-3 Pore diameter distribution for HX1-PHP and HX-SPHPA10

Thus, the hypercrosslinked sulphonated polyHIPEs HX-SPHPA10 obtained exhibited regular distribution of pores with surface area of 421 m^2/g. SEM images of HX-SPHPA10 are as shown in Figure 5-4. Microporous HX-SPHPA10 polyHIPE was also hydrophilic in nature.

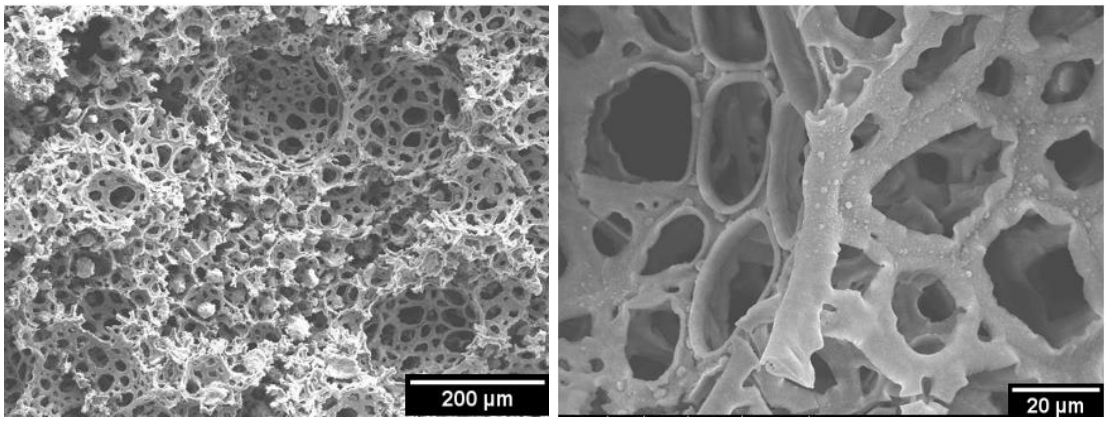

Figure 5-4 SEM images HX-SPHPA10 after hypercrosslinking

SEM images of HX-SPHPA10 shows highly porous open interconnected layout with evidence of interconnecting pores and curly edges. Newly formed micropores generated are evident on the walls of the polyHIPE. Moreover, the micropores were more pronounced on the walls in between two adjacent pores. It is worth noting, that the differentiating feature between the HX-SPHPA10 and HX1-PHP polyHIPEs is between the surface area enhancements. The surface area enhancement for HX1-PHP was almost double (802 m^2/g) than HX-SPHPA10 polyHIPEs. This is mainly due to the composition of the precursors,

where HX1-PHP were prepared with DVB-VBC precursors whereas HX-SPHPA10 were prepared by Sty-DVB precursors. Ahn *et al.* (2006) demonstrated hypercrosslinking studies with DVB-VBC polymers showing micropores in the resultant polymer structure were derived from the hypercrosslinking process. They reported that the crosslinking process with DVB-VBC precursor was intramolecular and leads to extremely efficient hypercrosslinking reaction. Similarly Veverka and Jerabek (1999) studies revealed polymers from DVB-VBC were excellent for the synthesis of hypercrosslinked materials as the chloromethyl (-CH_2Cl) substituent is the source of the internal electrophile used to link the bridges between the neighboring aromatic rings. Further research by Barbetta *et al.* (2000) in their comprehensive studies varying the ratio (wt%) of VBC to DVB concluded that the difference in the surface area and the pore sizes was due to the interfacial properties of the emulsion which is altered by the addition of VBC. Therefore consistent with the above theory for the polymers prepared with styrene and VBC precursors, HX-SPHPA10 exhibited BET surface area enhancement lower than that of HX1-PHP polyHIPEs. The pore and interconnect sizes further validated the effect of the precursors and porogens used on the polyHIPE morphology.

5.3.2 Catalyst precursor insertion

The polyHIPEs prepared with the use of $FeCl_3$ in the aqueous phase, HX2-PHP10, HX2-PHP20 and HX2-PHP30 were investigated for the catalyst distribution and size. All three polyHIPE samples showed hierarchically porous morphology. It was observed that the incorporation of $FeCl_3$ in the aqueous phase ensured homogenous distribution of iron catalyst and hypercrosslinking. The following Figure 5-5 illustrates the SEM images of polyHIPEs HX2-PHP10, HX2-PHP20 and HX2-PHP30 respectively. The SEM micrographs show fragile wall structure and connectivity, as a result after hypercrosslinking the polyHIPEs were brittle and crumbled on application of small compressions.

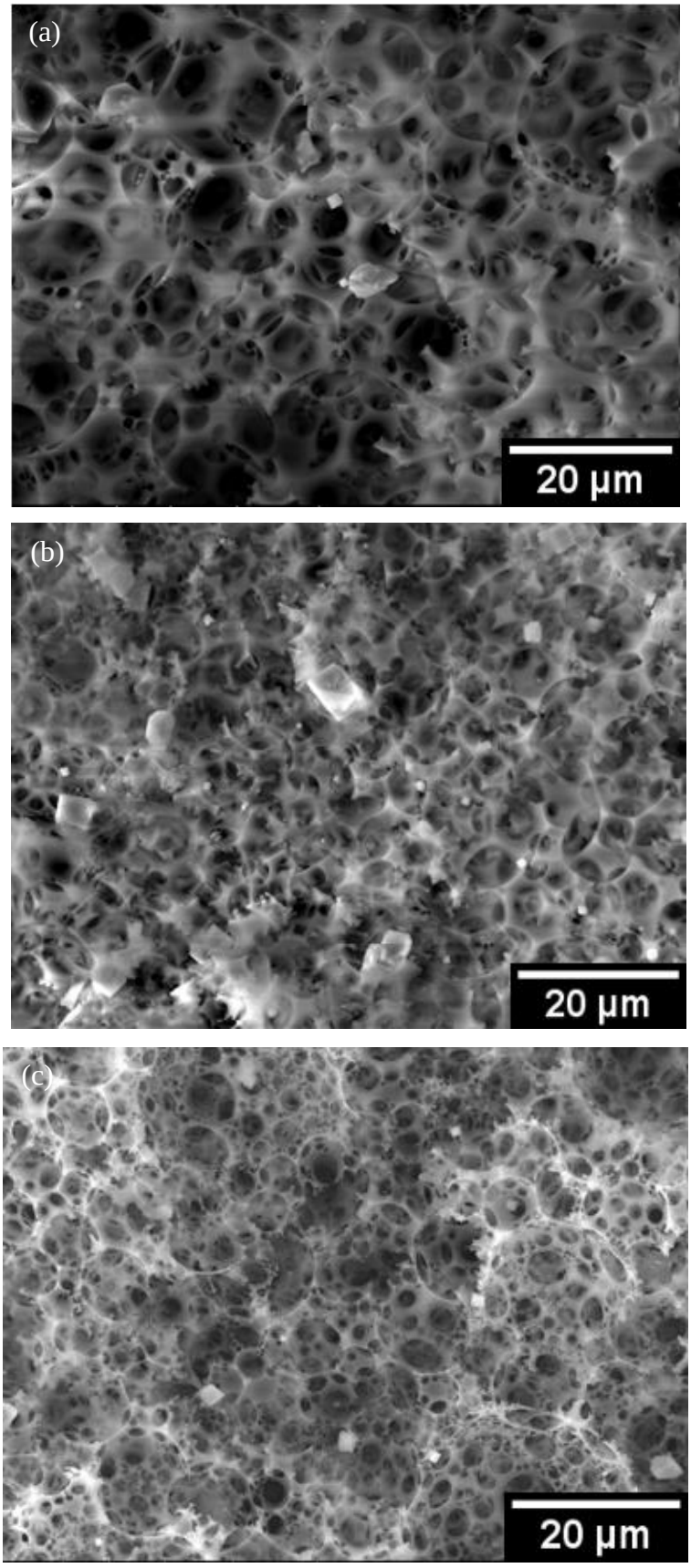

Figure 5-5 SEM micrographs showing catalyst distribution (a) HX2-PHP10, (b) HX2-PHP20 & (c) HX2-PHP30 (x 1500 magnification)

It was observed that increasing the homogenisation time plays a substantial role in catalyst size and its distribution throughout the polyHIPEs. Taylor (1934) first formulated the theory of droplet deformation and break up by viscous shear. Capillary number characterizes the ratio of the viscous forces to surface or interfacial tension forces of the emulsion (Sajjadi, 2007). It is represented in Equation 5-1

Equation 5-1

$$Ca = \frac{2\,\mu_c \gamma d}{\sigma}$$

Where, μ_c = viscosity of the continuous phase

γ = shear rate

σ = surface or Interfacial tension and

d = droplet diameter

Thus the above Equation 5-1 reflects that higher the mechanical shear applied and lower the interfacial tension, the droplet breaks down resulting in smaller droplets (DeRoussel *et al.*, 2001). It was noted that the pore size distribution and the catalyst size differ due to the increase in homogenization time. The polyHIPE samples showed narrow distribution of pores as there was increase in the shear stress with increase in the homogenization time. This also caused the catalyst particles to disperse evenly within structure. However due to repeat swelling during hypercrosslinking and the catalyst insertion, internal stresses generated within the monolithic polyHIPEs. Hence the polyHIPEs lacked good mechanical strength and showed evidence of cracking. SEM micrographs showing the catalyst distribution are shown in Figure 5-5. HX2-PHP10 shows agglomerated particles, whereas increasing the mixing time in HX2-PHP20 and HX2-PHP30 shows more uniform distribution with reduction in the particle sizes. The TEM image in Figure 5-6 shows the catalyst size within the polyHIPE HX2-PHP10 ranging from 1-5nm. HX2-PHP20 and HX2-PHP30 also had uniform distribution of particle size less than 3nm.

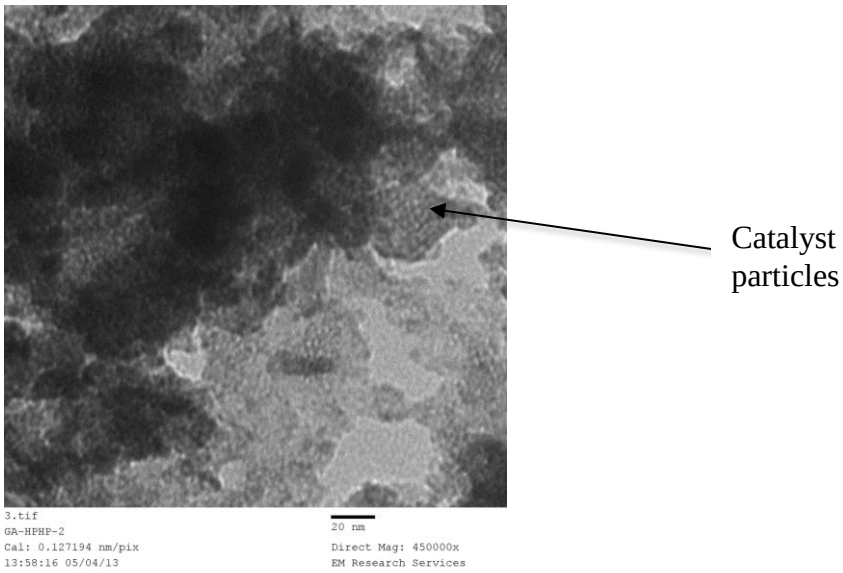

Figure 5-6 TEM image of the HX2-PHP10 after crushing the polymer showing catalyst size 1-5nm

Thus, the TEM and SEM images illustrates that the catalyst particle size significantly reduces with increase in the homogenization time.

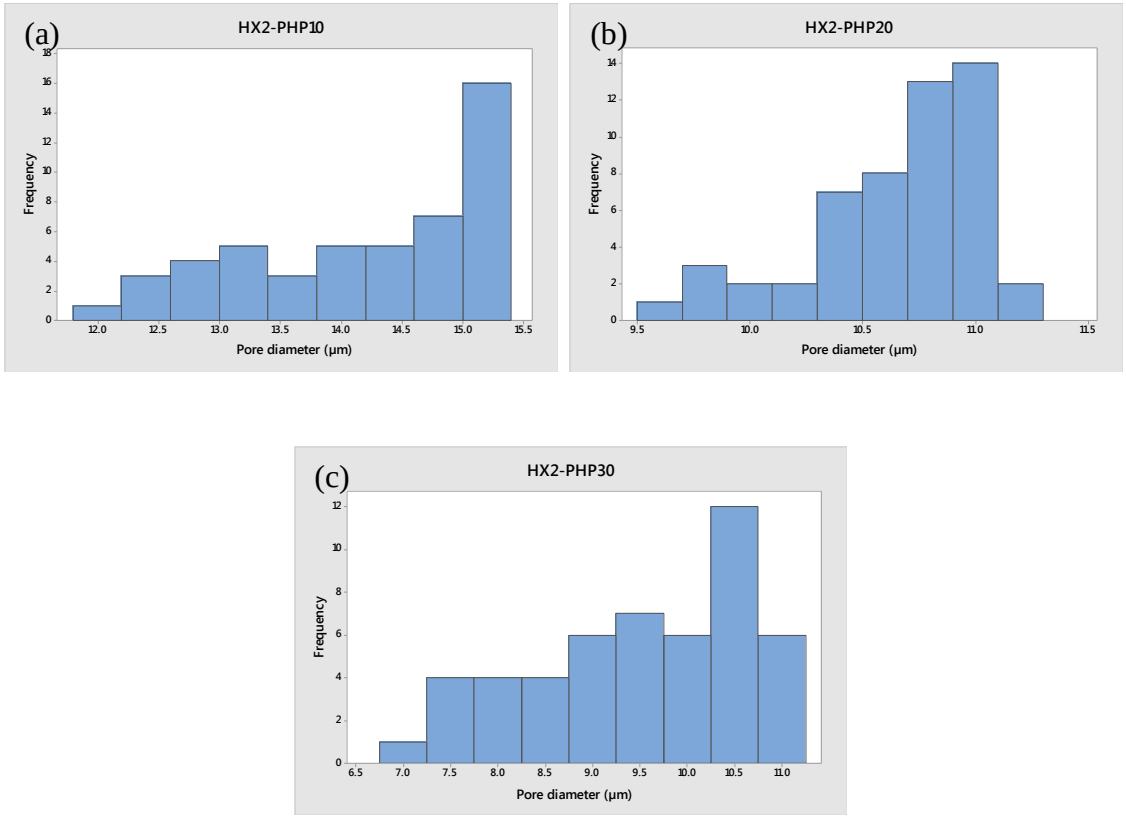

Figure 5-7 Pore diameter distribution for HX2-PHP10, HX2-PHP20 & HX2-PHP30

Figure 5-7 shows the pore diameter distribution for polyHIPEs HX2-PHP10, HX2-PHP20 and HX2-PHP30. The pore size distribution for HX2-PHP10 & HX2-PHP20 showed a left skewed distribution with mean pore diameter value of 14.1 and 10.6 µm respectively. HX2-PHP30 also showed asymmetrical pore size distribution with plateau region for the pore sizes between 7.5 to 9 µm. It is believed that the addition of $FeCl_3$ in the aqueous phase has a significant effect on the pore size distribution and the specific surface area of the polyHIPEs. The homogenous distribution of the catalyst within the polyHIPE structure aids in the hypercrosslinking process forming uniform small pores and interconnects leading to significant increase in the surface area. SEM image in Figure 5-8 shows the characteristics highly interconnected open pore network structure of HX2-PHP30 polyHIPE. The pores formed were more uniform and round with smooth interior surfaces having average interconnect of 2.4 µm. Similarly the average interconnects for HX2-PHP10 and HX2-PHP20 was found to be 5.2 and 3.8 µm respectively. The average pore and interconnect size data is tabulated in Table 5-3. The increase in the proportion of the smaller pores and interconnects for HX2-PHP10 and HX2-PHP20 correlates with the increase in the BET surface area as seen in Table 5-4. The BET surface area for the polyHIPEs before and after hypercrosslinking process is summarized in Table 5-4.

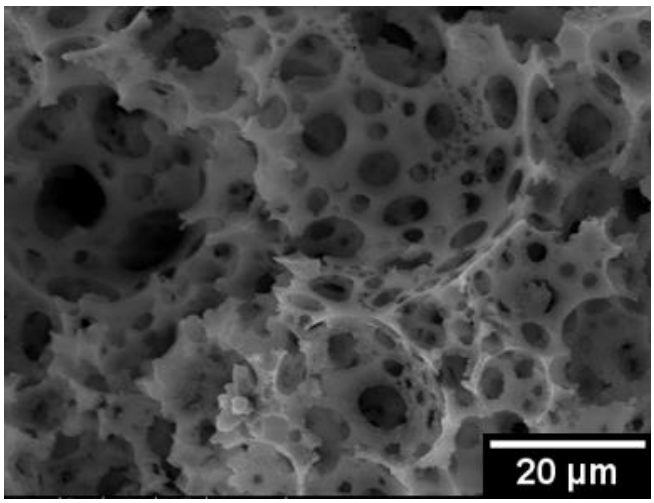

Figure 5-8 SEM micrograph for HX-PHP30 showing highly interconnected pore network formed due to hypercrosslinking process.

Table 5-3 Average pore and interconnect sizes for HX2-PHP10, HX2-PHP20 & HX2-PHP30

PolyHIPE sample code	Average pore size (μm)	Average interconnect size (μm)
HX2-PHP10	14.17 ± 1.6	5.2 ± 0.7
HX2-PHP20	10.64 ± 0.2	3.8 ± 1.5
HX2-PHP30	9.5 ± 0.3	2.4 ± 0.3

The use of porogens led to high specific surface area of 141.3, 162.5 and 189.6 m^2/g for HX2-PHP10, HX2-PHP20 and HX2-PHP30 polyHIPEs respectively. The surface area was significantly enhanced as summarized in Table 5-4 following hypercrosslinking which is in agreement with the pore size distributions and SEM observations.

Table 5-4 BET surface area for HX2-PHP10, HX2-PHP20 & HX2-PHP30

PolyHIPE sample code	BET before hypercrosslinking (m^2/g)	BET after hypercrosslinking (m^2/g)	Increase in surface area (%)
HX2-PHP10	141.3 ± 2.1	740.3 ± 1.25	425
HX2-PHP20	162.5 ± 2.23	882.4 ± 3.1	443
HX2-PHP30	189.6 ± 1.8	911.2 ± 1.5	381

The internal stresses developed within the monolith cause cracking of the pore walls which might explain the marginal difference in the average pore sizes

of HX2-PHP20 and HX2-PHP30 polyHIPEs. Also, the increase in surface area after hypercrosslinking in HX2-PHP30 was slightly lower as compared to HX2-PHP10 and HX2-PHP20. This can be attributed to the collapse of the pore wall due to internal stresses developed. Due to homogenous distribution of the catalyst and abundance of narrow micropores developed made the network more fragile. Moreover, the concentrations of VBC and porogens is too low to form stable and effective cross linking network in the resultant polymer. Hence the surface area is lowered, owing to the collapse of some nanopores during the drying processes (Ahn *et al.*, 2006). These results are in agreement with studies of Liu *et al.* (2008) for preparation of hypercrosslinked polystyrene with nano pore structure.

Thus the hypercrosslinked polyHIPEs prepared with the $FeCl_3$ in the aqueous phase exhibited distinguishing morphology compared to HX1-PHP and HX-SPHPA10 in two important properties. Firstly, the HX2-PHP morphology revealed considerable small pore sizes, very high surface area and porosity. Moreover, the higher the cross-linking degree of the polymeric network was marked with greater specific surface area. Secondly, in spite of the high degree of crosslinking, the polymeric network almost exhibit the same ability to be swollen in thermodynamically good solvent, such as dichloroethane (Zhang *et al.*, 2007). If the catalyst precursor is different than $FeCl_3$, then the polyHIPEs can be washed and soxhleted for the removal of $FeCl_3$, and finally dried. These hypercrosslinked polyHIPEs can be then inserted by a different catalyst by absorption of the catalyst precursor solution by the hypercrosslinked polyHIPEs. To further investigate the extent of hypercrosslinking, FTIR studies were conducted to confirm the chemical structure of the polyHIPEs before and after hypercrosslinking.

5.4 Fourier Transform Infrared

FTIR spectra were investigated to confirm the chemical structure of the hierarchically porous HX2-PHP10 and HX-SPHPA10 polyHIPEs and further modifications after hypercrosslinking. In order to assess the success of the hypercrosslinking reaction, the absorption peaks of the C-Cl bond were

compared before and after hypercrosslinking in the polyHIPE samples. Figure 5-9 illustrates the FTIR spectra for HX2-PHP10 and HX-SPHPA10 before and after the hypercrosslinking process.

In HX2-PHP10 polyHIPE, after hypercrosslinking, confirmation of the high level of cross-linking achieved was obtained by the decrease in intensity of the 1270 cm^{-1} band in the FTIR spectra confirming the loss of chlorine due to the hypercrosslinking reaction (Fontanals *et al.*, 2005; Ahn *et al.*, 2006; Hwang *et al.*, 2015). Thus this data corresponds to the formation of the methylene bridges. HX2-PHP10 polyHIPEs show that the consumption of the $–CH_2Cl$ groups which leads to disappearance of the peak at 1270 cm^{-1} after hypercrosslinking. In case of HX-SPHPA polyHIPEs, the polymers were subjected to sulphonation prior to hypercrosslinking hence the frequency 1000 – 1300 cm^{-1} is assigned to the stretching vibration of $–SO_3H$ groups discussed in Chapter 4. However, Bhunia *et al.* (2015) reported the peaks at 1022 and 1039 cm^{-1} as an evidence of additional crosslinking during sulphonation in their research demonstrating design of a new hypercrosslinked super microporous polymer. The high surface area (421 m^2/g) found in the HX-SPHPA10 can also be attributed to the presence of the OH vibrations seen in the region 3400 cm^{-1}. Two mechanisms can be predicted for the increase in the surface area. First, the extent of the chloromethyl group might increase when $FeCl_3$ chlorinate the hydroxymethyl groups. Second, the oxygen atom of the hydroxyl group reacts with $FeCl_3$, eliminating the hydroxyl group thus facilitating the formation of the methylene bridges (Fontanals *et al.*, 2005). This is reflected by the decline in the intensity of the 3400 cm^{-1} band after the hypercrosslinking process.

In both HX2-PHP10 and HX-SPHPA10 spectra, the peak at 710 cm^{-1} is attributed to mono substituted benzene ring and its intensity weakens after the hypercrosslinking process. This data exhibit that the hydrogens in the benzene ring were replaced during the hypercrosslinking reaction (Hwang *et al.*, 2015; Wang *et al.*, 2015). Similarly the intensity of the band in the region 2960-3010 cm^{-1} is attributed to the C-H stretching vibration of the benzene ring and the CH_3 group, which also show decline in the intensity after hypercrosslinking demonstrating that the hydrogens on the benzene ring were substituted in the hypercrosslinking process.

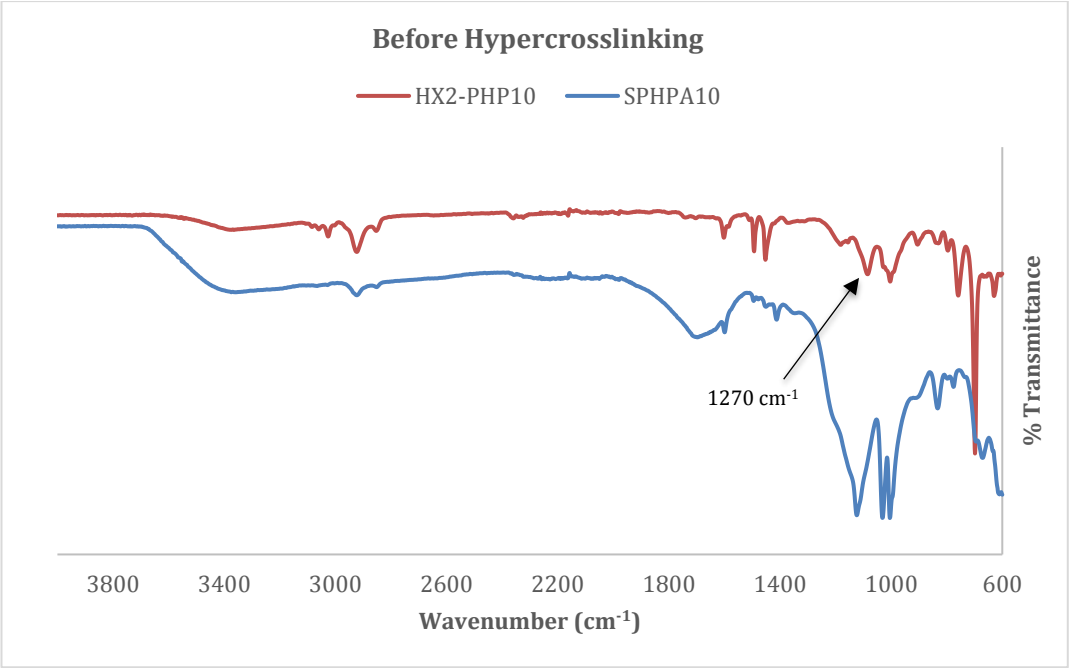

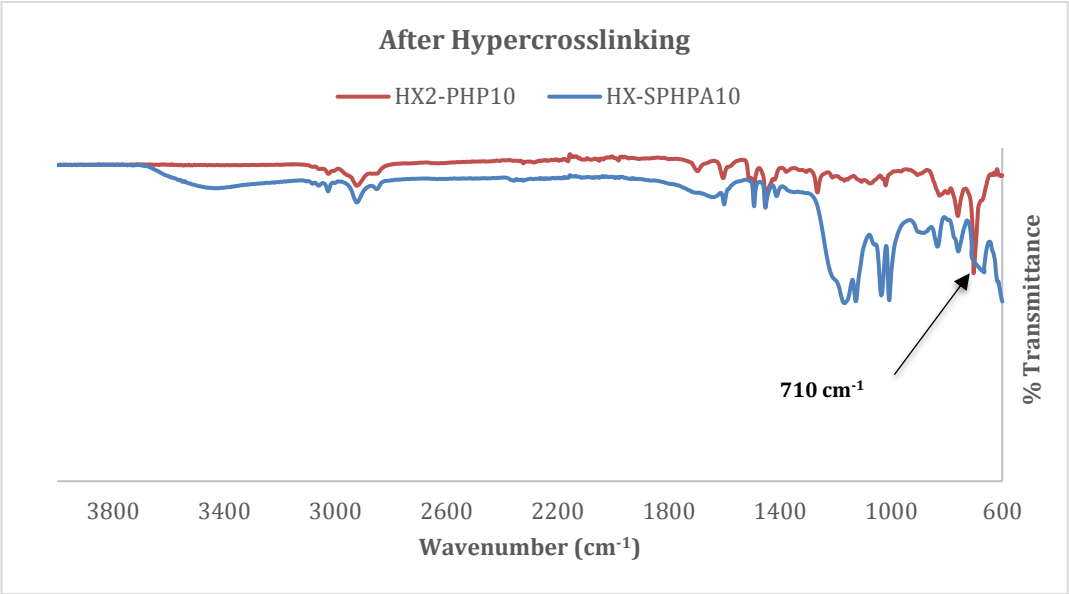

Figure 5-9 FTIR spectra of HX2-PHP10 and HX-SPHPA10 before and after hypercrosslinking.

Another remarkable difference between the HX2-PHP10 and HX-SPHPA10 was the surface area enhancement. HX2-PHP10 exhibited almost twice the specific surface area as compared to HX-SPHPA10. Fontanals *et al.* (2005) demonstrated that the degree of hypercrosslinking achieved with Lewis acid is mainly the function of the Cl content and to some extent the precursor monomer. HX2-PHP10 prepared with DVB-VBC and the aqueous phase compromised of

$FeCl_3$ during the preparation, will have a high chlorine content. Although it is difficult to quantify the level of crosslinking due to its initial content, the decline in intensity of the band at 1270 cm^{-1} reflect the formation of the methylene bridges thus increasing the surface area in HX2-PHP10 polyHIPEs as compared to HX-SPHPA10 polyHIPEs.

5.5 Thermogravimetric Analysis

It was observed that the addition of the porogen and hypercrosslinking weakens the polyHIPE structure. Hence the resultant polyHIPEs had low mechanical strength due to repeated swelling process and catalyst insertion.

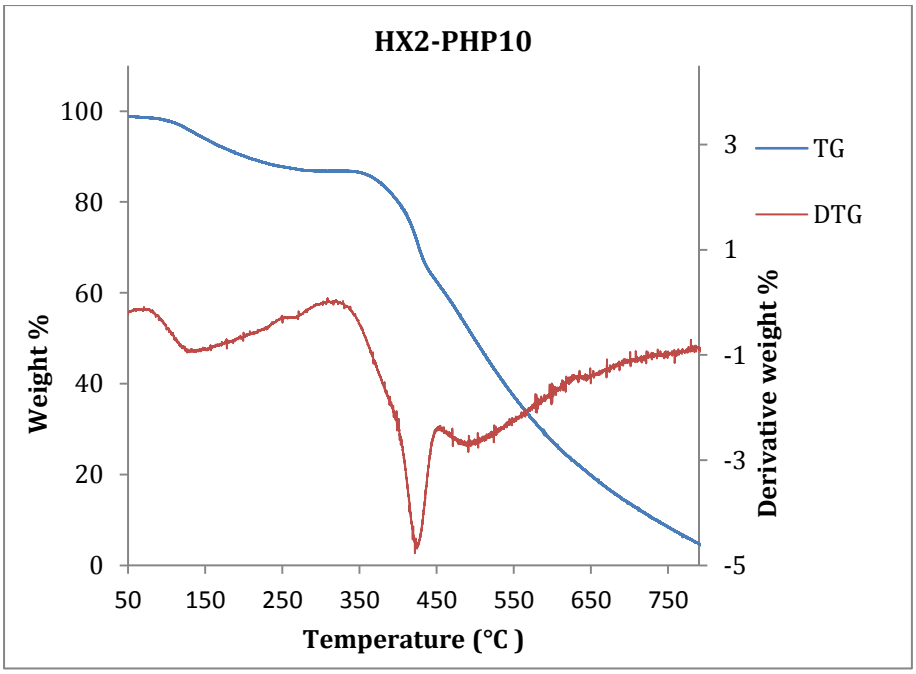

Figure 5-10 TGA for HX2-PHP10

The decomposition temperature was reduced on hypercrosslinking. TGA analysis on all hypercrosslinked polymers revealed that the onset of decomposition starts around 250^0C and at a maximum of 750^0C, the polyHIPEs are completely decomposed. TGA analysis on HX2-PHP10 is shown here to evaluate the decomposition temperatures. Figure 5-10 illustrates the TGA trace for HX2-PHP10 polyHIPE. The onset of decomposition starts around 300^0C. About 60%

of the polymer is present around 450^0C after which it rapidly decomposes. However, due to the presence of the $FeCl_3$ in the polymer matrix, it can be assumed that the presence of $FeCl_3$ particles catalyzes the decomposition of the polyHIPEs. Similar effect is reported by Schwickardi *et al.* (2002) where they reported the presence of metal ions accelerates the decomposition of templates, hence lower combustion temperatures are crucial.

5.6 Conclusions and Outlook

In summary, monolithic hydrophilic microporous polyHIPEs with enhanced surface area of 421 m^2/g were synthesized via post hypercrosslinking process. These hypercrosslinked sulphonated polyHIPEs were more robust then the polyHIPEs with porogenic solvents. Addition of porogens and hypercrosslinking affects the morphology of the polyHIPEs in terms of pores, interconnectivity and surface area. The incorporation of the catalyst precursor before polymerisation into a monolithic support was demonstrated for the first time. Our results confirm uniform distribution of the catalyst within the monolithic structure with enhanced specific surface area and well-defined pores and interconnects. Catalyst size can be controlled and BET surface area up to 911 m^2/g can be achieved with varying the homogenization time. These catalytic structures are important for development of hypercrosslinked polymers with accessible porosity and transport pores as they can remove diffusional barriers for the reactants and products.

FTIR analysis confirmed the hypercrosslinking process correlating to the increase in specific surface area of the polyHIPEs. However, TGA studies indicate that the decomposition temperatures decreases on hypercrosslinking. Thus, these materials can be further functionalised and utilised in agriculture, biotechnology, tissue engineering, separation processes, as well as catalyst applications, only if the service temperature remains low. Further research should aim at improving the mechanical properties of the hypercrosslinked polyHIPEs. Dielectric barrier discharge plasma can be used for catalyst precursor decomposition to metal oxide followed by catalyst reduction in the presence of hydrogen (In case of different catalyst precursor other than Fe used in the aqueous phase). We expect this technique to open up new method for some

applications where catalyst precursor decomposition stage is combined with catalyst reduction stage.

Chapter 6 Experimental evaluation of water absorption capacity of polyHIPE materials in different types of soil and their effect on soil characteristics

This chapter presents the discussion and experimental outputs from the application of sulphonated polyHIPE polymers (SPHPA10) in sandy loam and clay loam soils. The objective of the experiments was to evaluate the water absorption capacity of these hydrophilic polymers when mixed with soil and their effect in enhancing the soil characteristics. Plant growth is directly related to the amount of water in the soils and the soil parameters related to water retention include field capacity (FC), permanent wilting point (PWP) and available water holding capacity (AWC). Amending the soils with hydrophilic polymer is one of the known method which aids in providing additional water to plants (Huttermann *et al.*, 2009; Orikiriza *et al.*, 2009b; Agaba *et al.*, 2010).The water holding capacity of sulphonated polyHIPEs mixed with soil was studied using the pressure plate apparatus at 0.05bar, 2bar and 15bar pressures. These sulphonated polyHIPE polymers exhibited surface area of 214 m^2/g and average pore sizes of approximately 50 µm and interconnect sizes ranging from 2 to 10 µm. They also demonstrated high water uptake capacity almost 1500 times its own weight when completely saturated. The pressure plate extractor methodology used in determining the water holding characteristics of the soil samples is described in section 3.5.1 in Chapter 3.

We tested the hypothesis that enrichment of polyHIPEs with clay loam and sandy loam soils would aid in water absorption capacity and enhance the soil characteristics. Four treatments replicated five times were used on sandy loam and clay loam soils. Different amounts of polyHIPE samples were mixed with sandy loam and clay loam soils to give concentrations of 0%, 0.25%, 0.5% and 1% by weight. Field capacity is approximately equal to 0.3 bar matric potential and is the amount of water retained by the soil where the optimum wetness has reached and the downward drainage of water caused by gravity has ceased (Brady and Weil, 2008). It is the upper limit of the soil water availability. Permanent wilting point is the water content the soil holds where the plant roots are unable to draw any water from the soils, resulting in wilting of the plant. It

corresponds to the matric potential of about 15 bar (1500 kPa). Hence it is given as the lower limit of the soil water availability. At this condition, the water is held in smaller pores which the plant roots can no longer extract. The total available water capacity can be defined as the water held between the field capacity and permanent wilting point. Thus, the total soil water holding capacity in this study was determined using the pressure plate apparatus at pressures between 0.05 and 15bar.

Data obtained from both the sandy and clay loam soils was analyzed with a one-way analysis of variance (ANOVA). The Duncan test was used to separate the means and check the differences between treatments. $P<0.05$ was considered to be statistically significant.

6.1 Results and discussions

6.1.1 Saturation percentage of clay loam and sandy loam soils

The soils samples were saturated as described is section 3.5.1. After the saturation period the soil sample cores were wiped from the outside and weighed. The weight of the saturated soil sample was recorded as W_i after deducting the weight of the stainless steel core ring. D_i was the weight recorded of the dried soil sample which was dried in the oven at a temperature of 105^0C for 48 hours. Saturation percentage of the soils was calculated as per Mbah (2012). The following Equation 6-1 was used

Equation 6-1

$$\boldsymbol{SP} = \frac{W_i - D_i}{D_i} * 100$$

Where, SP = Saturation percentage,

W_i = wet soil sample (sandy or clay loam),

D_i = dry soil sample (sandy or clay loam)

Gravitational and capillary forces aid in the movement of water in soils. Water uptake in porous media depends on capillary forces, which allows or prevents water entry in pores. Rowell (2014) classified pores according to their size and function. The author reports pore size greater than 50 µm are termed as macropore which helps the transmission of water and nutrients in the soil. They cause water drainage after saturation. Pore sizes between 50 – 0.2 µm are called storage micropores which aid in making stored water available for the plants whereas, pores less than 0.2 µm are called residual micropores which hold the water strongly that it is not available to plants. Figure 6-1 shows the saturation percentage of moisture content in clay loam and sandy loam soils.

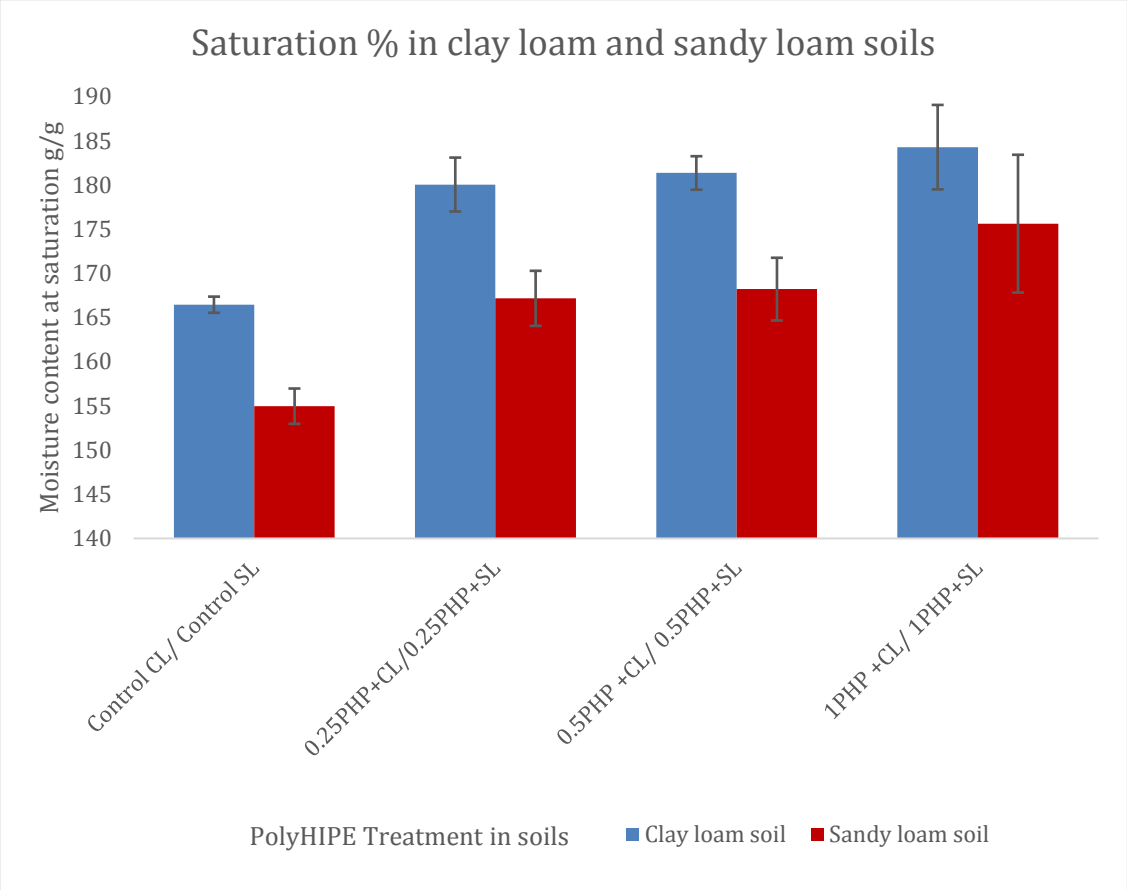

Figure 6-1 Saturation percentage in clay loam and sandy loam soils

It was observed that the sandy loam soil was slightly hydrophobic in nature and took more time (as compared to clay loam soil cores) to reach saturation. Dry soil readily adsorbs water due to the strong attraction between mineral soil particles and water. However, not all soils display this wettable characteristics

and repel water (Foth and Ellis, 1996). The clay loam soil saturated within 48 hours, however the sandy loam took 8-10hrs longer to reach saturation. The water penetration in sandy loam soil was slow and hence it took longer to wet the soil, delaying the movement of the water through the capillary rise. Clay loam soils showed higher water content and wetted easily as water retention is positively correlated with the clay content in the soil (Reichert *et al.*, 2009). The unbalanced electrical charges on the clay particles along with the hierarchical structure of the polyHIPEs with interconnected micropores aids in the capillary action and attract water molecules.

The average values of the soil moisture content at saturation state for control clay loam and sandy loam soils as seen from Figure 6-1 amounted to 37.1% and 27.7% respectively. The soil moisture content for the sandy loam soils was lower as expected as water molecules hold more tightly to the compacted particles of a clay loam soil than to coarser particles in sandy loam soils. There was a gradual increase in the soil moisture retention with increasing concentrations of polyHIPEs in both clay loam and sandy loam soils. The moisture content increased to 48.4% in clay loam and 37.8% in sandy loam soil respectively with 0.25% treatment of polyHIPEs as compared with the control variant. Further marginal increase (49.4% in clay loam and 38.6% in sandy loam soils) was observed in the moisture retention for 0.5% treatment of polyHIPEs. Finally, 1% polyHIPE amendments showed the highest increase in the moisture retention as compared to the untreated soil amounting to 51.9% and 44.7% in clay loam and sandy loam soils respectively. The water retention in the polyHIPEs amended soils implies that the coalescence pores along with the primary pores in SPHPA10 aid in water transmission in both the soil types. The high surface area of SPHPA10 correlates to the high water content in both the soils at saturation stage. The size and continuity of water filled pores can also help determine the hydraulic conductivity of soils (Troeh, 2005). It was observed that clay loam soils can retain more water than the sandy loam soils. This could more likely to be attributed to sandy loam soil having less water holding capacity compared to the clay loam soil texture.

Therefore, the addition of the polyHIPEs showed a gradual increase in the soil moisture content as compared to the control cores (0% polyHIPEs) with increasing concentration of the polyHIPEs in the soil. Similar results were

reported by Abedi-Koupai *et al.* (2008) in their studies on sandy loam, loamy and clay soils enriched with hydrogels in four levels, 2, 4, 6 and 8g/kg showed increase in saturated water content with increasing level of hydrogel application. Work done by Andry *et al.* (2009), in their study to evaluate the water retention of hydrophilic polymers in sandy soils also highlighted that the increase in mixing ratio of the two hydrophilic polymers from 0.1% to 0.2% had a significant effect on the available water content in sandy soils of arid and semi-arid regions.

6.1.2 Water retention at Field Capacity and Permanent Wilting Point

6.1.2.1 Effect of polyHIPE on moisture content at field capacity in clay loam soil

The application of polyHIPEs altered the soil water retention at field capacity in clay loam soils as compared with the control. It was observed that the soil moisture retention at the field capacity increased exponentially with increasing additions of the sulphonated polyHIPEs to the clay loam soils. Moisture content was 4.9% for the soil amended with 0.25% polyHIPE, 7.1% for the soil treated with 0.5% polyHIPE whereas, soil treated with 1% showed the highest water content at the field capacity with 14.72% increased moisture content as compared to the control.

Figure 6-2 shows the moisture content at field capacity for clay loam soils. Macropores which are mainly the transmission pores are drained at the field capacity whereas the storage and residual pores size of SPHPA10 48.6 µm benefitted in the transmission and storage of the water content. The average interconnect pore size 11.2 µm of the polyHIPE material acted as water reservoirs in storage and residual pores. Therefore, the results suggest high microporosity (storage and residual pores) within polyHIPEs amended clay loam soil as compared to the control. These results are in accordance to those obtained by Bai *et al.* (2010) which indicate that soil moisture increased by 6.2-32.8% with the application of super absorbent polymers in increasing concentrations (0.05%, 0.1%, 0.2% and 0.3%) mixed with sandy soils. They also reported that the effects on soil water retention varied according to the structure of the super absorbent polymers. Similar studies conducted by Orikiriza *et al.* (2009b) on different types

of soil including sandy loam and clay loam reported that hydrogel amendment enhanced the efficiency of water uptake. Although their results suggested that the water retention in the hydrogel amended soil cannot be directly correlated to increase in plant available water, they reported that hydrogel amendment clearly increased the biomass of plants grown in soils which have water content retention close to field capacity.

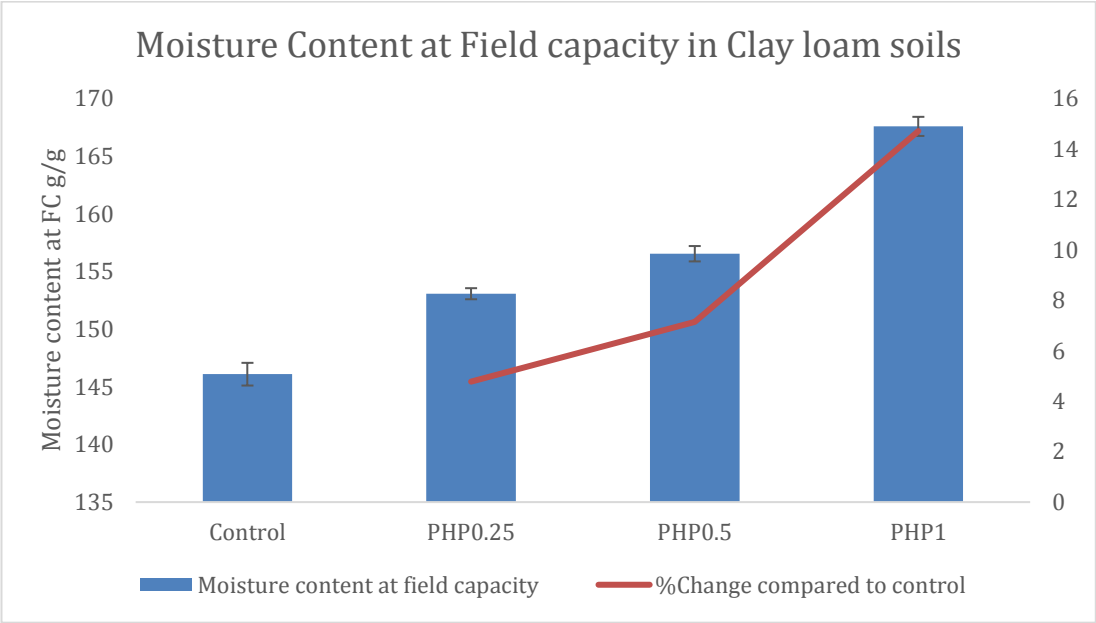

Figure 6-2 Moisture content at field capacity in clay loam soils

This study indicated that polyHIPE application increased the moisture retention at field capacity. A statistically significant difference was observed ($P<0.05$) between the control and the clay loam soil amended with 0.25%, 0.5% and 1% polyHIPEs. At soil field capacity, the moisture percentage increased by 22.4% with 0.25% polyHIPE concentration as compared to the control and was more than tripled with the highest concentration of polyHIPE which was 1%. Thus clay loam soil treated with various levels of sulphonated polyHIPEs showed higher values of moisture retention in comparison to the control. The combination of the micropores and the macropores along with the surface large area within the polyHIPEs allows the water movement and retention. Brady and Weil (2008) suggest about 10% of the pores must be large enough for aeration and water movement, so that root growth is not restricted.

It was also observed that the untreated clay loam soil (control) after oven drying, appeared to be more compact, tighter and cracked as compared to those amended with polyHIPE. Addition of the polyHIPE to the clay loam soil gave it more crumbly and granular structure aggregation thus altering the soils inherent properties. This may indicate that the addition of even small quantities of polyHIPE may improve the hydrological properties of the soil and thus may aid in increased performance of the crop.

6.1.2.2 Effect of polyHIPE on moisture content at permanent wilting point in clay loam soil

Water content at the permanent wilting point is mostly unavailable for the plants. Water will be held in the residual pores which cannot be extracted by the plant. The effect of polyHIPE at permanent wilting point was ambiguous. Soil mixed with smaller concentration of the polyHIPEs showed a decrease in soil retention capacity as compared with the control.

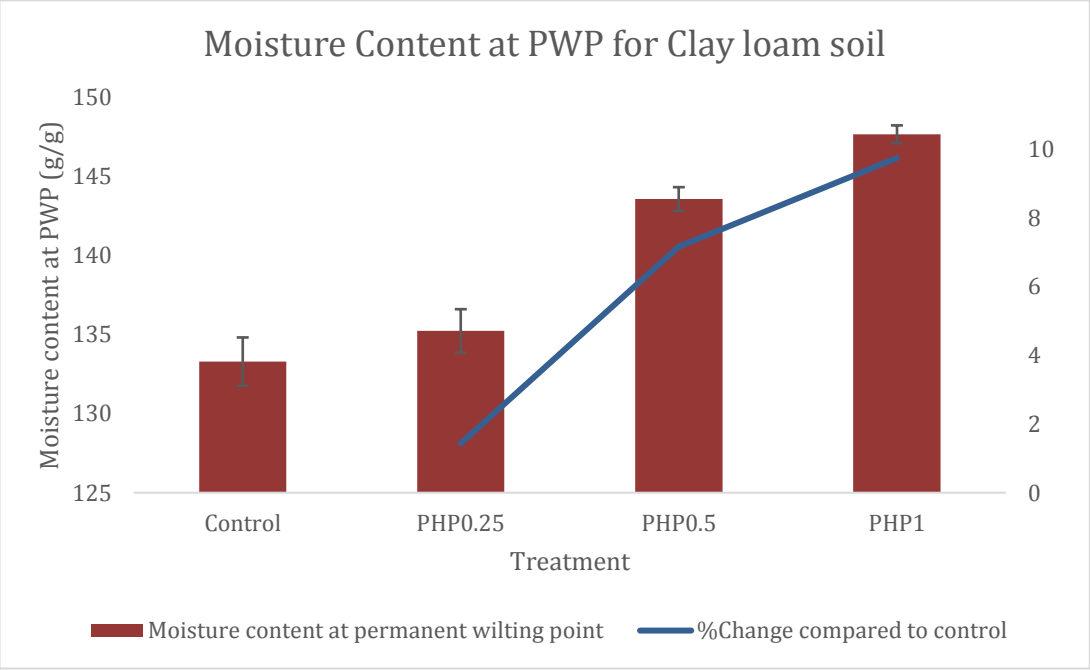

Figure 6-3 Moisture content at permanent wilting point for clay loam soils

Figure 6-3 shows the moisture content at permanent wilting point for clay loam soils. A significant difference was observed ($P<0.05$) for the moisture

content at PWP between the control and clay loam soil amended with 0.5% and 1% polyHIPEs. There was no significant increase in the moisture retention between the control and clay loam soil amended with 0.25% polyHIPEs. The water retention was 14.6%, 72.8% and 99.0% more as compared to the control for soil amended with 0.25%, 0.5% and 1% polyHIPEs respectively. Although the moisture content between the control and 0.25% polyHIPE treated soil was not significantly different, the 0.5% and 1% polyHIPE amendment in clay loam soils showed considerable moisture retention. Therefore, the addition of polyHIPEs can aid in water retention and delay the onset of the permanent wilting point.

This result is consistent with the findings of Yáñez-Chávez *et al.* (2014) which demonstrated that the permanent wilting point is reached more easily when no hydrogel is mixed with soil. Similarly Agaba *et al.* (2010) studies on the sandy loam and clay soils indicated that the soils amended with super absorbent polyacrylate hydrogel delayed the permanent wilting point and demonstrated prolonged tree survival compared to controls.

6.1.2.3 Effect of polyHIPE on moisture content at field capacity in sandy loam soil

Amending the sandy loam soil with the polyHIPEs significantly increased ($P<0.05$) the water retention at field capacity.

Figure 6-4 shows the moisture content at field capacity of sandy loam soil. Incorporation of the polyHIPEs in sandy loam soils showed almost a similar trend in moisture retention at field capacity as the clay loam soils. Moisture content was 5.2% for the soil amended with 0.25% polyHIPEs, 9.2% for the soil treated with 0.5% polyHIPEs whereas, soil treated with 1% showed the highest water content at the field capacity with 14.4% moisture content as compared to the control. This study demonstrated that polyHIPE application increased the moisture retention at field capacity in sandy loam soils. Statistically significant differences were observed ($P<0.05$) between the control and the sandy loam soil amended with 0.25%, 0.5% and 1% polyHIPEs respectively. From Figure 6-2 and Figure 6-4, it can be seen that the sandy loam soil amended with 1% polyHIPEs showed a

similar trend of water retention at field capacity for 0.5% polyHIPE amended clay loam soils.

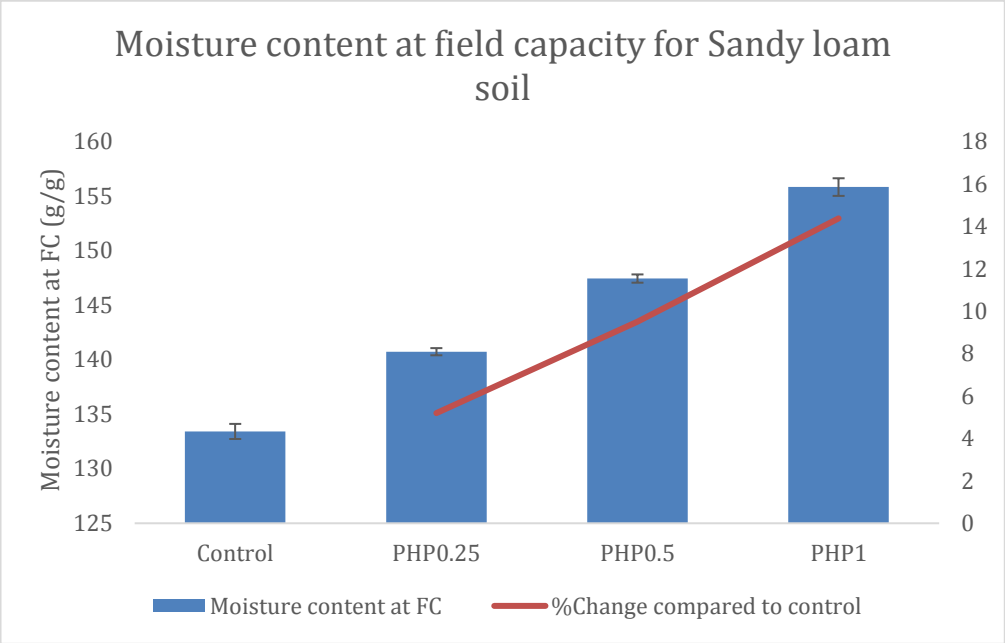

Figure 6-4 Moisture content at field capacity for sandy loam soil

At soil field capacity, the moisture percentage increased to 52.2% with 0.25% polyHIPEs concentration and was further increased to 95.6% with the incorporation of 0.5% polyHIPEs. The amendment with 1% polyHIPE resulted in 3 fold increase in moisture content at field capacity as compared to the control. Sandy loam soil amended with 1% polyHIPEs showed 145% moisture increase as compared to the untreated soil. Swelling of the polyHIPEs after absorption of water would expand in the soil and may block the soil pores, thereby affecting the soil water movement. This may prevent the water loss due to seepage, thus changing the physical properties of the soil. Abedi-Koupai *et al.* (2008) demonstrated similar results for water retention capacity with two different hydrogels in sandy loam soils. They reported increased residual water content with increasing hydrogel application. Their studies suggested, as sandy loam soil have less cation holding capacity compared with other soil textures, the increase in expansion of the polymers in the soil enhances water adsorption.

Thus sandy loam soil treated with various levels of sulphonated polyHIPEs showed higher values of moisture retention in comparison to the control. A similar

effect has been discussed by Sivapalan (2006), where the effect of crosslinked polyacrylamide was assessed for water holding capacity in sandy soil. Their study demonstrated a 12 and 18 fold increase in water use efficiency of plants grown in sandy soils treated with 0.03 and 0.07% polyacrylamide respectively. Consequently, they reported incorporation of polyacrylamide can increase the water holding capacity in sandy soils and reduce losses due to deep percolation. Han *et al.* (2013) reported super absorbent polymer application can alter the soil water diffusivity and may assist in inhibiting evaporation of soil moisture and prevention water seepage. In comparison to our current results, Shahid *et al.* (2012a) demonstrated increase of up to 60 to 100% of water retention at field capacity in sandy loam soils with the application of 0.1 to 0.4w/w% of a superabsorbent hydrogel nanocomposite.

Therefore, these results suggest that with the aid of sulphonated polyHIPEs, it is possible to increase the moisture content in sandy loam soils. Incorporating an appropriate amount of sulphonated polyHIPEs can significantly improve the ability of sandy loam soil to hold water. However, unlike the clay loam soils, addition of polyHIPEs did not change the sandy loam soils inherent properties. After oven drying, the untreated sandy loam soil (control) and amended soil showed a similar gritty texture.

6.1.2.4 Effect of polyHIPE on moisture content at permanent wilting point in sandy loam soil

A significant difference was observed ($P<0.05$) for the moisture content at PWP between the control and sandy loam soil amended with 0.25%, 0.5% and 1% polyHIPEs.

Figure 6-5 shows the moisture content at PWP for the sandy loam soils. The water retention was 72.5%, 141.3% and 213.8% more as compared to the control for soil amended with 0.25%, 0.5% and 1% polyHIPEs respectively. Although an increase in the water retention capacity was observed in 0.25% and 0.5% treatments, enrichment of soil with 1% polyHIPEs significantly increased the retention capacity of the soil water at the point of permanent wilting.

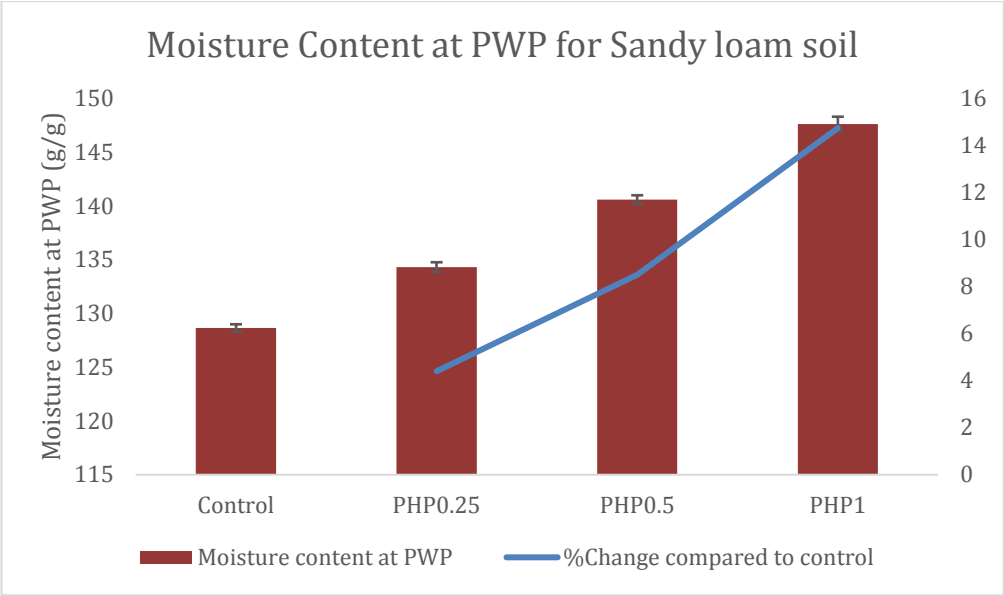

Figure 6-5 Moisture content at PWP for sandy loam soil

Similar results were reported by Leciejewski (2009), in which their study demonstrated soil treatment with hydrogel increased the soil water retention properties of sandy soil from a forest nursery in Julinek. Their study highlighted that the hydrogel accumulated the gravitational water in the soil, which under natural conditions could have been rapidly lost due to the permeability of the sandy soils, thus becoming unavailable for plants. They also found that sandy soil treated with highest amount of hydrogel (6 g/dm^3) showed maximum increase in water retention capacity at the permanent wilting point, which is similar to our results for 1% treatment of polyHIPEs. Studies from Paluszek (2011) also suggest that higher hydrogel doses increase the water retention at the point of permanent wilting in soils which is due to the strong attraction of the water with the polymer structure. Sivapalan (2006) indicated that the immobilized part of the water retained in the hydrogel is unavailable for plants.

Although the results obtained for the effect of polyHIPEs at PWP may be ambiguous, they suggest addition of the polyHIPEs can improve sandy loam soil properties by retaining water in the soil matrix for a longer duration, thus reducing the frequency of irrigation. This may also have an impact on the soil inherent properties.

6.1.3 Available water capacity (AWC) in clay loam and sandy loam soils

PolyHIPE treatment increased soil water capacity in both clay loam and sandy loam soils. AWC is the amount of water that is stored in the soil, which is then gradually absorbed by the plant roots. Soils with high total available water capacity can supply adequate moisture to plants during water scarcity (Troeh and Thompson, 2005). Hence AWC affects plants growth directly because it influences water uptake, nutrient transport and aeration (Batey, 2009).

Brady and Weil (2008) defines total available water capacity (TAWC) is the amount of water content available, stored, and absorbed by the plant between field capacity and permanent wilting point, whereas readily available water content (RAWC) is the amount of water content plants can uptake from the root zone without getting stressed. In this study, RAWC is calculated between 0.05 bar and 2 bar. Figure 6-6 illustrates the total available water capacity in clay loam and sandy loam soils.

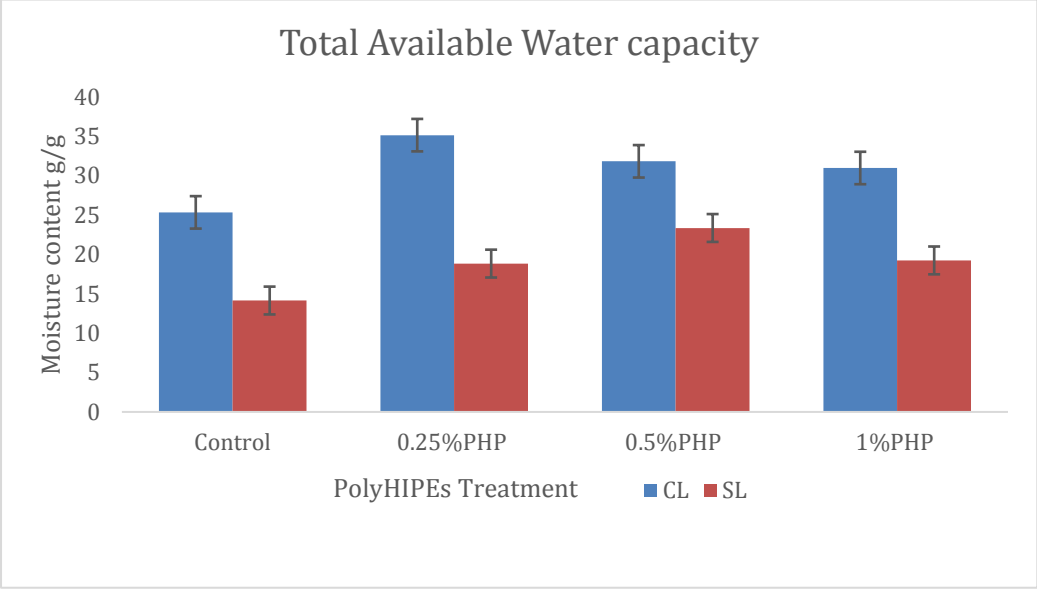

Figure 6-6 Total available water capacity in clay loam and sandy loam soils

A significant difference was observed ($P<0.05$) for TAWC between the control and clay and sandy loam soils amended with 0.25%, 0.5% and 1% polyHIPE respectively. The largest increment in TAWC was 65.1% in sandy loam and 38.7% in clay loam soils compared to the control, which was obtained with 0.5%

and 0.25% treatment of polyHIPEs respectively. The high retention of the TAWC in both the soils can also be attributed to the cation exchange capacity. The productivity and fertility of the soil is highly dependent on its cation exchange capacity (Troeh and Thompson, 2005). The CEC of soils is mainly function of amount of clay and organic matter present and the soil pH (Foth and Ellis, 1996). With enrichment of the soils with polyHIPE, an additional cation exchange system is added to the soil. Under completely saturated state, it can occupy a certain percentage of the total soil volume. The ion exchange capacity of polyHIPE was evaluated as 3.22 meq/g. Hence addition of the polyHIPEs can alter the ion composition of the soil water and its retention capacity. Our results are consistent with the findings of Orikiriza *et al.* (2009b) in which the application of super absorbent polyacrylate hydrogels not only enhanced the efficiency of water uptake but also increased the cation exchange capacity of the soil (13.9meq/g) consequently increasing the biomass of the nine tree species potted in five soil types.

In contrast to the water retention data obtained during soil saturation and field capacity, the trend of high water retention with high doses of polyHIPEs was not found in AWC. Thus in our study, polyHIPEs did not gradually increase AWC in both the soils despite increasing the polyHIPE doses. Conversely, the smallest increment (22.2%) in the TAWC was noted at highest polyHIPE concentration of 1% in the clay loam soil. This can be attributed to the water held in smaller/residual pores or the polyHIPEs did not swell and expand to its maximum capacity in the compacted clay loam soils. The latter effect was also observed by Abedi-Koupai *et al.* (2008), where they reported the application of higher level of hydrogels (6-8 g/kg) did not increase the volumetric water content as compared to the application of low level of hydrogels (2-4 g/kg) in clay soils. They stated that water retention was lower than the other soil texture (sandy loam and loamy) due to less expansion of hydrogels in clay soils. To determine the macro and microporosity in the soils amended with polyHIPEs, soil volumetric content was determined by multiplying the gravimetric water content by the ratio of the soil bulk density (Rowell, 1994). The measurement of the water content at the field capacity corresponds to the volume of the micropores. Therefore, (Dinnis, 1994) states that the microporosity can be divided into residual and storage pore volume by measuring the water content at the wilting point. Clay loam soil

amended with 1% polyHIPEs showed storage pore volume of 0.1 cm^3 cm^{-3} indicating that the TAWC is held in smaller pores and hence restricted. This results suggest that the addition of larger amount of polyHIPEs may affect the microporosity of the soil with the dominance of smaller pores. Pores and interconnects allow the transport of water, however it will be held in residual pores and hence will not be available to the plant growth. On the other hand, the storage pore volume for the clay loam soil amended with 0.25% treatment of polyHIPEs was 0.21 cm^3 cm^{-3}. This correlates with the higher TAWC as seen in Figure 6-6.

Our data obtained for sandy loam soil enriched with 1% concentration of PolyHIPEs had low TAWC (36%) which was almost similar to the 0.25% treatment of polyHIPEs (33.1% of TAWC) in sandy loam soils. This can be attributed to the position of the polyHIPEs in the soil and the pore size. Larger pores can easily drain the water reducing the water retention.

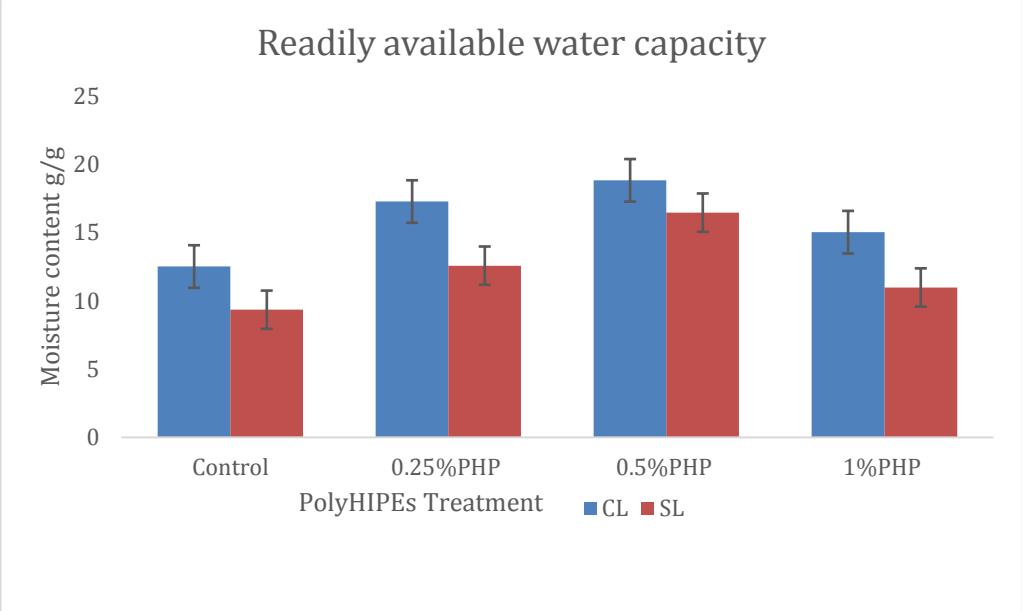

Figure 6-7 Readily available water capacity in clay loam and sandy loam soils

Figure 6-7 shows the readily available water capacity in clay loam and sandy loam soils. A significant difference was observed ($P<0.05$) for RAWC between the control and clay and sandy loam soils amended with 0.25%, 0.5% and 1% polyHIPEs respectively. The most intensive impact in RAWC was seen in 0.5% polyHIPE treatment in both sandy loam and clay loam soils which showed increased retention capacity of 76.1% and 50.4% respectively as compared with

the control variant. These findings are consistent with the studies of (Abedi-Koupai *et al.*, 2008) and Yu *et al.* (2011), where hydrogels increases the water holding capacity of sand to a greater degree as compared to the clay soils. As discussed earlier, this is attributed to the limited expansion of the polyHIPE due to the fine textured soil, thereby impeding the water absorption. The lowest retention in RAWC was seen with 1% polyHIPE treatment, 20.1% in clay loam and 17.4% in sandy loam soils. This data obtained is in contrast to the findings of Abedi-Koupai *et al.* (2008) where they reported approximately 3 fold increase in AWC as compared to that of the control by addition of 8 g/kg of hydrogel in sandy loam soils. In our study, the effect of the polyHIPEs on RAWC can be more likely related to the pores and interconnect size and polyHIPE morphology than the soil texture.

The data obtained here suggest that although higher concentration of polyHIPE mixed with the soils showed greater amount of water retention at saturation point and field capacity, the higher doses did not necessarily increase the RAWC in both the soils. This may suggest that the water is held in residual pores and interconnects in polyHIPE which is not easily accessible to the plant roots. Another reason which may affect the water content, is the degree of sulphonation which provides the hydrophilicity to the sulphonated polyHIPEs. If some of the interior structure is not efficiently sulphonated, the water uptake capacity of the monolith can be affected. Furthermore, cracks developed in the polyHIPEs may also lead to drainage of the water. Clay soils can form aggregates which may limit the swelling of the polymer, thus hindering the water absorption. Thus, the microporosity and macroporosity of the polyHIPEs treated soil influence the water retention capacity. Hydrophilic polymeric material developed by Burke *et al.* (2010) showed water adsorption capacities of 10 fold and 18 fold for pore sizes of 20 and 150 µm respectively. Their work showed that application of these polymers as a soil additive at 0.5% by weight with normal, semiarid and arid conditions increased the dry biomass yield by 30, 140, and 300% respectively after 21 days of cultivation.

Our results suggest that application of lower levels of polyHIPEs (0.25-0.5%) may be recommended in both type of soils. Sulphonated polyHIPEs can function as an additional water reservoir for the plant soil system. However, further research is required about the longevity and effectiveness along with the

application rate of the polyHIPEs in different types of soil. Hence information of the available water content and the characteristics of the soil amended with polyHIPEs to retain water can be critical in planning water management in water scarce areas.

6.2 Conclusion

The results of our current study confirm that the addition of sulphonated polyHIPEs could improve the soil water holding capacity in both sandy and clay loam soils. Incorporation of the polyHIPEs was found to increase the saturation percentage in both types of soil. A trend of gradual increase in the soil water retention characteristics was observed with increasing concentration of the polyHIPEs in sandy and clay loam soils during saturation, field capacity and PWP. It was observed that addition of small quantities of polyHIPEs may alter the soil inherent properties in clay loam soils. This may improve the hydrological properties of the clay loam soil. Incorporation of 1% polyHIPEs had significant effect on soil water retention characteristics in sandy loam soils, resulting in 3 fold increase in moisture content at field capacity as compared to the control. The largest increment in TAWC, 60.4% in sandy loam and 38.9% in clay loam soils compared to the control, was obtained with 0.5% and 0.25% application of polyHIPEs respectively. The most intensive impact in RAWC was seen in 0.5% polyHIPE treatment in both sandy loam and clay loam soils which showed increased retention capacity of 68.9% and 52.8% respectively as compared with the control variant. Our experiments suggest that application of lower levels of polyHIPE (0.25-0.5%) may be recommended in both type of soils. With enrichment of the soils with polyHIPEs, an additional cation exchange system is added to the soil, which aided to the water retention. However, further investigation is needed to determine if it significantly alters the soils productivity along with the water retention.

Thus, these results indicate that the application of sulphonated polyHIPEs markedly improved retention capacity in both type of soils. The obtained data indicate that a significant reduction in the required irrigation frequency for sandy loam soils is possible. This understanding of the water retention characteristics

of the polyHIPE with sandy loam and clay loams soils would be of help in water management. Further studies are needed to estimate, if the water retained by the polyHIPEs is available for plants and how it impacts the plant growth, polymers rehydration cycle and its decomposition over time. Hence the tested sulphonated polyHIPEs in this study are suitable for potential use in agriculture.

Chapter 7 Conclusions and Recommendation for Future Work

7.1 Summary and Conclusions

Over the past few year, microporous materials have attracted considerable attention because they are widely used as adsorbents and catalyst supports. Compared to the conventional microporous materials such as silica, zeolites and metal organic frameworks (MOF) porous polymers have an advantage due to the ease and variation in their synthesis, their controlled morphology, the ease of chemical modification, and their thermal stability. Therefore this study focus on the preparation of functional polyHIPE materials via high internal phase emulsion for specific applications. Two primary aims were set and the sequential chapters in this thesis were carried out based on them. The work carried out in this thesis has successfully met both of these aims. This final chapter summarizes the findings of this research and includes recommendation for future work.

Firstly, the preparation and functionalization of polymeric material developed by polymerization of high internal phase emulsion has been reported. Variation in the mixing time controlled the pore and interconnect pore sizes of the highly porous, open cellular polymer. The SEM images suggested that pore and interconnect sizes are reduced significantly with an increase in mixing time. The average pore size for the sulphonated polyHIPE was reduced by 34.3% from 46.9 µm to 30.8 µm, whereas the average interconnect size decreased similarly by 34.8% with an increase in mixing time from 10 minutes to 30 minutes. Thus polyHIPEs with tunable pore and interconnect sizes were successfully prepared. Sulphonation via microwave irradiation imparts hydrophilicity to the polymers. Microwave irradiation results in the formation of blisters eventually forming micro and nano pores within the walls of the polymer. Enhancement in the specific surface area of the sulphonated polyHIPEs was also observed as detailed in Chapter 4. Moreover, the water uptake capacity of these sulphonated polyHIPE was increased by 18 fold. Thus functionalization by microwave irradiation is efficient and enhances the structure of the resultant polymer. Characterization by a variety of techniques (*i.e.,* Fourier transfer infrared, titration, thermogravimetric analysis) all confirmed the modification in the sulphonated polyHIPE. Titrimetric

analysis assisted in the quantitative assessment of the ion exchange capacity of the sulphonated polyHIPE. These functionalized polyHIPEs exhibited good ion exchange capacity of 3.42 meq/g. FTIR analysis clearly establised the success of the sulphonation process and the incorporation of the suphonate groups in the polyHIPE structure Thermogravimetric analysis demonstrated that the incorporation of the sulphonic groups thermally stabilized the polymer backbone by shifting the degradation temperature to 650^0C. Thus, in this work we prepared sulphonated polyHIPEs with high ion exchange capacity, hydrophilicity and thermal stability which can be used as catalyst support or proton exchange membrane. The irregular and rough surface with hierarchy of pores and interconnects in sulphonated polyHIPEs was found favorable for the growth of *Shewanella Oneidensis* MR-1 forming a catalytic biofilm. Hence sulphonated polyHIPE were investigated further for water absorption capacity in sandy loam and clay loam soils.

The second aim was to prepare and functionalize catalytic hypercrosslinked polyHIPE materials. Hypercrosslinked polymers with different co-monomers and porogens were successfully prepared as detailed in Chapter 5. The incorporation of the Lewis acid catalyst ($FeCl_3$) dissolved in the aqueous phase during the emulsification stage resulted in homogenous distribution of the catalyst throughout the polymer structure. Addition of porogens improved the specific surface area in VBC-DVB polyHIPEs which was further enhanced by hypercrosslinking. SEM images revealed the highly interconnected porous morphology. The pores were well defined and smooth as compared to the sulphonated polyHIPEs. Catalyst size can be controlled and BET surface area up to 911 m^2/g can be achieved with varying the mixing time. FTIR analysis confirmed the success of the hypercrosslinking process correlating with the increase in specific surface area of the polyHIPEs. However, due to the increase in micropores and interconnectivity, with the average pore sizes remaining constant a weakened mechanical structure is produced in the hypercrosslinked polyHIPEs. Moreover, due to the homogenous distribution of the catalyst and the abundance of narrow micropores developed within the structure the polyHIPE network became more fragile. On the other hand, post hypercrosslinking carried out on sulphonated polyHIPEs resulted in enhanced surface area of 421 m^2/g

and a more robust structure. The hypercrosslinked polyHIPEs prepared with VBC monomers exhibited almost twice the specific surface area as compared to the hypercrosslinked sulphonated polyHIPEs. Characterization by FTIR and BET indicated the success of hypercrosslinking and effective enhancement of the surface area in VBC based polyHIPEs prepared with $FeCl_3$ in the aqueous phase. However, thermogravimetric analysis indicated that thermal stability decreases on hypercrosslinking.

Finally, application of sulphonated polyHIPEs in sandy loam and clay loam soils suggested improved water holding capacity in both the soils was discussed in Chapter 6. Being highly hydrophilic they increase the plant available water in the soil which enables the plant to survive under water stress conditions. A trend of gradual increase in the soil water retention characteristics was observed with increasing concentration of the polyHIPEs in sandy and clay loam soils during saturation and field capacities. It was found that the addition of small quantities of polyHIPE may alter the soil inherent properties in clay loam soils. With enrichment of the soils with sulphonated polyHIPEs, an additional cation exchange system is added to the soil, which aids water retention. The highly porous morphology with interconnected pores in sulphonated polyHIPEs suggests that application of lower levels of polymer (0.25-0.5%) may be recommended in both types of soils.

7.2 Recommendations for future work

The work discussed in this thesis opens new approaches to the application of polyHIPE material as catalyst support and in agriculture as a soil additive. Further testing and developments in the following areas can deliver valuable information in developing these monolithic materials:

- The work in this study has used styrene, divinyl benzene and vinyl benzene chloride monomers. A more detailed understanding of the morphology with different comonomers and surfactants and how their composition and ratio can be altered to influence the resultant polymer properties needs to be investigated. The potential for development of a

biodegradable polyHIPEs should also be investigated to respond to concerns about the persistence of styrene in the soil.

- Sulphonation via microwave irradiation was found effective and significantly reduces the sulphonation process time to a few minutes whilst enhancing the polyHIPE morphology. Developing methods for uniform sulphonation is of fundamental scientific interest. Monoliths could be tailored with the addition of the sulphonic acid functionality which aids in transport of protons. Moreover, these tailored monolith can be tested for the production of proton exchange material considering specific applications such as electrodialysis and polymer fuel cells.

- To further investigate and understand the biofilm formation of *Shewanella Oneidensis* MR-1, on sulphonated polyHIPE material. Understanding the metabolic pathways used to form a robust catalytic biofilm will open new methods and its successful application in soil bioremediation.

- Mechanical stability in hypercrosslinked network is still underexplored. Process parameters and comonomers which will influence the resultant hypercrosslinked material and their mechanical properties need to be further investigated.

- Dielectric barrier discharge plasma can be used for catalyst precursor decomposition to metal oxide followed by catalyst reduction in the presence of hydrogen (In case of different catalyst precursor other than Fe used in the aqueous phase). This technique can open up new approach for some applications where catalyst precursor decomposition stage is combined with catalyst reduction stage.

- Laboratory experiments showed that clay and sandy loam soils amended with hydrophilic sulphonated polyHIPEs have a positive effect on the total plant available water and soil characteristics. However, further investigation needs to be carried out with field trials to check if similar results could be achieved in a more varied suboptimal field environment.

The ion exchange capacity of the polyHIPEs can be investigated for controlled release of essential nutrient for plant growth for example phosphorus. Hydraulic conductivity can be assessed for the soils amended with sulphonated polyHIPEs. Bio compatibility of the sulphonated polyHIPEs can be explored by impregnating the polymer with plant growth promoting and bio control agents such as *Streptomyces spp*., *Tricoderma spp*., *Pseudomonas spp*., and *Bacillus spp* which promote diverse microbial population in the rhizosphere enhancing plant growth and productivity (Gopalakrishnan *et al.*, 2013; Han *et al.*, 2015)

References

Abedi-Koupai, J. and Asadkazemi, J. (2006) 'Effects of a hydrophilic polymer on the field performance of an ornamental plant (Cupressus arizonica) under reduced irrigation regimes', *Iranian Polymer Journal*, 15(9), pp. 715-725.

Abedi-Koupai, J., Sohrab, F. and Swarbrick, G. (2008) 'Evaluation of Hydrogel Application on Soil Water Retention Characteristics', *Journal of Plant Nutrition*, 31(2), pp. 317-331.

Agaba, H., Orikiriza, L.J.B., Esegu, J.F.O., Obua, J., Kabasa, J.D. and Huttermann, A. (2010) 'Effects of Hydrogel Amendment to Different Soils on Plant Available Water and Survival of Trees under Drought Conditions', *Clean-Soil Air Water*, 38(4), pp. 328-335.

Ahmed, M., Malik, M.A., Pervez, S. and Raffiq, M. (2004) 'Effect of porosity on sulfonation of macroporous styrene-divinylbenzene beads', *European Polymer Journal*, 40(8), pp. 1609-1613.

Ahn, J.H., Jang, J.E., Oh, C.G., Ihm, S.K., Cortez, J. and Sherrington, D.C. (2006) 'Rapid generation and control of microporosity, bimodal pore size distribution, and surface area in Davankov-type hyper-cross-linked resins', *Macromolecules*, 39(2), pp. 627-632.

Akay, G. (2004) *Microporous Polymer*. Int. Patent Publication, PCT WO/2004/005355.

Akay, G. (2006) in Lee, S. (ed.) *Encyclopedia of Chemicals Processing*. New York: Taylor & Francis Group.

Akay, G. (2012). Int. Patent Publication, PCT WO/2012/025767.

Akay, G., Birch, M.A. and Bokhari, M.A. (2004) 'Microcellular polyHIPE polymer supports osteoblast growth and bone formation in vitro', *Biomaterials*, 25(18), pp. 3991-4000.

Akay, G., Bokhari, M.A., Byron, V.J. and Dogru, M. (2005a) 'Development of Nano-Structured Micro-Porous Materials and their Application in Bioprocess-Chemical Process Intensification and Tissue Engineering', in Galan, M.A. and Del Valle, E.M. (eds.) *Chemical Engineering Trends and Development*. Wiley, pp. 171-197.

Akay, G. and Burke, D.R. (2010). Int. Patent Publication, PCT WO/2010/040996.

Akay, G. and Burke, D.R. (2012) 'Agro-Process Intensification through Synthetic Rhizosphere Media for Nitrogen Fixation and Yield Enhancement in Plants', *American Journal of Agricultural & Biological Science*, 7(2), pp. 150-172.

Akay, G., Downes, S. and Price, V.J. (2002a) *Microcellular polymers as cell growth media and novel polymers*. European Patent, EP 1183328.

Akay, G., Downes, S. and Price, V.J. (2002b) 'Microcellular polymers as cell growth media and novel polymers'. Google Patents. Available at: http://www.google.co.uk/patents/EP1183328A2?cl=en.

Akay, G., Erhan, E. and Keskinler, B. (2005b) 'Bioprocess intensification in flow-through monolithic microbioreactors with immobilized bacteria', *Biotechnology and Bioengineering*, 90(2), pp. 180-190.

Akay, G. and Fleming, S. (2012) 'Agro-process intensification: micro-reactors as soil additives with nitrogen fixing bacterium *Azospirillum brasilense* to enhance its potential as self-sustaining biofertiliser', *Green Process Synth 2012*, pp. 427-437.

Akay, G. and Jordan, C.A. (2011) 'Gasification of Fuel Cane Bagasse in a Downdraft Gasifier: Influence of Lignocellulosic Composition and Fuel Particle Size on Syngas Composition and Yield', *Energy & Fuels*, 25(5), pp. 2274-2283.

Akay, G., Noor, Z.Z., Calkan, O.F., Ndlovu, T.M. and Burke, D.R. (2010) *A process for preparing functionalised microporous polymers (which are also known as micro-cellular polymers or polyHIPE polymers (PHPs)) using intensified internal heating (for example by microwave irradiation).* U.S Patent 7820729.

Akay, G., Pekdemir, T., Shakorfow, A.M. and Vickers, J. (2012) 'Intensified demulsification and separation of thermal oxide reprocessing interfacial crud (THORP-IFC) simulants', *Green Processing and Synthesis*, 1(1), pp. 109-127.

Akay, G. and Vickers, J. (2003) *Method for seperating oil in water emulsions*. European Patent, EP 1307402.

Akay, G. and Vickers, J. (2010) *Methods of separating oil & water*. US Patent 7780854.

Akkaramongkolporn, P., Ngawhirunpat, T. and Opanasopit, P. (2009) 'Preparation and Evaluation of Differently Sulfonated Styrene-Divinylbenzene Cross-linked Copolymer Cationic Exchange Resins as Novel Carriers for Drug Delivery', *Aaps Pharmscitech*, 10(2), pp. 641-648.

Anderson, C.D. and Daniels, E.S. (2003) *Emulsion Polymerisation and Latex Applications*. Smithers Rapra Technology.

Andry, H., Yamamoto, T., Irie, T., Moritani, S., Inoue, M. and Fujiyama, H. (2009) 'Water retention, hydraulic conductivity of hydrophilic polymers in sandy soil as affected by temperature and water quality', *Journal of Hydrology*, 373(1-2), pp. 177-183.

Aronson, M.P. and Petko, M.F. (1993) 'Highly Concentrated Water-In-Oil Emulsions - Influence of Electrolyte on their Properties and Stability', *Journal of Colloid and Interface Science*, 159(1), pp. 134-149.

Bai, W., Zhang, H., Liu, B., Wu, Y. and Song, J. (2010) 'Effects of super-absorbent polymers on the physical and chemical properties of soil following different wetting and drying cycles', *Soil Use and Management*, 26(3), pp. 253-260.

Bancroft, W.D. (1913) 'The theory of emulsification, V', *The Journal of Physical Chemistry*, 17(6), pp. 501-519.

Barbetta, A. and Cameron, N.R. (2004) 'Morphology and surface area of emulsion-derived (PolyHIPE) solid foams prepared with oil-phase soluble porogenic solvents: Three-component surfactant system', *Macromolecules*, 37(9), pp. 3202-3213.

Barbetta, A., Cameron, N.R. and Cooper, S.J. (2000) 'High internal phase emulsions (HIPEs) containing divinylbenzene and 4-vinylbenzyl chloride and the morphology of the resulting PolyHIPE materials', *Chemical Communications*, (3), pp. 221-222.

Barbetta, A., Dentini, M., De Vecchis, M.S., Filippini, P., Formisano, G. and Caiazza, S. (2005) 'Scaffolds based on biopolymeric foams', *Advanced Functional Materials*, 15(1), pp. 118-124.

Barby, D. and Haq, Z. (1982) *Low density porous cross-linked polymeric materials and their preparation and use as carriers for included liquids*. European Patent 0,060,138.

Barby, D. and Haq, Z. (1985) *Low Density Porous Cross-Linked Polymeric Materials And Their Preparation And Use As Carriers For Included Liquids*. US Patent 4522953.

Barlik, N., Keskinler, B., Kocakerim, M.M. and Akay, G. (2015) 'Surface modification of monolithic PolyHIPE Polymers for anionic functionality and their ion exchange behavior', *Journal of Applied Polymer Science*, 132(29).

Barrios, V.A.E., Espinosa, G.A., Rodríguez, J.L.D., Méndez, J.R.R. and Aguilar, N.V.P. (2012) *FTIR - An Essential Characterization Technique for Polymeric Materials*. INTECH Open Access Publisher.

Batey, T. (2009) 'Soil compaction and soil management – a review', *Soil Use and Management*, 25(4), pp. 335-345.

Becher, P. (2001) *Emulsions: Theory and Practice*. Third edn. New York: Oxford University Press.

Bellamy, K., Findlay, P.H., Rannard, S.P. and Ryan, P.M. (2008) *Aqueous media purification method and device comprising a functionalised polyhipe resin*. European Patent, EP 1 889 811 A1.

Bhardwaj, A.K., Shainberg, I., Goldstein, D., Warrington, D.N. and J.Levy, G. (2007) 'Water Retention and Hydraulic Conductivity of Cross-Linked Polyacrylamides in Sandy Soils', *Soil Science Society of America Journal*, 71(2), pp. 406-412.

Bhumgara, Z. (1995) 'Polyhipe Foam Materials as Filtration Media', *Filtration & Separation*, 32(3), pp. 245-251.

Bhunia, S., Banerjee, B. and Bhaumik, A. (2015) 'A new hypercrosslinked supermicroporous polymer, with scope for sulfonation, and its catalytic potential for the efficient synthesis of biodiesel at room temperature', *Chemical Communications*, 51(24), pp. 5020-5023.

Binkley, D., Dunkin, K.A., Debell, D. and Ryan, M.G. (1992) 'Production and nutrient cycling in mixed plantations of eucalyptus and albizia in Hawaii', *Forest Science*, 38(2), pp. 393-408.

Binks, B.P. (ed.) (1998) *Modern Aspects of Emulsion Science*. Cambridge : Royal Society of Chemistry

Blackley, D.C. (1975) *Emulsion Polymerisation: Theory and Practice*. London: Applied Science Publishers Ltd.

Blanco, J.F., Nguyen, Q.T. and Schaetzel, P. (2001) 'Novel hydrophilic membrane materials: sulfonated polyethersulfone Cardo', *Journal of Membrane Science*, 186(2), pp. 267-279.

Bokhari, M.A., Akay, G., Zhang, S.G. and Birch, M.A. (2005) 'Enhancement of osteoblast growth and differentiation in vitro on a peptide hydrogel - polyHIPE polymer hybrid material', *Biomaterials*, 26(25), pp. 5198-5208.

Brady, N.C. and Weil, R.R. (2008) *The Nature and Properties of Soils*. Pearson Prentice Hall.

Brown, G.O. (2002) 'Henry Darcy and the making of a law', *Water Resources Research*, 38(7).

Buchholz, F.L. and Graham, A.T. (1998) *Modern superabsorbent polymer technology*. Wiley-VCH.

Burke, D.R. (2007) *Bioprocess Intensification: Development of Novel Materials for Soil Enhancement to Maximise Crop Yield. PhD Thesis. Newcastle University.*

Burke, D.R., Akay, G. and Bilsborrow, P.E. (2010) 'Development of Novel Polymeric Materials for Agroprocess Intensification', *Journal of Applied Polymer Science*, 118(6), pp. 3292-3299.

Busby, W., Cameron, N.R. and Jahoda, C.A. (2001) 'Emulsion-derived foams (PolyHIPEs) containing poly(epsilon-caprolactone) as matrixes for tissue engineering', *Biomacromolecules*, 2(1), pp. 154-64.

Butler, R., Hopkinson, I. and Cooper, A.I. (2003) 'Synthesis of porous emulsion-templated polymers using high internal phase CO2-in-water emulsions', *Journal of the American Chemical Society*, 125(47), pp. 14473-14481.

Çalkan, B. (2007) *Preparation of novel nano-structured macro- and meso-porous metal foams for process intensification and miniaturization*. Ph. D. thesis. University of Newcastle upon Tyne,

University of Newcastle upon Tyne.

Cameron, N.R. (2005) 'High internal phase emulsion templating as a route to well-defined porous polymers', *Polymer*, 46(5), pp. 1439-1449.

Cameron, N.R. and Barbetta, A. (2000) 'The influence of porogen type on the porosity, surface area and morphology of poly(divinylbenzene) PolyHIPE foams', *Journal of Materials Chemistry*, 10(11), pp. 2466-2472.

Cameron, N.R., Sherrington, D.C., Albiston, L. and Gregory, D.P. (1996a) 'Study of the formation of the open cellular morphology of poly(styrene/divinylbenzene) polyHIPE materials by cryo-SEM', *Colloid and Polymer Science*, 274(6), pp. 592-595.

Cameron, N.R., Sherrington, D.C., Ando, I. and Kurosu, H. (1996b) 'Chemical modification of monolithic poly(styrene-divinylbenzene) PolyHIPE(R) materials', *Journal of Materials Chemistry*, 6(5), pp. 719-726.

Carnachan, R.J., Bokhari, M., Przyborski, S.A. and Cameron, N.R. (2006) 'Tailoring the morphology of emulsion-templated porous polymers', *Soft Matter*, 2(7), pp. 608-616.

Chakrabarti, A. and Sharma, M.M. (1993) 'Cationic Ion -Exchange Resins as Catalyst', *Reactive Polymers*, 20(1-2), pp. 1-45.

Chern, C.S. (2006) 'Emulsion polymerization mechanisms and kinetics', *Progress in Polymer Science*, 31(5), pp. 443-486.

Chesworth, W. (2008) *Encyclopedia of Soil Sciences*. University of Guelph, Canada: Springer.

Clayton, W. (1928) *The Theory of Emulsions and Their Technical Treatment*. 2nd edn. London: J.& A.Churchill Ltd.

Cooper, A.I., Butler, R. and Davies, C.M. (2001) 'Emulsion templating using high internal phase supercritical fluid emulsions', *Advanced Materials*, 13(19), pp. 1459-1463.

Cummins, D., Wyman, P., Duxbury, C.J., Thies, J., Koning, C.E. and Heise, A. (2007) 'Synthesis of functional photopolymerized macroporous PolyHIPEs by atom transfer radical polymerization surface grafting', *Chemistry of Materials*, 19(22), pp. 5285-5292.

Davankov, V.A., Rogozhin, S.V. and Tsyurupa, M.P. (1973) *Macronet Polystyrene Structures For Ionites and Method of Producing Same*. U.S. Patent No. 3729457.

Dechant, J. (1987) 'Emulsions and solubilization. Von K. SHINODA und S. FRIBERG. New York/Chichester/Brisbane/Toronto/Singapore: John Wiley & Sons 1986.', *Acta Polymerica*, 38(7), pp. 459-459.

Deleuze, H., Maillard, B. and Mondain-Monval, O. (2002) 'Development of a new ultraporous polymer as support in organic synthesis', *Bioorganic & Medicinal Chemistry Letters*, 12(14), pp. 1877-1880.

Deleuze, H., Richez, A., Vedrenne, P. and Collier, R. (2005) 'Preparation of ultra-low-density microcellular materials', *Journal of Applied Polymer Science*, 96(6), pp. 2053-2063.

DeRoussel, P., Khakhar, D.V. and Ottino, J.M. (2001) 'Mixing of viscous immiscible liquids. Part 2: Overemulsification - interpretation and use', *Chemical Engineering Science*, 56(19), pp. 5531-5537.

Desforges, A., Arpontet, M., Deleuze, H. and Mondain-Monval, O. (2002) 'Synthesis and functionalisation of polyHIPE (R) beads', *Reactive & Functional Polymers*, 53(2-3), pp. 183-192.

Dinnis, E.R. (1994) 'Soil science: Methods & applications D. L. Rowell, Longman Scientific & Technical, Longman Group UK Ltd, Harlow, Essex, UK', *Journal of the Science of Food and Agriculture*, 66(4), pp. 573-574.

Dizge, N., Aydiner, C., Imer, D.Y., Bayramoglu, M., Tanriseven, A. and Keskinlera, B. (2009a) 'Biodiesel production from sunflower, soybean, and waste cooking oils by transesterification using lipase immobilized onto a novel microporous polymer', *Bioresource Technology*, 100(6), pp. 1983-1991.

Dizge, N., Keskinler, B. and Tanriseven, A. (2008) 'Covalent attachment of microbial lipase onto microporous styrene-divinylbenzene copolymer by means of polyglutaraldehyde', *Colloids and Surfaces B-Biointerfaces*, 66(1), pp. 34-38.

Dizge, N., Keskinler, B. and Tanriseven, A. (2009b) 'Biodiesel production from canola oil by using lipase immobilized onto hydrophobic microporous styrene-divinylbenzene copolymer', *Biochemical Engineering Journal*, 44(2-3), pp. 220-225.

Dogru, M. and Akay, G. (2011). Japanese Patent, 2006-53894.

Eberhardt, M. and Theato, P. (2005) 'RAFT polymerization of pentafluorophenyl methacrylate: Preparation of reactive linear diblock copolymer', *Macromolecular Rapid Communications*, 26(18), pp. 1488-1493.

Elabd, Y.A. and Napadensky, E. (2004) 'Sulfonation and characterization of poly (styrene-isobutylene-styrene) triblock copolymers at high ion-exchange capacities', *Polymer*, 45(9), pp. 3037-3043.

Erhan, E., Yer, E., Akay, G., Keskinler, B. and Keskinler, D. (2004) 'Phenol degradation in a fixed-bed bioreactor using micro-cellular polymer-immobilized Pseudomonas syringae', *Journal of Chemical Technology and Biotechnology*, 79(2), pp. 195-206.

Fernandez-Lafuente, R., Armisen, P., Sabuquillo, P., Fernandez-Lorente, G. and Guisan, J.M. (1998) 'Immobilization of lipases by selective adsorption on hydrophobic supports', *Chemistry and Physics of Lipids*, 93(1-2), pp. 185-197.

Flannery, R.L. and Busscher, W.J. (1982) 'Use Of A Synthetic-Polymer In Potting Soils To Improve Water Holding Capacity', *Communications in Soil Science and Plant Analysis*, 13(2), pp. 103-111.

Fontanals, N., Cortes, J., Galia, M., Marce, R.M., Cormack, P.A.G., Borrull, F. and Sherrington, D.C. (2005) 'Synthesis of Davankov-type hypercrosslinked resins using different isomer compositions of vinylbenzyl chloride monomer, and application in the solid-phase extraction of polar compounds', *Journal of Polymer Science Part a-Polymer Chemistry*, 43(8), pp. 1718-1728.

Fontanals, N., Manesiotis, P., Sherrington, D.C. and Cormack, P.A.G. (2008) 'Synthesis of spherical ultra-high-surface-area monodisperse amphipathic polymer sponges in the low-micrometer size range', *Advanced Materials*, 20(7), pp. 1298-+.

Fontanals, N., Marce, R.M., Borrull, F. and Cormack, P.A.G. (2015) 'Hypercrosslinked materials: preparation, characterisation and applications', *Polymer Chemistry*, 6(41), pp. 7231-7244.

Foth, H.D. and Ellis, B.G. (1996) *Soil Fertility*. 2nd Edition,CRC Press LLC, Boca Raton, FL.

Foth, H.D. and Ellis, B.G. (1997) *Soil fertility*. Boca Raton: CRC Press Inc.

Freire, M.G., Dias, A.M.A., Coelho, M.A.Z., Coutinho, J.A.P. and Marrucho, I.M. (2005) 'Aging mechanisms of perfluorocarbon emulsions using image analysis', *Journal of Colloid and Interface Science*, 286(1), pp. 224-232.

Germain, J., Frechet, J.M.J. and Svec, F. (2007) 'Hypercrosslinked polyanilines with nanoporous structure and high surface area: potential adsorbents for hydrogen storage', *Journal of Materials Chemistry*, 17(47), pp. 4989-4997.

Gokmen, M.T. and Du Prez, F.E. (2012) 'Porous polymer particles-A comprehensive guide to synthesis, characterization, functionalization and applications', *Progress in Polymer Science*, 37(3), pp. 365-405.

Goldstein, J., Newbury, D.E., Joy, D.C., Lyman, C.E., Echlin, P., LIfshin, E., Sawyer, L. and Michael, J.R. (2003) *Scanning Electron Microscopy and X-ray Microanalysis*. 3 edn. Springer US.

Goodwin, J. (2004) 'Emulsions and Microemulsions, Chap. 7, in: ' *Colloids and Interfaces with Surfactants and Polymers - An Introduction (2004), Edited by J. W. Goodwin, John Wiley and Sons, Ltd*.

Gopalakrishnan, S., Srinivas, V., Sree Vidya, M. and Rathore, A. (2013) 'Plant growth-promoting activities of Streptomyces spp. in sorghum and rice', *SpringerPlus*, 2, p. 574.

Gralnick, J.A. and Newman, D.K. (2007) 'Extracellular respiration', *Molecular Microbiology*, 65(1), pp. 1-11.

Greco, P.P. (2014) *Development of novel polymeric and composite Nano-Structured Micro-Porous Materials for impact resistance applications*. University of Newcastle upon Tyne.

Griffin, W.C. (1949) 'Classification of surface-active agents by HLB', *Journal of the Society of Cosmetic Chemists*, (1), pp. 311-326.

Griffin, W.C. (1954) 'Calculation of HLB Values of Non-ionic Surfactants', *Journal of the Society of Cosmetic Chemists*, (5), pp. 249-256.

Hamblin, A.P. (1985) 'The Influence Of Soil Structure On Water-Movement, Crop Root-Growth, And Water -Uptake', *Advances in Agronomy*, 38, pp. 95-158.

Han, J.-H., Shim, H., Shin, J.-H. and Kim, K.S. (2015) 'Antagonistic Activities of Bacillus spp. Strains Isolated from Tidal Flat Sediment Towards Anthracnose Pathogens Colletotrichum acutatum and C. gloeosporioides in South Korea', *The Plant Pathology Journal*, 31(2), pp. 165-175.

Han, Y.G., Yu, X.X., Yang, P.L., Li, B., Xu, L. and Wang, C.Z. (2013) 'Dynamic study on water diffusivity of soil with super-absorbent polymer application', *Environmental Earth Sciences*, 69(1), pp. 289-296.

Harkins, W.D. (1947) 'A general theory of the mechanism of emulsion polymerization', *Journal of the American Chemical Society*, 69(6), pp. 1428-44.

Hayman, M.W., Smith, K.H., Cameron, N.R. and Przyborski, S.A. (2005) 'Growth of human stem cell-derived neurons on solid three-dimensional polymers', *Journal of Biochemical and Biophysical Methods*, 62(3), pp. 231-240.

Helfferich, F. (1962) *Ion Exchange*. McGraw-Hill Inc., New York.

Hilgen, H., Dejong, G.J. and Sederel, W.L. (1975) 'Styrene -Divinylbenzene Copolymers .2. Conservation Of Porosity In Styrene-Divinylbenzene Copolymer Matrices And Derived Ion-Exchange Resins', *Journal of Applied Polymer Science*, 19(10), pp. 2647-2654.

Hudson, B.D. (1994) 'Soil organic matter and available water capacity', *Journal of Soil and Water Conservation*, 49(2), pp. 189-194.

Huttermann, A., Orikiriza, L.J.B. and Agaba, H. (2009) 'Application of Superabsorbent Polymers for Improving the Ecological Chemistry of Degraded or Polluted Lands', *Clean-Soil Air Water*, 37(7), pp. 517-526.

Hwang, K.S., Choi, W.J., Kim, J.H. and Lee, J.Y. (2015) 'Preparation of Hypercrosslinked Poly(DVB-VBC) Particles with High Surface Area and Structured Meso- and Micropores', *Macromolecular Research*, 23(11), pp. 1051-1058.

Ikem, V.O., Menner, A., Horozov, T.S. and Bismarck, A. (2010) 'Highly Permeable Macroporous Polymers Synthesized from Pickering Medium and High Internal Phase Emulsion Templates', *Advanced Materials*, 22(32), pp. 3588-+.

Islam, M.R., Hu, Y., Mao, S., Mao, J., Eneji, A.E. and Xue, X. (2011) 'Effectiveness of a water-saving super-absorbent polymer in soil water conservation for

corn (Zea mays L.) based on eco-physiological parameters', *Journal of the Science of Food and Agriculture*, 91(11), pp. 1998-2005.

Jerabek, K., Pulko, I., Soukupova, K., Stefanec, D. and Krajnc, P. (2008) 'Porogenic solvents influence on morphology of 4-vinylbenzyl chloride based polyHIPEs', *Macromolecules*, 41(10), pp. 3543-3546.

Johnson, M.S. (1984) 'The Effects Of Gel-Forming Polyacrylamides On Moisture Storage In Sandy Soils', *Journal of the Science of Food and Agriculture*, 35(11), pp. 1196-1200.

Junkar, I., Koloini, T., Krajnc, P., Nemec, D., Podgornik, A. and Strancar, A. (2007) 'Pressure drop characteristics of poly(high internal phase emulsion) monoliths', *Journal of Chromatography A*, 1144(1), pp. 48-54.

Kaniappan, K. and Latha, S. (2011) 'Certain Investigations on the Formulation and Characterization of Polystyrene/Poly (methyl methacrylate) Blends'.

Kazanskii, K.S. and Dubrovskii, S.A. (1992) 'Chemistry and physics of "agricultural" hydrogels', in *Polyelectrolytes Hydrogels Chromatographic Materials*. Springer Berlin Heidelberg, pp. 97-133.

Khaddazh, M., Gritskova, I.A. and Litvinenko, G.I. (2012) 'An Advanced Approach on the Study of Emulsion Polymerization: Effect of the Initial Dispersion State of the System on the Reaction Mechanism, Polymerization Rate, and Size Distribution of Polymer-Monomer Particles', in Gomes, A.D.S. (ed.) *Polymerization*. InTech, pp. 163-200.

Kimmins, S.D. and Cameron, N.R. (2011) 'Functional Porous Polymers by Emulsion Templating: Recent Advances', *Advanced Functional Materials*, 21(2), pp. 211-225.

Kimmins, S.D., Wyman, P. and Cameron, N.R. (2014) 'Amine-functionalization of glycidyl methacrylate-containing emulsion-templated porous polymers and immobilization of proteinase K for biocatalysis', *Polymer*, 55(1), pp. 416-425.

Kircher, L., Theato, P. and Cameron, N.R. (2013) 'Reactive thiol-ene emulsion-templated porous polymers incorporating pentafluorophenyl acrylate', *Polymer*, 54(7), pp. 1755-1761.

Kita, R., Svec, F. and Frechet, J.M.J. (2001) 'Hydrophilic polymer supports for solid-phase synthesis: Preparation of poly(ethylene glycol) methacrylate polymer beads using "classical" suspension polymerization in aqueous medium and their application in

the solid-phase synthesis of hydantoins', *Journal of Combinatorial Chemistry*, 3(6), pp. 564-571.

Kizling, J. and Kronberg, B. (1990) 'On the formation and stability of concentrated water-in-oil emulsions, aphrons', *Colloids and Surfaces*, 50, pp. 131-140.

Klute, A. and Dirksen, C. (1986) 'Hydraulic conductivity and diffusivity. Laboratory methods', in *Methods of soil analysis - part 1. Physical and mineralogical methods, A. Klute (ed.). S.S.S.A./A.S.A., Madison (1986) 687-734.*

Kovacic, S. and Krajnc, P. (2009) 'Macroporous Monolithic Poly(4-vinylbenzyl chloride) Columns for Organic Synthesis Facilitation by In Situ Polymerization of High Internal Phase Emulsions', *Journal of Polymer Science Part a-Polymer Chemistry*, 47(23), pp. 6726-6734.

Krajnc, P. (2002) 'The influence of some polymerization conditions on the morphology of poly(styrene-co-divinylbenzene) monoliths', *Polimery*, 47(3), pp. 180-183.

Krajnc, P., Brown, J.F. and Cameron, N.R. (2002) 'Monolithic scavenger resins by amine functionalizations of poly(4-vinylbenzyl chloride-co-divinylbenzene) PolyHIPE materials', *Organic Letters*, 4(15), pp. 2497-2500.

Lal, R. (2001) 'World cropland soils as a source or sink for atmospheric carbon', in *Advances in Agronomy*. Academic Press, pp. 145-191.

Leciejewski, P. 13a (2009) 'The effect of hydrogel additives on the water retention curve of sandy soil from forest nursery in Julinek' *Journal of Water and Land Development*. p. 239. Available at: //www.degruyter.com/view/j/jwld.2009.13a.issue--1/v10025-010-0031-8/v10025-010-0031-8.xml (Accessed: 2016-09-07t13:49:00.319+02:00).

Lee, J.Y., Wood, C.D., Bradshaw, D., Rosseinsky, M.J. and Cooper, A.I. (2006) 'Hydrogen adsorption in microporous hypercrosslinked polymers', *Chemical Communications*, (25), pp. 2670-2672.

Li, F.F., Wang, C.F., Shen, X.N., Huang, F.R. and Du, L. (2011) 'Synthesis and characterization of novel silicon-containing aromatic bispropargyl ether resins and their composites', *Polymer Journal*, 43(7), pp. 594-599.

Li, X., He, J.-Z., Hughes, J.M., Liu, Y.-R. and Zheng, Y.-M. (2014) 'Effects of super-absorbent polymers on a soil-wheat (Triticum aestivum L.) system in the field', *Applied Soil Ecology*, 73, pp. 58-63.

Li, Y.F., Li, X.Z., Zhou, L.C., Zhu, X.X. and Li, B.N. (2004) 'Study on the synthesis and application of salt-resisting polymeric hydrogels', *Polymers for Advanced Technologies*, 15(1-2), pp. 34-38.

Lin-Vien, D., Colthup, N.B., Fateley, W.G. and Grasselli, J.G. (1991) *The Handbook of Infrared and Raman Characteristic Frequencies of Organic Molecules*. San Diego: Academic Press.

Lissant, K.J. (1966) 'The Geometry of High-Internal-Phase-Ratio Emulsions', *Journal Of Colloid And Interface Science*, 22, pp. 462-468.

Lissant, K.J. (1988) 'Emulsification and Demulsification- An Historical Overview', *Colloids and Surfaces*, 29(1), pp. 1-5.

Lissant, K.J., Peace, B.W., Wu, S.H. and Mayhan, K.G. (1974) 'Structure of High Internal Phase Emulsions', *Journal of Colloid and Interface Science*, 47(2), pp. 416-423.

Liu, Q.Q., Wang, L., Xiao, A.G., Yu, H.J. and Tan, Q.H. (2008) 'A hyper-cross-linked polystyrene with nano-pore structure', *European Polymer Journal*, 44(8), pp. 2516-2522.

Liu, Q.Q., Wang, L., Yu, W.T., Xiao, A.G., Yu, H.J. and Huo, J. (2010) 'Hypercrosslinked Polystyrene Microspheres with Bimodal Pore Size Distribution and Controllable Macroporosity', *Journal of Applied Polymer Science*, 116(1), pp. 84-92.

Lucchesi, C., Pascual, S., Dujardin, G. and Fontaine, L. (2008) 'New functionalized polyHIPE materials used as amine scavengers in batch and flow-through processes', *Reactive & Functional Polymers*, 68(1), pp. 97-102.

Luo, Y.W., Wang, A.N. and Gao, X. (2012) 'Pushing the mechanical strength of PolyHIPEs up to the theoretical limit through living radical polymerization', *Soft Matter*, 8(6), pp. 1824-1830.

Macintyre, F.S., Sherrington, D.C. and Tetley, L. (2006) 'Synthesis of ultrahigh surface area monodisperse porous polymer nanospheres', *Macromolecules*, 39(16), pp. 5381-5384.

Malik, M.A. (2009) 'Carbonyl Groups in Sulfonated Styrene-Divinylbenzene Macroporous Resins', *Industrial & Engineering Chemistry Research*, 48(15), pp. 6961-6965.

Manley, S.S., Graeber, N., Grof, Z., Menner, A., Hewitt, G.F., Stepanek, F. and Bismarck, A. (2009) 'New insights into the relationship between internal phase level of emulsion templates and gas-liquid permeability of interconnected macroporous polymers', *Soft Matter*, 5(23), pp. 4780-4787.

Marques, M.P.C. and Fernandes, P. (2011) 'Microfluidic Devices: Useful Tools for Bioprocess Intensification', *Molecules*, 16(10), pp. 8368-8401.

Marquez, A.L., Medrano, A., Panizzolo, L.A. and Wagner, J.R. (2010) 'Effect of calcium salts and surfactant concentration on the stability of water-in-oil (w/o) emulsions prepared with polyglycerol polyricinoleate', *Journal of Colloid and Interface Science*, 341(1), pp. 101-108.

Marrucci, G. (1969) 'A Theory of Coalescence', *Chemical Engineering Science*, Vol. 24, pp. 975-985.

Maya, F. and Svec, F. (2013) 'Porous polymer monoliths with large surface area and functional groups prepared via copolymerization of protected functional monomers and hypercrosslinking', *Journal of Chromatography A, Article in Press*.

Mbah, C.N. (2012) 'Determining the Field Capacity, Wilting point and Available Water Capacity of some Southeast Nigerian Soils using Soil Saturation from Capillary Rise', *Nigerian Journal of Biotechnology*, 24, pp. 41-47.

McCornick, P., Smakhtin, V., Bharati, L., Johnston, R., McCartney, M., Sugden, F., Clement, F. and McIntyre, B. (2013) *Tackling change: Future-proofing water, agriculture, and food security in an era of climate uncertainty*. International Water Management Institute (IWMI), Colombo, Sri Lanka 36p: International Water Management Institute (IWMI).

McKeown, N.B. and Budd, P.M. (2011) 'Polymers with Inherent Microporosity', in *Porous Polymers*. John Wiley & Sons, Inc., pp. 1-29.

Menner, A. and Bismarck, A. (2006) 'New evidence for the mechanism of the pore formation in polymerising High Internal Phase Emulsions or why polyHIPEs have an interconnected pore network structure', *Macromolecular Symposia*, 242, pp. 19-24.

Menner, A., Haibach, K., Powell, R. and Bismarck, A. (2006) 'Tough reinforced open porous polymer foams via concentrated emulsion templating', *Polymer*, 47(22), pp. 7628-7635.

Mercier, A., Deleuze, H., Maillard, B. and Mondain-Monval, O. (2002) 'Synthesis and application of an organotin functionalised highly porous emulsion-derived foam', *Advanced Synthesis & Catalysis*, 344(1), pp. 33-36.

Mercier, A., Deleuze, H. and Mondain-Monval, O. (2000) 'Preparation and functionalization of (vinyl)polystyrene polyHIPE (R) - Short routes to binding functional groups through a dimethylene spacer', *Reactive & Functional Polymers*, 46(1), pp. 67-79.

Mercier, A., Deleuze, H. and Mondain-Monval, O. (2001) 'Thiol addition to the pendant vinylbenzene groups of (vinyl)polystyrene PolyHIPE via a batch and a cross-flow method', *Macromolecular Chemistry and Physics*, 202(13), pp. 2672-2680.

Moglia, R.S., Holm, J.L., Sears, N.A., Wilson, C.J., Harrison, D.M. and Cosgriff-Hernandez, E. (2011) 'Injectable PolyHIPEs as High-Porosity Bone Grafts', *Biomacromolecules*, 12(10), pp. 3621-3628.

Nimmo, J.R. (2004) 'Porosity and Pore Size Distribution', *in Hillel, D.,ed Encyclopedia of Soils in the Environment:* , London, Elsevier, v. 3, pp. 295-303.

Okay, O. (1987) 'Styrene-Divinylbenzene Copolymers .5. Inhomogeneity In The Structure And The Average Degree Of Swelling', *Angewandte Makromolekulare Chemie*, 153, pp. 125-134.

Okay, O. (2000) 'Macroporous copolymer networks', *Progress in Polymer Science*, 25(6), pp. 711-779.

Opawale, F.O. and Burgess, D.J. (1998) 'Influence of interfacial properties of lipophilic surfactants on water-in-oil emulsion stability', *Journal Of Colloid And Interface Science*, 197(1), pp. 142-150.

Ordomsky, V.V., Schouten, J.C., van der Schaaf, J. and Nijhuis, T.A. (2012) 'Foam supported sulfonated polystyrene as a new acidic material for catalytic reactions', *Chemical Engineering Journal*, 207, pp. 218-225.

Orikiriza, L.J.B., Agaba, H., Tweheyo, M., Eilu, G., Kabasa, J.D. and Huettermann, A. (2009a) 'Amending Soils with Hydrogels Increases the Biomass of Nine Tree Species under Non-water Stress Conditions', *Clean-Soil Air Water*, 37(8), pp. 615-620.

Orikiriza, L.J.B., Agaba, H., Tweheyo, M., Eilu, G., Kabasa, J.D. and Huttermann, A. (2009b) 'Amending Soils with Hydrogels Increases the Biomass of Nine Tree Species under Non-water Stress Conditions', *Clean-Soil Air Water*, 37(8), pp. 615-620.

Ottens, M., Leene, G., Beenackers, A., Cameron, N. and Sherrington, D.C. (2000) 'PolyHipe: A new polymeric support for heterogeneous catalytic reactions: Kinetics of hydration of cyclohexene in two- and three-phase systems over a strongly acidic sulfonated PolyHipe', *Industrial & Engineering Chemistry Research*, 39(2), pp. 259-266.

Paluszek, J. (2011) 'Physical quality of eroded soil amended with gel-forming polymer', *International Agrophysics*, 25(4), pp. 375-382.

Pierre, S.J., Thies, J.C., Dureault, A., Cameron, N.R., van Hest, J.C.M., Carette, N., Michon, T. and Weberskirch, R. (2006) 'Covalent enzyme immobilization onto photopolymerized highly porous monoliths', *Advanced Materials*, 18(14), pp. 1822-+.

Poritchett, W.L. and Fisher, R.F. (1987) *Properties and management of forest soils*. 2nd Ed edn. New York: John Wiley and Sons, Inc.

Princen, H.M. (1983) 'Rheology of Foams and Highly Concentrated Emulsions .1. Elastic Properties and Yield Stress of a Cylindrical Model System', *Journal of Colloid and Interface Science*, 91(1), pp. 160-175.

Pulko, I., Kolar, M. and Krajnc, P. (2007) 'Atrazine removal by covalent bonding to piperazine functionalized PolyHIPEs', *Science of the Total Environment*, 386(1-3), pp. 114-123.

Pulko, I. and Krajnc, P. (2008) 'Open cellular reactive porous membranes from high internal phase emulsions', *Chemical Communications*, (37), pp. 4481-4483.

Pulko, I. and Krajnc, P. (2012) 'High Internal Phase Emulsion Templating - A Path To Hierarchically Porous Functional Polymers', *Macromolecular Rapid Communications*, 33(20), pp. 1731-1746.

Pulko, I., Wall, J., Krajnc, P. and Cameron, N.R. (2010) 'Ultra-High Surface Area Functional Porous Polymers by Emulsion Templating and Hypercrosslinking: Efficient Nucleophilic Catalyst Supports', *Chemistry-a European Journal*, 16(8), pp. 2350-2354.

Regas, F.P. (1984) 'Physical Characterization of Suspension- Crosslinked Polystyrene Particles and Their Sulfonated Products .2. Ionic Networks', *Polymer*, 25(2), pp. 249-253.

Reichert, J.M., Albuquerque, J.A., Kaiser, D.R., Reinert, D.J., Urach, F.L. and Carlesso, R. (2009) 'Estimation Of Water Retention And Availability In Soils Of Rio Grande Do Sul', *Revista Brasileira De Ciencia Do Solo*, 33(6), pp. 1547-1560.

Reynolds, P.A., Gilbert, E.P. and White, J.W. (2000) 'High internal phase water-in-oil emulsions studied by small-angle neutron scattering', *Journal of Physical Chemistry B*, 104(30), pp. 7012-7022.

Rosche, B., Li, X.Z., Hauer, B., Schmid, A. and Buehler, K. (2009) 'Microbial biofilms: a concept for industrial catalysis?', *Trends in Biotechnology*, 27(11), pp. 636-643.

Rowell, D.L. (1994) *Soil science: methods and applications*. Longman Scientific & Technical.

Rowell, D.L. (2014) *Soil Science: Methods & Applications*. Taylor & Francis.

Sajjadi, S. (2007) 'Formation of fine emulsions by emulsification at high viscosity or low interfacial tension; A comparative study', *Colloids and Surfaces a-Physicochemical and Engineering Aspects*, 299(1-3), pp. 73-78.

Schoo, H.F.M., Challa, G., Rowatt, B. and Sherrington, D.C. (1992) 'Immobilization of flavin on highly porous polymeric disks- 3 Routes to catalytically active membrane', *Reactive Polymers*, 16(2), pp. 125-136.

Schwab, M.G., Senkovska, I., Rose, M., Klein, N., Koch, M., Pahnke, J., Jonschker, G., Schmitz, B., Hirscher, M. and Kaskel, S. (2009) 'High surface area polyHIPEs with hierarchical pore system', *Soft Matter*, 5(5), pp. 1055-1059.

Schwickardi, M., Johann, T., Schmidt, W. and Schuth, F. (2002) 'High-surface-area oxides obtained by an activated carbon route', *Chemistry of Materials*, 14(9), pp. 3913-3919.

Shahid, S.A., Qidwai, A.A., Anwar, F., Ullah, I. and Rashid, U. (2012a) 'Improvement in the water retention characteristics of sandy loam soil using a newly synthesized poly(acrylamide-co-acrylic acid)/AlZnFe2O4 superabsorbent hydrogel nanocomposite material', *Molecules*, 17(8), pp. 9397-412.

Shahid, S.A., Qidwai, A.A., Anwar, F., Ullah, I. and Rashid, U. (2012b) 'Improvement in the Water Retention Characteristics of Sandy Loam Soil Using a Newly Synthesized Poly(acrylamide-co-acrylic Acid)/AlZnFe2O4 Superabsorbent Hydrogel Nanocomposite Material', *Molecules*, 17(8), p. 9397.

Sherman, P. (1968) *Emulsion Science*. London and New York: Academic Press Inc.

Shiklomanov, I.A. (1991) *In:Proceedings of the International Symposium to Commemorate 25 Years of the IHP*. UNESCO/IHP,pp. 93–126.

Sikavitsas, V.I., Bancroft, G.N. and Mikos, A.G. (2002) 'Formation of three-dimensional cell/polymer constructs for bone tissue engineering in a spinner flask and a rotating wall vessel bioreactor', *Journal of Biomedical Materials Research*, 62(1), pp. 136-148.

Sing, K.S.W., Everett, D.H., Haul, R.A.W., Moscou, L., Pierotti, R.A., Rouquerol, J. and Siemieniewska, T. (1985) 'Reporting Physisorption Data For Gas Solid Systems With Special Reference to the Determination of Surface Area and Porosity', *Pure and Applied Chemistry*, 57(4), pp. 603-619.

Singare, P.U., Lokhande, R.S. and Madyal, R.S. (2011) 'Thermal degradation studies of some strongly acidic ca-tion exchange resins', *Open Journal of Physical Chemistry*, 1(02), p. 45.

Sivapalan, S. (2006) 'Benefits of treating a sandy soil with a crosslinked-type polyacrylamide', *Australian Journal of Experimental Agriculture*, 46(4), pp. 579-584.

Smith, C.J., Goh, K.M., Bond, W.J. and Freney, J.R. (1995) 'Effects Of Organic And Inorganic Calcium Compounds On Soil-Solution pH and Aluminum Concentration', *European Journal of Soil Science*, 46(1), pp. 53-63.

Smith, W.V. and Ewart, R.H. (1948) 'Kinetics of Emulsion Polymerization', *The Journal of Chemical Physics*, 16(6), pp. 592-607.

Smitha, B., Sridhar, S. and Khan, A.A. (2003) 'Synthesis and characterization of proton conducting polymer membranes for fuel cells', *Journal of Membrane Science*, 225(1-2), pp. 63-76.

Sulman, E.M., Nikoshvili, L.Z., Matveeva, V.G., Tyamina, I.Y., Sidorov, A.I., Bykov, A.V., Demidenko, G.N., Stein, B.D. and Bronstein, L.M. (2012) 'Palladium Containing Catalysts Based on Hypercrosslinked Polystyrene for Selective Hydrogenation of Acetylene Alcohols', *Topics in Catalysis*, 55(7-10), pp. 492-497.

Sulman, E.M., Valetsky, P.M., Sulman, M.G., Bronstein, L.M., Sidorov, A.I., Doluda, V.Y. and Matveeva, V.G. (2011) 'Nanosized catalysts as a basis for intensifications of technologies', *Chemical Engineering and Processing*, 50(10), pp. 1041-1053.

Taylor, G.I. (1934) 'The Formation of Emulsions in Definable Fields of Flow', *Proceedings of the Royal Society of London. Series A, Containing Papers of a Mathematical and Physical Character*, 146(858), pp. 501-523.

Taylor, P. (1995) 'Ostwald ripening in emulsions', *Colloids and Surfaces A: Physicochemical and Engineering Aspects*, 99, pp. 175-185.

Theato, P. (2008) 'Synthesis of Well-Defined Polymeric Activated Esters', *Journal of Polymer Science Part a-Polymer Chemistry*, 46(20), pp. 6677-6687.

Thormann, K.M., Saville, R.M., Shukla, S., Pelletier, D.A. and Spormann, A.M. (2004) 'Initial phases of biofilm formation in Shewanella oneidensis MR-1', *Journal of Bacteriology*, 186(23), pp. 8096-8104.

Toro, C.A., Rodrigo, R. and Cuellar, J. (2008) 'Sulfonation of macroporous poly(styrene-co-divinylbenzene) beads: Effect of the proportion of isomers on their cation exchange capacity', *Reactive & Functional Polymers*, 68(9), pp. 1325-1336.

Troeh, F.R. (1993) *Soils and soil fertility*. 5th ed.. edn. New York: New York : Oxford University Press.

Troeh, F.R. (2005) *Soils and Soil Fertility*. Wiley.

Troeh, F.R. and Thompson, L.M. (2005) *Soils and soil fertility*. Ames, Iowa [etc.]: Blackwell.

Tsyurupa, M.P. and Davankov, V.A. (2002) 'Hypercrosslinked polymers: basic principle of preparing the new class of polymeric materials', *Reactive & Functional Polymers*, 53(2-3), pp. 193-203.

Vernon-Parry, K.D. (2000) 'Scanning electron microscopy: an introduction', *III-Vs Review*, 13(4), pp. 40-44.

Veverka, P. and Jerabek, K. (1999) 'Mechanism of hypercrosslinking of chloromethylated styrene-divinylbenzene copolymers', *Reactive & Functional Polymers*, 41(1-3), pp. 21-25.

Wakeman, R.J., Bhumgara, Z.G. and Akay, G. (1998) 'Ion exchange modules formed from polyhipe foam precursors', *Chemical Engineering Journal*, 70(2), pp. 133-141.

Wallace, J.S. (2000) 'Increasing agricultural water use efficiency to meet future food production', *Agriculture Ecosystems & Environment*, 82(1-3), pp. 105-119.

Walstra, P. (1993) 'Principles of Emulsion Formation', *Chemical Engineering Science*, 48(2), pp. 333-349.

Wang, H., Bai, H. and Li, L. (2015) 'Hierarchically porous polystyrene membranes fabricated via a CO2-expanded liquid selective swelling and in situ hyper-cross-linking method', *RSC Advances*, 5(84), pp. 68639-68645.

Weil, R.R. (2016) *The nature and properties of soils*. Global edition of the 15th revised edition.. edn. Harlow, Essex : Pearson Education.

Williams, J., Prebble, R.E., Williams, W.T. and Hignett, C.T. (1983) 'The influence of texture, structure and clay mineralogy on the soil moisture characteristic', *Soil Research*, 21(1), pp. 15-32.

Williams, J.M. (1991) 'High Internal Phase water-in-oil Emulsions- Influence of surfactants and Co-surfactants on emulsion stability and foam quality', *Langmuir*, 7(7), pp. 1370-1377.

Williams, J.M., Gray, A.J. and Wilkerson, M.H. (1990) 'Emulsion Stability and Rigid Foams from Styrene or Divnylbenzene Water-In-Oil Emulsions', *Langmuir*, 6(2), pp. 437-444.

Williams, J.M. and Wrobleski, D.A. (1988) 'Spatial-Distribution of the Phases in Water-in-oil emulsions - Open and Closed Microcellular Foams from Cross-linked Polystyrene', *Langmuir*, 4(3), pp. 656-662.

Wu, D., Xu, F., Sun, B., Fu, R., He, H. and Matyjaszewski, K. (2012) 'Design and Preparation of Porous Polymers', *Chemical Reviews*, 112(7), pp. 3959-4015.

Xu, S., Luo, Y. and Tan, B. (2013) 'Recent Development of Hypercrosslinked Microporous Organic Polymers', *Macromolecular Rapid Communications*, 34(6), pp. 471-484.

Yamak, H.B. (2013) 'Emulsion Polymerisation: Effects of Polymerization Variables on the Properties of Vinyl Acetate Based Emulsion Polymers', in Yilmaz, F. (ed.) *Polymer Science*. InTech, pp. 35-72.

Yan, J., Wang, X. and Chen, J. (2000) 'Swelling of porous styrene–divinylbenzene copolymers in water', *Journal of Applied Polymer Science*, 75(4), pp. 536-544.

Yáñez-Chávez, L.G., Pedroza-Sandoval, A., Sánchez-Cohen, I. and Samaniego-Gaxiola, J.A. (2014) 'Assessment of the Impact of Compost and Hydrogel as Soil Moisture Retainers on the Growth and Development of Forage Maize (Zea mays L.)', *Journal of Agriculture and Environmental Sciences*, Vol. 3(No. 4), pp. pp. 93-106.

Yeo, L.Y., Matar, O.K., Ortiz, E.S. and Hewitt, G.F. (2000) 'Phase Inversion and Associated Phenomena', *Multiphase Science and Technology*, 12, pp. 51-116.

Yu, J., Shainberg, I., Yan, Y.L., Shi, J.G., Levy, G.J. and Mamedov, A.I. (2011) 'Superabsorbents and Semiarid Soil Properties Affecting Water Absorption', *Soil Science Society of America Journal*, 75(6), pp. 2305-2313.

Zatz, J.L. (1987) 'Nonionic Surfactants: Physical Chemistry, Edited by Martin J. Schick. Marcel Dekker, New York. 1987. 1,' *Journal of Pharmaceutical Sciences*, 78(4), p. 150pp.

Zhang, X., Shen, S.H. and Fan, L.Y. (2007) 'Studies progress of preparation, properties and applications of hyper-cross-linked polystyrene networks', *Journal of Materials Science*, 42(18), pp. 7621-7629.

Zhou, W.Q., Gu, T.Y., Su, Z.G. and Ma, G.H. (2007) 'Synthesis of macroporous poly(styrene-divinyl benzene) microspheres by surfactant reverse micelles swelling method', *Polymer*, 48(7), pp. 1981-1988.

Appendices

Appendix-A

PolyHIPE materials (containing Phosphoric acid)

Oil Phase: Styrene 76%, DVB 10%, Span 80 14%

Aqueous Phase: Phosphoric acid 10%, Potassium persulphate 1%

Phase volume: 90%

Dosing Time: 5 minutes Mixing Time: 10 min

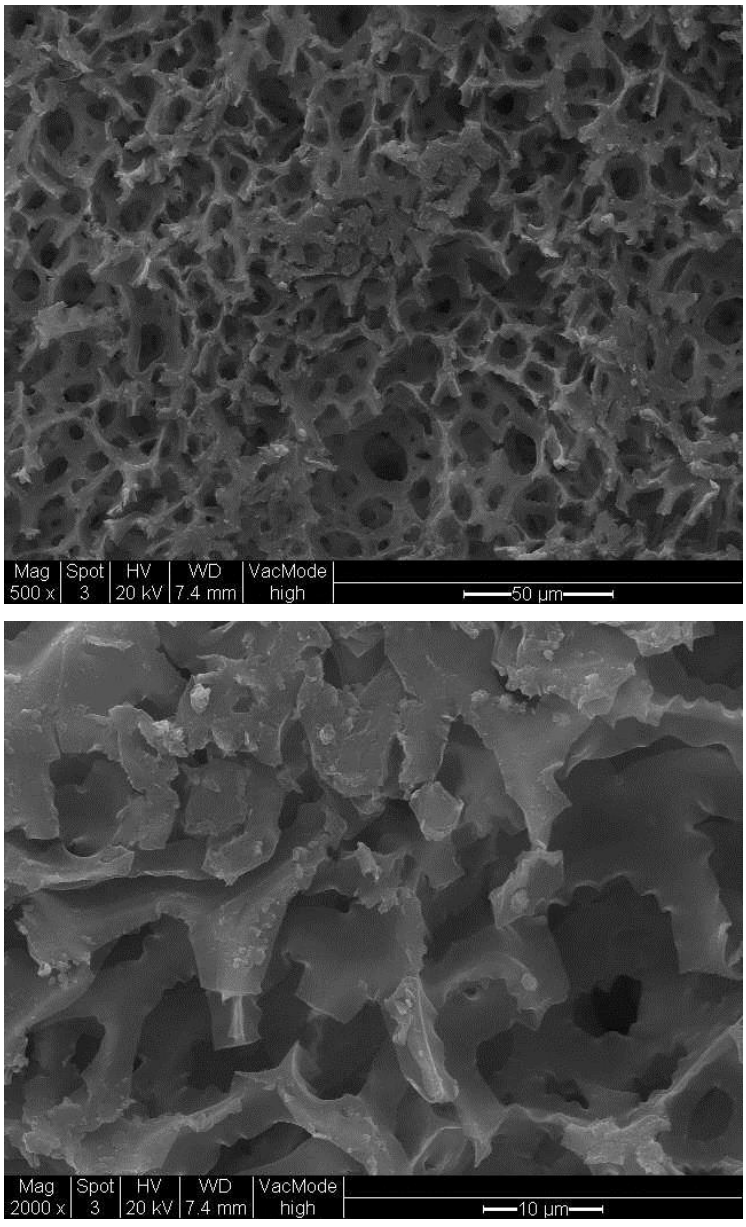

Figure A-1 SEM images of polyHIPE material with phophoric acid in aqueous phase.

Resultant polyHIPE material obtained is hydrophobic. SEM images show an open pore network. Pores are irregular with thick walls. Surface area measurement (BET) = 3 ± 1.5 m^2/g

Appendix –B

Media Preparation

1) Preparation of LB broth:

   In an autoclave bottle, 25gms of LB broth powder is dissolved in 1 litre of distilled water. Mix well. Seal the bottle and sterilize by autoclaving at 121^0C for 20 minutes. Cool and store.

2) Preparation of Lactate medium:

   In an autoclave bottle, 1gm of lactate powder is dissolved in 1 litre of distilled water. Mix well. Seal the bottle and sterilize by autoclaving at 121^0C for 20 minutes. Cool and store.